ΕΘΝΙΚΟ ΜΕΤΣΟΒΙΟ ΠΟΛΥΤΕΧΝΕΙΟ

ΣΧΟΛΗ ΕΦΑΡΜΟΣΜΕΝΩΝ ΜΑΘΗΜΑΤΙΚΩΝ
ΚΑΙ ΦΥΣΙΚΩΝ ΕΠΙΣΤΗΜΩΝ

Δ.Π.Μ.Σ. ΜΙΚΡΟΣΥΣΤΗΜΑΤΑ ΚΑΙ
ΝΑΝΟΔΙΑΤΑΞΕΙΣ

Χρήση της τεχνικής LIFT για την κατασκευή πολύ-στρωματικών Οργανικών Φωτοδιόδων

Μεταπτυχιακή Εργασία

Βεργυρή Παναγιώτη

Μάιος 2014

National Technical University of Athens

"Laser Induced Forward Transfer of Stacked layers for Organic Light Emitting diodes"

Master Thesis

Vergyris Panagiotis

May 2014

Author: Vergyris Panagiotis

Date: 30 May 2014

National Technical University of Athens, Greece

Holst Center, TNO, High Tech Campus, Eindhoven, Netherlands

Supervisors : Ioanna Zergioti, NTUA, Athens

: Jack Levell, Holst Center, HTC, Eindhoven

Σύνοψη

Η παρούσα διπλωματική εργασία αφορά την παρασκευή οργανικών φωτοδιόδων (Organic Light Emitting Diodes) με την χρήση της τεχνικής Laser Induced Forward Transfer Technique (LIFT). Η εν λόγω εργασία έγινε στα πλαίσια της ολοκλήρωσης του μεταπτυχιακού διπλώματος Μικροσυστήματα και Νανοδιατάξεις στο Εθνικό Μετσόβιο Πολυτεχνείο Αθηνών.

Μελετήθηκε η δυνατότητα εκτύπωσης λεπτών υμενίων (100nm/tris(8-hydroxyquinoline)aluminum/Alq_3) οργανικών μέταλλο-πολυμερικών συμπλεγμάτων όπως και πολυμερών με την χρήση ενός Nd:YAG picosecond-laser και ενός nanosecond excimer laser σε αδρανές περιβάλλον και σε περιβάλλον ατμοσφαιρικών συνθηκών. Διάφορες παραλλαγές της τεχνικής LIFT εφαρμόστηκαν και ιδιαίτερη έμφαση δόθηκε στην τεχνική Dynamic Release Layer LIFT. Το πολυμερές της τριαζήνης χρησιμοποιήθηκε ως το ενδιάμεσο προς αποδόμηση στρώμα για την συγκεκριμένη τεχνική. Όλες οι προηγούμενες απόπειρες εκτύπωσης οργανικών φωτοδιόδων χρησιμοποιούν ένα μεταλλικό υποστηρικτικό στρώμα. Αντιθέτως στη παρούσα εργασία επιχειρείτε η άμεση εκτύπωση καθαρού ενεργού υλικού χωρίς την χρήση του επιπλέον μεταλλικού υμενίου. Στόχος είναι, η παρασκευή πολύ-στρωματικών συσκευών με διαδοχική χρήση της τεχνικής LIFT. Μερικές παραλλαγές βασιζόμενες στη εκτύπωση με χρήση laser εφαρμόστηκαν, χρησιμοποιώντας διαφορετική αρχιτεκτονική δομή του δότη σε κάθε περίπτωση. Επιτεύχθηκε η κατασκευή pixel με διάμετρο από 30μm μέχρι 70μm και με μέγιστη ανάλυση μικρότερη από 20μm. Ύστερα από μετρήσεις της φωταύγειας του μέσου παρατηρήθηκε μικρή μείωση στις επιθυμητές ακτινοβολιτικές του ιδιότητες.

Στα πρώτα δύο κεφάλαια του κειμένου γίνετε μία σύντομη περιγραφή του απαιτούμενου θεωρητικού υποβάθρου και της βασικής αρχής της τεχνικής LIFT. Στη συνέχεια γίνεται μία ανασκόπηση των διαφορετικών παραλλαγών της τεχνικής LIFT που συναντώνται στην βιβλιογραφία και μία αναλυτική ανασκόπηση των εφαρμογών τους για την παρασκευή OLEDs όπως και των περιορισμών που συναντώνται σε αυτές. Επίσης αναφέρονται τα διάφορα ήδη οργανικών ημιαγωγών εκπομπής φωτός που σχετίζονται με την αντίστοιχη τεχνολογία

.

Στο τρίτο κεφάλαιο παρουσιάζονται τα εργαλεία που χρησιμοποιήθηκαν στην παρούσα εργασία. Το βασικό εργαστήριο στο οποίο δούλεψα ήταν εξοπλισμένο με ένα Nd:YAG picosecond-laser ενώ μερικά πειράματα έγιναν με την χρήση ενός nanosecond excimer laser. Επίσης στο παρών κεφάλαιο αναλύεται η διαδικασία προετοιμασίας των δοτών όπως και του θαλάμου ελεγχόμενων συνθηκών που συναρμολογήθηκε για της ανάγκες της συγκεκριμένης μελέτης.

Στο τέταρτο κεφάλαιο παρουσιάζονται τα σχετικά πειράματα με την ανάπτυξη των υμενίων της τριαζήνης, του Alq_3, και του πολυμερούς Super Yellow, όπως επίσης και ο υπολογισμός της ελάχιστης απαιτούμενης ενέργειας για την πλήρη αποδόμηση του υμενίου της τριαζήνης σε όλο το πάχος του με την χρήση του picosecond-laser στα 355nm.

Στο κεφάλαιο πέντε, παρουσιάζω την εφαρμογή της τεχνικής LIFT στην εναπόθεση Alq_3. Μελετήθηκε η επίδραση του πάχους της τριαζήνης και της απόστασης μεταξύ δότη και αποδέκτη και βελτιστοποιήθηκαν οι παραπάνω παράμετροι. Επίσης παρουσιάζονται τα αποτελέσματα ύστερα από τον χαρακτηρισμό των κατασκευασμένων pixel μέσω ατομικής μικροσκοπίας, οπτικής μικροσκοπίας και φασματοσκοπικές μετρήσεις. Στη συνέχεια κάποιες απόπειρες εξομάλυνσης των μορφολογικών ανωμαλιών στην επιφάνεια των pixel παρουσιάζονται στο ίδιο κεφάλαιο.

Στο κεφάλαιο έξι καταγράφονται κάποιες διαφορετικές προσεγγίσεις της τεχνικής που περιλαμβάνουν κυρίως διαφορετική αρχιτεκτονική δομή του δότη. Επίσης διαφορετικό ενεργό υλικό χρησιμοποιείτε προς εκτύπωση σε ένα μέρος των πειραμάτων.

Στο κεφάλαιο εφτά παρουσιάζονται τα αποτελέσματα τα οποία συνοπτικά αναφέρονται παρακάτω:

- Το παραγόμενο ωστικό κύμα επηρεάζει σημαντικά την μορφολογία των pixel.
- Το ωστικό κύμα μπορεί να ελεγχθεί αλλάζοντας την απόσταση μεταξύ δότη-αποδέκτη, την ατμοσφαιρική πίεση ή και τα δύο.

- Αλλάζοντας την εστίαση της δέσμη laser μπορούμε να ελέγξουμε το μέγεθος των pixel.
- Το κατώφλι αποδόμησης, για την τριαζήνη με το picosecond-laser στα 355nm για πάχος τριαζήνης στα 100nm, 240nm, και 300nm είναι αντίστοιχα 11,2mJ/cm^2, 11,8mJ/cm^2 και 12,7mJ/cm^2.
- Με την τεχνική Dynamic Release Layer-LIFT pixel μεγέθους από 20μm μέχρι 80μm μπορούν να κατασκευαστούν με το παρόν σύστημα.
- Όταν η διάμετρος των pixel μεγαλώνει, μεγαλύτερες μορφολογικές ανωμαλίες παρατηρούνται.
- Μετά από φασματοσκοπικές μετρήσεις των pixel από Alq_3 παρατηρείται ότι οι ιδιότητες του υλικού παραμένουν σχεδόν ανεπηρέαστες.
- Το υλικό από την IMEC είναι πολύ ευαίσθητο και μετά από την διαδικασία LIFT υποβαθμίζεται πλήρως.
- Το διάλυμα των Alq_3 στο χλωροφόρμιο δεν μπορεί να εναποτεθεί με τη μέθοδο του spin coating χωρίς να προκαλέσει αποκλίσεις στο πάχος της τριαζήνης.
- Στην περίπτωση που ο χαλκός χρησιμοποιείται σαν το στρώμα απορρόφησης φωτός και μετατροπής του σε θερμότητα για την θερμό-αποδόμηση της τριαζήνης το συνολικό σχεδόν στρώμα της τριαζήνης εκτυπώνεται μαζί με τα στρώμα των Alq3.
- Τα Alq_3 pixels μετά από ανόπτηση παρουσία ατμών μεθανόλης διογκώνοντας βελτιώνοντας σημαντικά της μορφολογικές ατέλειες τους.

Στο ίδιο κεφάλαιο προτείνω σχετικές μελλοντικές προοπτικές όσον αφορά στην παραπάνω εργασία.

Το παρακάτω κείμενο είναι γραμμένο στην Αγγλική στα πλαίσια της εκπόνησης της εργασίας στο Holst Center στο Eindhoven της Ολλανδίας. Για την διευκόλυνση του ελληνικού αναγνωστικού κοινού μία σύντομη περίληψη του παρακάτω κειμένου στα Ελληνικά γίνεται στο κεφάλαιο οχτώ.

Abstract

This thesis concerns the fabrication of Organic Light Emitting Diodes by using the Laser Induced Forward Transfer Technique (LIFT). This study is part of my Master's Degree in National Technical University of Athens (NTUA) and the purpose of this thesis is to investigate further the potentiality of LIFT technique for the fabrication of multilayer OLEDs .

In this study, we demonstrated the feasibility of direct dry patterning of thin layer's (100 nm) of tris(8-hydroxyquinoline)aluminum (Alq_3) organic (luminophores) small molecules by Nd:YAG picosecond-laser and by a nanosecond Excimer laser at ambient and vacuum conditions. Triazene polymer was utilized as a dynamic release layer to transfer the small molecules. All the previous laser pulse deposition attempts of small molecules utilized metal shield's to support transfer. On contrary, we directly transferred the small molecules which opens up the possibility of a potential technique for a full colour OLED by sequential steps. Some varied laser based transfer processes has been performed by using varied architectures on the donor preparation. Feature size down to 50μm and patterns with high resolution up to 20μm between the pixels was achieved by this technique. The fluorescence measurements of small molecules before and after laser transfer collaborated that there is no material modification.

This thesis is divided into different chapters. In the first two chapters, a brief discussion about the theoretical background and also the basic principal of the LIFT technique is explained. An overview of various Laser material transfer approaches are described in this section. In addition, I present a detailed literature review on the OLEDs patterning by LIFT technique. Furthermore, the basic working principle of Organic Light Emitting Diodes (OLEDs), different types of organic light emitting materials, their limitations, and various fabrication approaches are detailed in chapter two.

In the Chapter 3, we present the tools that have been utilized to perform the LIFT experiments. The basic tool was the Pico-laser Nd:YAG system. Some experiments were also performed with a nanosecond excimer laser. The environmental chamber, built in order to provide vacuum or nitrogen condition during

LIFT is also discussed in this section. Also, the process for the preparation of the donors for the LIFT process is described here.

In the Chapter 4 are presented the background experiments, about the spin coating of Alq_3, triazene and Super Yellow, as also the calculation of the ablation threshold of Triazene

In Chapter 5, I present the extensive study of the LIFT process for the deposition of small molecules. We studied the influence of the triazene thickness, the influence of the gap and we optimize those two parameters. In the same chapter are presented the results from the characterisation of the fabricated pixels, be atomic force microscopy and by photoluminescence measurements as well. Finally, it is also mentioned one attempt of healing the pixel's surface by exposing them in methanol vapours.The biggest part of the experiments done by using the Dynamic Release Layer LIFT technique. The as transferred layer was a layer from Alq_3 which is an organic light emitting material.

In Chapter 6 some additional LIFT experiments, which include different sacrificial layer approach and donor material (polymer) was tested. More detailed, it has been checked the Hydrogen Assisted –LIFT and the Light Induced Forward Transfer on a Super Yellow layer and also, the Light Induced Thermal Imaging process on a Alq3 layer by using a copper layer as a light to heat conversion layer.

The conclusions (Chapter 7) are:

- The shock wave can cause serious damage on the fabricated pixels
- The shock wave can be controlled by changing the gap or the environmental conditions.
- Getting out of focus on the picosecond laser system, bigger pixels can be patterned.
- The ablation threshold for the picosecond laser system (wavelength=355nm) for a bilayer of triazene layer with 100nm, 240nm and 300nm thickness and a 100nm layer of Alq_3 above, is 11,2mJ/cm^2, 11,8mJ/cm^{2}and 12,7mJ/cm^2 respectively.

- By the Dynamic Release Layer-LIFT technique pixels from 20μm to 80μm were demonstrated.
- The photoluminescence properties of Alq_3 small molecules remain almost unaltered after the LIFT process with the Dynamic Release Layer-LIFT technique.
- The IMEC's Light Emitting Layer is very sensitive to the ambient environment and in combination with the transfer process we are using, the emitting layer is totally degraded after the transferring.
- The solution of Chloroform/ Alq_3 dissolve the triazene layer making unaccepted the spin coating method for the deposition of Alq_3 above a triazene layer.
- Triazene layer transfers with the Alq_3 in the case where an interlayer of copper is used as Light to Heat Conversion Layer
- When the patterns getting bigger the quality of the pixels getting worse.
- Alq_3 pixels can be healed by methanol vapors but after the process they suffer from degradation.

Finally in Chapter 7, I am proposing some paths, and some ideas how this study can be improved.

Preface

The term “Laser Induced Forward Transfer (LIFT)” was coined by Bohandy et. al. in the year 1986, the group successfully transferred metallic copper deposited on a glass substrate to a receiver substrate. After more than two decades of the invention, LIFT has made great advances and gained attention in the research community as well as microelectronics industry. The simplicity and versatility of this process made it a sought after technique for transferring a large number of materials such as metals, inks, pastes, semiconductors, oxides, dielectric and biomolecules. But there are still many parameters that need to be optimized and tools to be developed for LIFT to be commercially successful. This technique finds applications in fabrication of organic light emitting diodes, interconnects and transfers of biomolecules. LIFT has many variants which are similar in processes such as Laser Induced Thermal Imaging (LITI), Dynamic release Layer-LIFT (DRL-LIFT), Matrix Assisted Pulsed Laser Evaporation-LIFT (MAPLE-LIFT) etc. In this thesis, LIFT process is investigated with an emphasis on the DRL-LIFT technique for the fabrication of OLEDs.

This master thesis is carried out at Holst Centre, located at High Tech Campus Eindhoven, The Netherlands, founded in the year 2014 by TNO. Holst Centre is an open innovation research and development center that develops generic technologies for Wireless Autonomous Sensor Technologies and Flexible Electronics. It works in large collaboration with academia and with over 40 industrial partners. The technological program (TP) which with this master thesis is involved with is the TP5: Flexible OLED Displays.

The flexible OLED display technology integration program aims to develop an economically scalable route to high-volume manufacturing of such a display. It targets improvements in display size resolution, power consumption, outdoor readability, flexibility and weight. To do this, the program tackles a number of individual challenges in an integrated approach. These challenges include:

- Developing new OLED, organic and metal oxide semiconductor materials for printing and self-aligned lithographic processes

- Redesigning pixel circuits and backplane matrices to support larger, higher-resolution displays, and developing new addressing schemes
- Developing new display manufacturing techniques such as fine patterning equipment for backplanes and tools for integrated roll-to-roll manufacturing
- Process integration

The program brings together partners from across the value chain including materials and equipment suppliers as well as component and device manufacturers. Large multinationals, SMEs and startups with specific know-how can all add value to and benefit from the program.

Acknowledgments

With this master thesis, I conclude my Master of Science, Microsystems and Nanodevices at National Technical University of Athens. I would like to thank all my Professors at NTUA who gave the opportunity to engage me in the fascinating world of Sciences.

My sincere thanks to my advisor Mr. Jack Levell for showing trust in me and for introducing me to the exciting world of science as also Mr. Sandeep Menon Perinchery who through numerous valuable discussions and arguments, he have helped me develop a scientific approach towards my work. I am ready to apply this attitude to my future projects and in other aspects of my life.

Furthermore through that very pleasant experience I met some very knowledgeable persons as Mr. Rajesh Mandamprambil and Mr. Henri Fledderus. I own them a lot for their support during this thesis and their time. Mr. Henri Fledderus introduced me in the laser lab and help me in personal with his advices to understand what I have to do to succeed in an multicultural and professional environment of a company as Holst Center. Mr. Rajesh Mandamparambil share with me his enthusiasm, with which was always interact with the daily obstacles, we meet during that project. I cannot forget to give my kind regards to Mr. Edsger Smits and Mr.Merijn Giesbers for their time and their valuable advices, as also all my friends and colleagues at Holst Center.

Last but not least I would like to thank Mrs. Iwanna Zergioti which help me and advise me during this thesis and gave me the opportunity with supervising me in distance from Greece to learn about the strength of myself.

And, most importantly, I want to thank my parents. I am the person I am, because of you.

Thank you.

Contents

List of abbreviations

a.u.	Arbitrary units
AFM	Atomic force microscopy
Alq_3	tris (8-hydroxyquinoline) aluminium (ı ı ı)
a-Si:H	Hydrogenated amorphous Silicon
BA-LIFT	Blister Actuated Laser Induced Forward Transfer
BLAST	Ballistic Laser- Assisted Solid Transfer
DRL	Dynamic Release Layer
EL	Electro-luminescent
FED	Field Emission Display
FMM	Fine-Metal Masking
FWHM	Full width at half maximum
HA-LIFT	Hydrogen Assisted Light Induced Forward Transfer
HOMO	Highest Occupied Molecular Orbital
ITO	Indium Tin Oxide
LDW	Laser Direct-Write
LEDs	Light Emitted Diodes
LEL	Light Emitting Layer
LIBT	Light Induced Backward Transfer
LIFT	Light Induced Forward Transfer
LITI	Laser Induced Thermal Imaging
LTHC	Light-to-Heat Conversion layer
LUMO	Lowest Unoccupied Molecular Orbital
MAPLE-DW	Matrix-Assisted Pulsed Laser Evaporation-Direct Write
MMA	Methyl methacrylate
OEL	Organic Electroluminescence
OFET	Organic Field Effect Transistor
OLEDs	Organic Light Emitting Diodes
PFO	Poly(9,9-di-n-octyl-2,7-fluorene)
PFs	Polyfluorenes

PhOLEDs	Phosphorescent Organic Light Emitting Diodes
PL	Photo-luminescent
PLEDs	Polymer Light Emitting Diodes
POLEDs	Polymer OLEDs
PPV	Polyphenylene vinylene
PVK	Poly(vinylcarbazole)
RIST	Radiation Induced Sublimation Transfer
SBS	Styrene-Butadiene-Styrene
SM	Small Molecules
SMOLEDs	Small Molecules Organic Light Emitting Diodes
TP	Triazene Polymer
UV	Ultraviolet
Vp	4-vinylpyridine
WOLEDs	White Organic Light Emitting Devices

List of symbols

OD	optical penetration	nm
F_{th}	threshold fluence	mJ/cm^2
$I_{(\lambda)}$	intensity	W/cm^2
$a_{(\lambda)}$	linear attenuation coefficient	nm^{-1}
a_{eff}	effective absorption coefficient	nm^{-1}
A	absorbance	
$d(F)$	etch rate (etch depth per pulse)	nm
T	transmittance	
λ	wavelength	nm

1 Laser Induced Forward Transfer

Introduction

The application of laser forward transfer techniques has steadily grown since the first reports of patterned copper deposition 20 years ago [1]. These general techniques employ a pulsed laser to locally transfer material from a source film onto a substrate in close proximity or in contact with the film. The source is typically a coated laser transparent substrate, referred to as the target, donor, or ribbon. Laser pulses propagate through the transparent ribbon until they are absorbed by the film. Above an incident laser energy threshold, material is ejected from the film and transferred toward the acceptor, receptor, waiting or receiving substrate. These laser forward transfer techniques, belong to a class of processes capable of generating a high-resolution pattern without the need for lithographic processes afterwards. Furthermore there are other examples of laser direct-write techniques include pyrolitic or photolytic decomposition of gas- or liquid-phase precursors, also known as laser CVD or laser-assisted deposition [2].

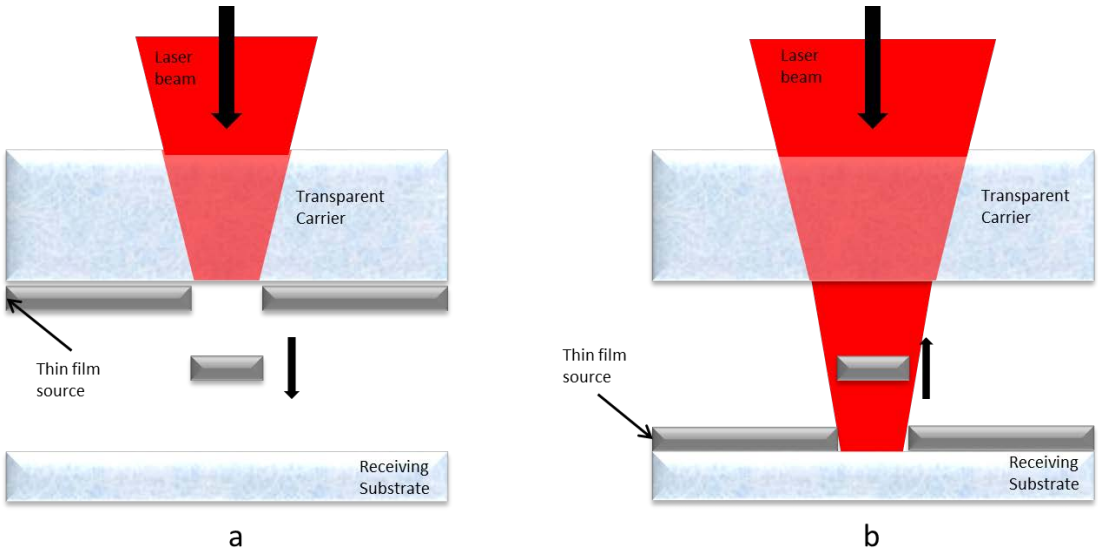

Figure 1-1: Laser transfer techniques: (a) Laser Induced Forward Transfer (LIFT) (b) Laser Induced Backward Transfer (LIBT).

Laser induced material transfer, based on the arrangement of laser, donor thin film and acceptor substrate, can be classified into two groups: laser induced forward transfer (LIFT) and the laser induced backward transfer (LIBT).

LIFT is the mainstream technique and has been reported in more paper and applications than LIBT. In this thesis it is studied the laser induced forward transfer which is also the technique I am using during our experiments.

1.1 LIFT-Theoretical Background

Various mechanisms of interactions at the thin layers with lasers (ablation, transfer and deposit) has been studied the last decades according to different conditions of irradiation: wavelength (from ultraviolet to infrared radiation), pulse duration (nanosecond and sub-nanosecond) and fluence [3]. The laser induced forward transfer (LIFT) technique consists in removing a small piece of a thin layer previously deposited on a transparent substrate and transferring it on another substrate using a pulsed laser (Figure 1-2). This simple, single step, direct printing technique offers the ability to make surface micro-patterning or localized deposition of material.

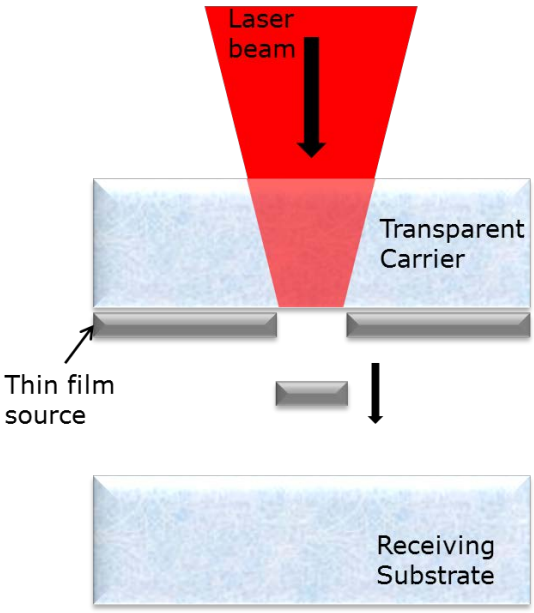

Figure 1-2: Illustration of the Laser Induced Forward Transfer technique

The extreme simplicity of the technique, which can be performed in ambient environment and offers deposited feature sizes of 100's of nm to 100's of μm, relative

to many other micro-fabrication methods led to it being intensively studied the late 1980's until today.

1.1.1 Light-Matter interaction

In that technique what plays critical role is the interaction of the matter with the light from the laser beam. When laser light is incident on a material surface, a part is reflected back in the medium, parts get transmitted and some gets absorbed. The attenuation of incident laser intensity inside the target material can be explained by Lambert-Beer's law, and can be expressed mathematically by **1.2**.

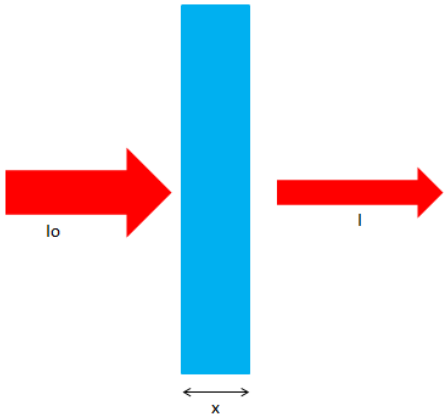

Figure 1-3: The transmittance of a monochromatic laser beam through a layer.

Absorption is observed as decrease of the number photons in the beam while transmitting in the material. In linear optics the incremental decrease of the intensity $I_{(x)}$ is proportional to the intensity itself:

$$dI_{(x)} = -aI_{(x)} \qquad \textbf{1.1}$$

What is assumed is that we are talking about monochromatic radiation, the system not saturated in light, and the absorbers behave independently and are distributed homogenously.

Integration of equation **1.1** leads to the Beer-Lambert law:

$$I_{(\lambda)} = I_{0(\lambda)} e^{-a_{(\lambda)}\chi} \qquad \textbf{1.2}$$

The intensity (W/cm^2) of the light decreases exponentially with depth in the material. I is the amount of light that is transmitted to the detector once it has passed through the layer and I_0 is the original amount of light (Figure 1-3). Linear attenuation coefficient $a_{(\lambda)}$ usually expressed in units of cm^{-1} and is a function of the radiated wavelength.

The transmittance (T) is defined as:

$$\frac{I}{I_0} = e^{-a_{(\lambda)}\chi} = T \qquad \textbf{1.3}$$

We also define the absorbance (A) and the relations between transmittance (T) and absorbance (A) can be expressed by the following equations:

$$A = log_{10}\frac{I_0}{I} = log_{10}\frac{1}{T} \qquad \textbf{1.4}$$

Quite common is the optical density (OD) especially for optical filters which is defined as:

$$OD = -log_{10}T \; or \; T = 10^{-OD} \qquad \textbf{1.5}$$

1.1.2 Laser Ablation

Originally, UV laser ablation of polymers was believed to be a pure photochemical effect, resulting from the direct bond breaking by UV photons. Gradually, investigators obtained evidence that laser heating of materials is significant and a pure thermal nature of laser ablation was considered. Here we use the term ‘photothermal’ for the process resulting from laser heating of material.

The ablation parameters, a_{eff} (effective absorption coefficient) and F_{th} (threshold fluence) were calculated according to the equation **1.6** which is generated from the equation **1.2**:

$$d(F) = \frac{1}{a_{eff}} ln\left(\frac{F}{F_{th}}\right) \qquad \textbf{1.6}$$

Where $d(F)$ is the etch rate (etch depth per pulse).

The effective absorption coefficient, which is a measure for the penetration depth of the laser, depends strongly on the applied laser fluence and the wavelength. We also have to mention that usually a larger crater is made due to a shock wave which was created by the ablation process [4]. That behavior is also reflected to the LIFT process on the transferring material.

1.2 Modified LIFT

Conventional LIFT technique has an inherent limitation. The material to be patterned is required to act as its own propellant for transfer (chemical degradation, bad quality patterns), which in practice limited the materials that could be transferred. Hence, a number of complementary techniques have been developed to expand the range of applications. The most important of those techniques are presented in the next pages.

1.2.1 Dynamic Release Layer - LIFT (DRL-LIFT)

DRL-LIFT eliminates the need to directly irradiate the donor film by inserting a sacrificial layer of a second material, often referred to as a Dynamic Release Layer (DRL), not intended for deposition, between the donor and the carrier.

The potential of a range of materials, including metals, and polymers, to be used for the sacrificial layers has received significant study in recent years. Particular success has been achieved in transferring ‘hard’, e.g. metals and ceramics, and ‘soft’ materials, e.g. biomaterials in solution, polymers and liquids can be transferred without damage.

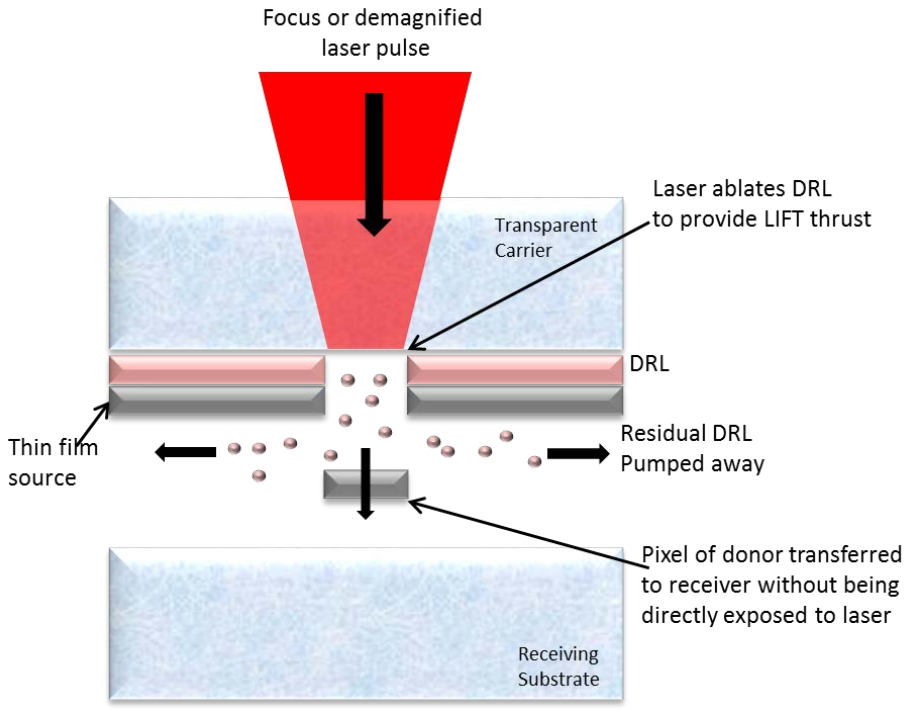

Figure 1-4: Illustration of the Dynamic Release Layer-LIFT technique

Recently the deposition of all the components required for an organic LED, in a single deposition event from a layered donor film, was demonstrated using a designed triazene polymer as the sacrificial layer. However, it is important to mention that DRL and donor material must be compatible. For example, in case of a fully spin coating structured donor the different layers should be chemically compatible. Plus there is always the possibility of residual DRL contamination of the deposited material if the DRL is not completely evaporated in the process. In cases, some debris from the DRL follow the transfer layer contaminating the final deposited layer and causing undesirable results. The most common DRL is the triazene polymer and I will further explain, in paragraph 4.4.

1.2.2 Matrix-Assisted Pulsed Laser Evaporation-Direct Write (MAPLE-DW)

One LIFT variant commonly encountered in the literature involves preparing the donor material in particulate form and mixing it with a sacrificial matrix material. It utilizes an optically transparent substrate coated on one side with a matrix consisting of the material to be transferred mixed with a polymer or organic binder as in LIFT, the laser is focused through the transparent substrate onto the matrix. When a laser pulse strikes the matrix, the binder decomposes and aids the transfer of the

material of interest to an acceptor substrate placed parallel to the matrix surface. This technique is known as Matrix-Assisted Pulsed Laser Evaporation-Direct Write (MAPLE-DW)(Figure 1-5) [5].

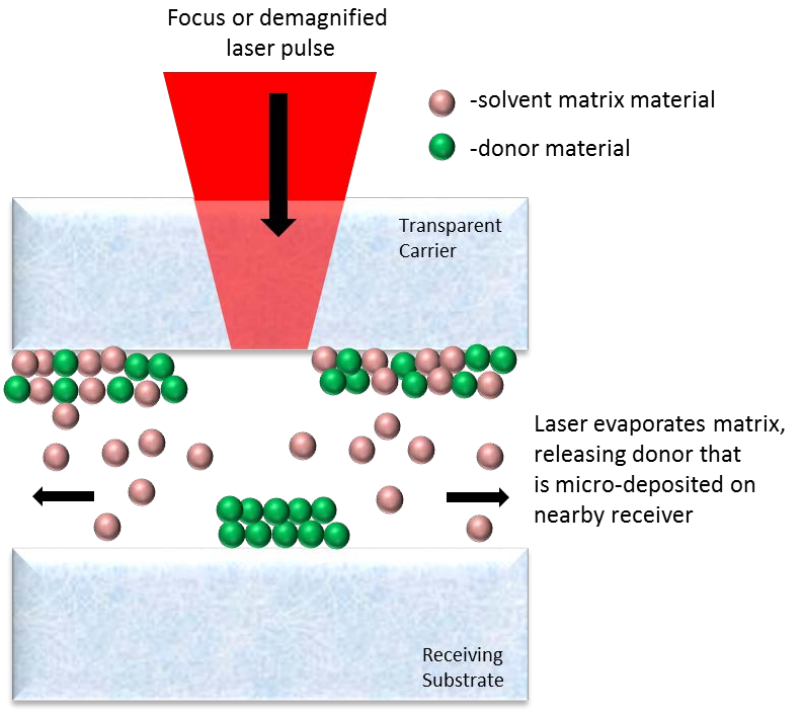

Figure 1-5: Illustration of the Matrix-Assisted Pulsed Laser Evaporation-Direct Write technique (MAPLE-DW)

MAPLE-DW has been demonstrated to be suitable for the micro manufacture of various devices including electronic components and chemical sensors and biomaterials. The main challenge with MAPLE-DW is the necessity to use donor material in a particulate form. This can mean that deposited material properties can be significantly different from those of the bulk. MAPLE-DW is distinguished from other forward transfer techniques in that it is a pyrolytic method for the matrix material only. The matrix material is normally volatile so only a small amount of heating is required for evaporation and significant heating of the donor material can be avoided. By using that technique various metals, organics, and biomaterials have been forward-transferred.

1.2.3 Blister Actuated Laser Induced Forward Transfer (BA-LIFT)

In its conventional form , the bottom of a laser-transparent glass substrate (donor) is coated with an ink and placed 50–500 μm above a receiver substrate. Upon

pulsed-laser irradiation, a confined region of ink near the glass interface is vaporized, and ink volumes as small as picoliters are ejected onto the receiver substrate. Special care must be taken when the material of interest is particularly susceptible to thermal, optical, or mechanical damage . Conversely, when the ink material does not strongly absorb incident laser energy, transmitted radiation inevitably interacts with the receiver substrate and can cause undesired vaporization of the transparent conducting oxide. Usually a polymer film absorbing layer (thickness = 2–8 μm) is incorporated between the glass substrate and ink material on the donor. Upon laser irradiation, a small volume of polymer nearest the polymer/glass interface absorbs the energy, forming an enclosed high pressure vapor that deforms the remaining polymer film into the adjacent ink and induces its transfer [6].

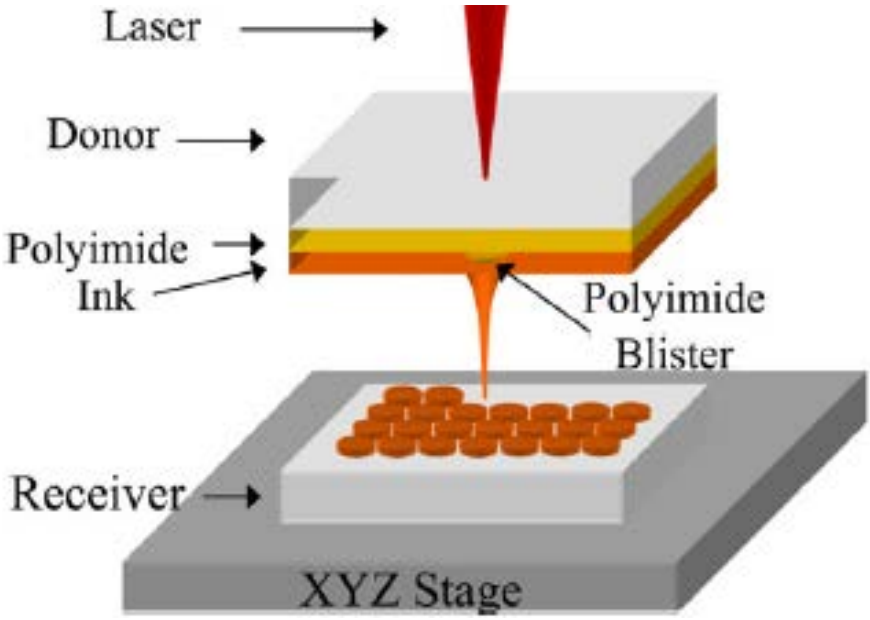

Figure 1-6: Illustration of Blister Actuated Laser-Induced Forward Transfer technique. (BA-LIFT) [6]

This modified LIFT technique is termed blister actuated laser-induced forward transfer (BA-LIFT) because the ink transfer is a consequence of laser-generated blister motion, shown in Figure 1-6. BA-LIFT eliminates possible contamination issues associated with laser-absorbing additives or thinner laser absorbing layers by tuning the process for the absorption of laser energy solely in the polymer film and by selecting a thick enough polymer layer that will not fully decompose. In addition, BA-LIFT has been shown to successfully deposit weak laser-absorbing organic and

biological materials, including systems that are optically and thermally sensitive [6], [7].

1.2.4 Laser Induced Thermal Imaging (LITI)

The Laser-Induced Thermal Imaging (LITI) technique, shown in Figure 1-7, is a forward transfer method designed exclusively for the printing of conducting polymers. As with DRL-LIFT, an extra film, not intended for transfer is included between the carrier and the donor layers to protect the donor. However in the case of LITI, this extra layer is not ablated but instead is designed to absorb the incident laser and heat up sufficiently to decompose surrounding organics into gaseous fragments to provide the LIFT thrust. The layer (typically metallic) is known as a Light-to-Heat Conversion (LTHC) layer in LITI literature.

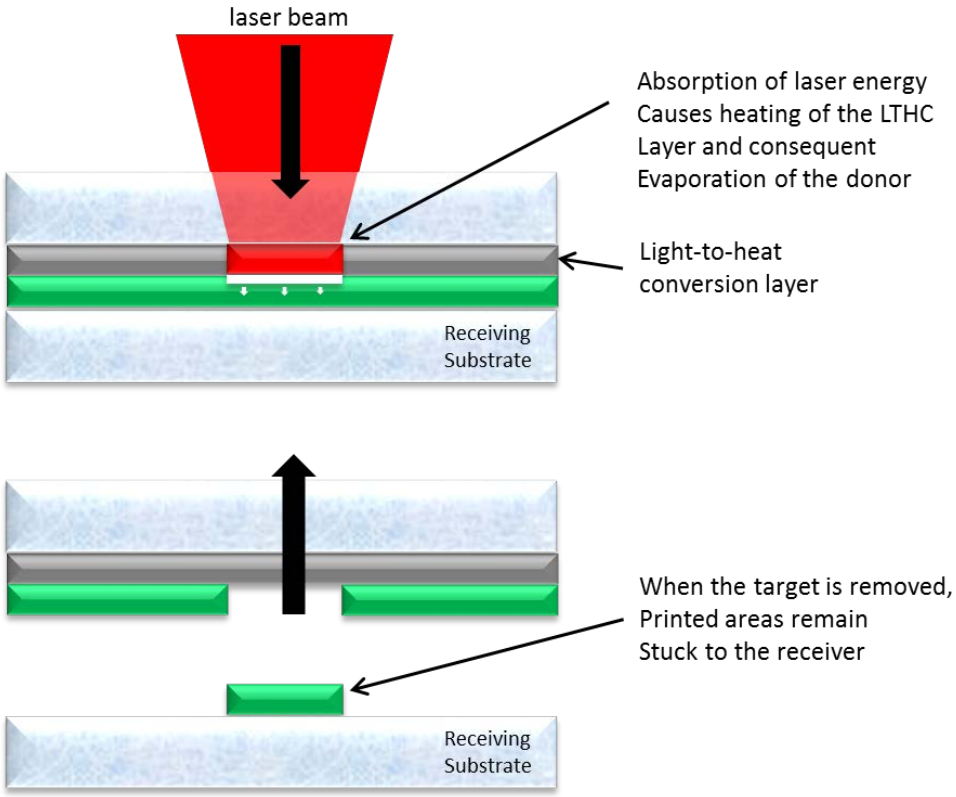

Figure 1-7: Illustration of the Laser- Induced Forward Thermal Imaging technique.(LITI)

By not requiring ablation of the LTHC, the issue of contamination of the deposited material by residual LTHC is eliminated. However, to further protect the donor material, a second polymer layer is sometimes included between the LTHC

layer and the donor; this layer is then akin to a DRL. Typically is a photocured layer that acts to protect the transfer layer from chemical, mechanical, and thermal damage. Depending upon the transfer layer requirements, the interlayer may consist of more than one layer. [8].

Laser Induced Thermal Imaging (LITI) have developed as a patterning technique with a large number of potential applications including the patterning of digital color proofs, plates and film; LCD color filters, black matrix, and spacers; field emission display (FED) anodes, contrast enhancement filters, and nano-emitters; organic field effect transistor (OFET) fabrication; and OLED emitters, color filters, and color conversion filters [8].

1.2.5 Hydrogen Assisted LIFT (HA-LIFT)

Another alternative method of achieving LIFT without direct ablation was proposed by Toet and coworkers [9]. In this technique the donor film is hydrogenated amorphous silicon (a-Si:H). The trust for forward transfer comes from the explosive release of hydrogen when the a-Si:h film is melted at the carrier-donor interface. The Si is then transferred in a mixture of molten droplets and particles, and is deposited as a poly-Si pixel. This technique is sometimes known as Hydrogen-Assisted Laser Induced Forward transfer (HA-LIFT) and is shown in Figure 1-8.

The a-Si: films can also be used as DRLs for the deposition of other donor materials. During the experiments for this thesis this technique was used to transfer Alq_3 small molecules for OLED fabrication. However, as the HA-LIFT process normally only releases the Hydrogen from the a-Si:H film and transfers the Si, contamination of deposited donor with poly-Si is a potential issue. Especially in our case where our goal is the fabrication of OLEDs this could be a serious issue for a final device.

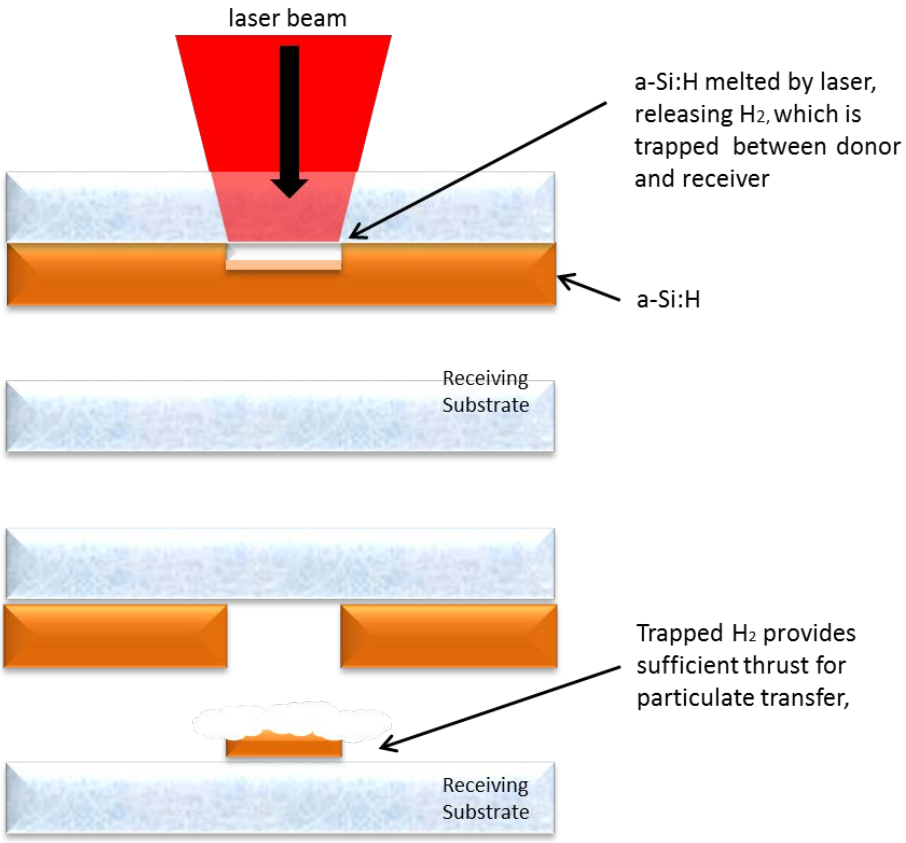

Figure 1-8: Illustration of Hydrogen Assisted-LIFT technique. (HA-LIFT)

1.2.6 Ballistic Laser-Assisted Solid Transfer (BLAST)

Despite the great progress made using LIFT techniques, there is still no way to directly print solid segments from ’hard’ films, i.e. metals, glasses, crystals, ceramics etc., essentially intact after transfer to maintain the as-deposited properties of the donor. Such a capability would be ideal for the LIFT of, for example, single-crystal, oriented, or single domain donor films, or for donors containing pre-made structures. DRL-LIFT technique using triazene polymer DRL has shown promise in this area. One more modified LIFT technique named Ballistic Laser-Assisted Solid Transfer (BLAST) does not require a DRL material and so is potentially applicable for the forward transfer deposition of any ’hard’ donor [10].

It is known that LIFT has a well-defined fluence threshold, dependent on the specifics of the donor film (e.g. thickness, absorption, and thermal properties) and patterning laser (e.g. wavelength and pulse duration), below which no forward transfer occurs. However, it is also known that evaporation of small amounts of

material from a laser-irradiated surface can occur below the fluence threshold for significant bulk modification. Whilst the amount of evaporation is small enough to be considered insignificant for micromachining, in a LIFT environment any evaporated material would be trapped between donor film and carrier. The idea behind BLAST (see Figure 1-9) is to delaminate the donor from the carrier prior to transfer using a pulse with fluence below the threshold fluence.

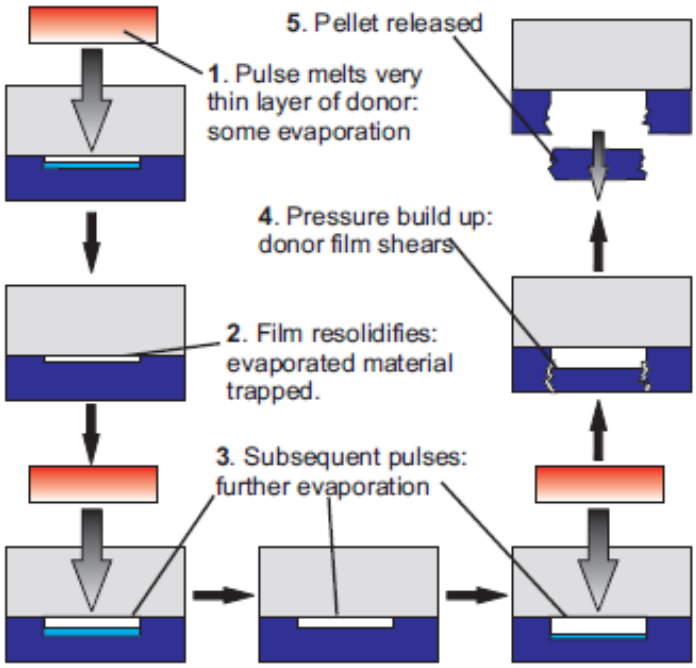

Figure 1-9: Schematics of Ballistic Laser Assisted Solid Transfer. (BLAST) [10]

2 Organic Light Emitting Diodes (OLEDs)

Introduction

Lighting is one of the oldest electronics industries, and has been characterized throughout its history by its adoption and extension of new technologies. Organic electroluminescence (OEL) display has been paid much attention as a next-generation flat panel display, since they have a lot of outstanding feature such as high definition, high emission intensity, less restriction of a viewing angle, high speed of response and small power consumption of monochrome and color displays and they could be applied to low cost production. But, in spite of the high efficiency, low drive voltage, and color tunability of OLED, its device lifetimes remain a major concern, especially in the presence of water and oxygen [11].

The rapid progress in performance and lifetime make organic light-emitting diodes (OLED) suitable candidates for flat panel display applications. Since the early 1990s highly significant improvements were brought out in material synthesis, structure design and device technology. So far OLED displays are already used in mobile phones and more applications are expected in the near coming future with [12].

2.1 Organic Light Emitting Materials

The two main categories which organic electronic materials are divided, based on their chemical structure, are small molecules and polymers. Consequently the two main structural categories of OLEDs are small molecule OLEDs (SMOLEDs) and polymer OLEDs (POLEDs) [13]. A third category of dye-doped devices using phosphorescent dyes, known as PhOLEDs (phosphorescent OLEDs) is based on exciton transfer to small molecule emitters from a matrix which can be either polymeric or small molecule, so both SMOLEDs and POLEDs can be PhOLEDs [14].

2.1.1 Polymers

The first PLEDs were conjugated polymers, poly(phenylvinylene) (PPV), and due to the improved charge transport rates along the conjugated polymeric backbone compared to inter-molecular hopping rates, most subsequent PLED work has focused on conjugated polymers. Polymers based on PPV remain of great interest with a structure known as super Yellow commonly used as a model polymer. Nevertheless, another class of polymers called polyfluorenes (PFs) have taken over as the dominant class of conjugated polymer in organic electronics. One non-conjugated polymer widely used is poly(N-vinylcarbazole) (PVK), widely used as both a hole-injecting material and as a host for dyes. Overall, polymers remain of great interest due to the low cost of manufacture and the potential of solution-processable deposition techniques, but one of the main barriers to commercialization is that they are generally far less pure than small molecules.

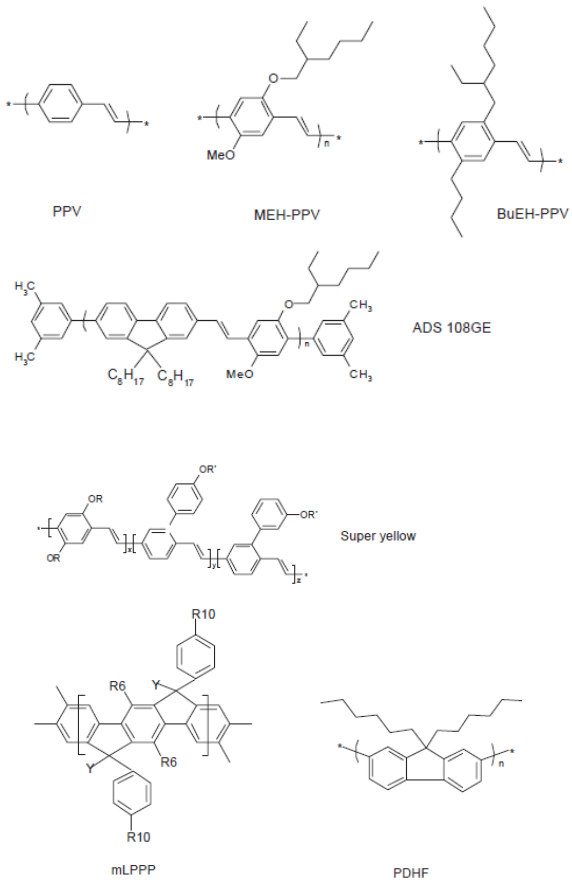

Figure 2-1:Chemical structures of luminescent conjugated polymers commonly used.

PFN is a standard polymeric OLED material, well studied in the literature, but normally used as an electron injecting layer or a host for phosphorescent dopants. PFN is particularly useful for sequential LIFT, because it is soluble in methanol, which does not dissolve most of the other polymeric films soluble in other organic solvents. This means that it can be spin-coated directly on top of TP, enabling the transfer of single PFN films [15].

2.1.2 Small Molecules

The initial modern OLED breakthrough came with Alq_3, a SMOLED material [16]. Although an organo-metallic complex, it is considered an organic compound. SMOLEDs have been researched in great detail, and improvements in efficiency and stability have surpassed PLEDs. In this thesis, Alq_3 and IMEC'S LEL are the small molecules investigated.

Full-scale commercial displays have been made using patterned thermal evaporation through a mask of metal, otherwise known as fine-metal masking (FMM). A disadvantage of this method is the difficulty of simultaneously having small pixels for high resolution and large-scale mother glass for high-volume manufacturing ([17]) as also the cost of the material evaporation, where over 50%-90% ,depending on the source, of the material is wasted. PLEDs have more potential in this regard, being solution processable, but the technology is not as well-developed as evaporation. During this thesis the Alq_3 layers were prepared both by spin coating and vacuum evaporation technique.

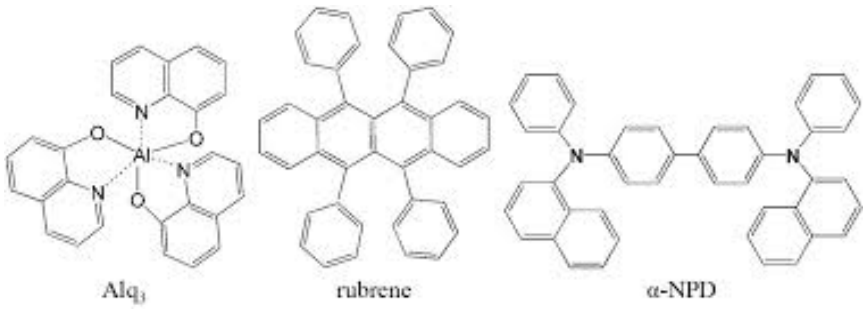

Figure 2-2:Organic small molecules electronic materials.

The most common electron-transport and light-emitting layer in commercial organic light-emitting diodes (OLEDs) is aluminum tris(8-hydroxyquinoline) (Alq_3)

[18].The Alq_3-polymers, both in solution and in the solid-state, show outstanding emission properties. The results demonstrate the potential of the Alq_3-polymer system as emission layer in organic light-emitting diodes. [19]

The deposited Alq_3 films exhibit an efficient and stable photoluminescence (PL) under air condition. Exposure to humid atmosphere for a week does not cause discernible change in the film composition and crystallinity [11].

2.1.3 Phosphorescent Dyes

Doping of a host material with an electroluminescent emitter was an early development in the history of OLEDs, and the idea was based on the well-known principles of Förster and Dexter energy transfer. The efficiency of electroluminescent organic light-emitting devices can be improved by the introduction of a fluorescent dye. Energy transfer from the host to the dye occurs via excitons, but only the singlet spin states induce fluorescent emission; these represent a small fraction (about 25%) of the total excited-state population (the remainder are triplet states). Phosphorescent dyes, however, offer a means of achieving improved light-emission efficiencies, as emission may result from both singlet and triplet states [20].

When the absorption spectrum of the acceptor (dye) overlaps the emission spectrum of the donor (host), efficient energy transfer from the host to the dye can occur via a singlet-allowed, induced dipole coupling between the molecular species. Induced dipole (or Forster) energy transfer to the triplet state is disallowed by spin conservation. However, energy transfer may occur by the parallel combination of Forster transfer to the singlet state, along with electron exchange (Dexter energy transfer).

Fluorescent emitters radiatively recombine only from the singlet state, with non-radiative triplet decomposition predominant due to the inability of a triplet exciton to recombine, which gives long lifetimes, which inevitably lead to a non-radiative energy dissipation process. Nevertheless, there are some materials which exhibit significant phosphorescent emission (radiative triplet recombination) by increased spin-orbit coupling. These materials are normally organometallic complexes of second and third row transition metals such as platinum and iridium.

2.2 Conventional Fabrication Methods for OLEDs

There are huge range of methods which have been employed to deposit the thin-films required to make functioning OLEDs. These can be roughly divided into evaporative processes (‘dry’), and solvent-based processes (‘wet’). Vacuum thermal evaporation (or sublimation of materials) is the most commercially advanced technology for both display applications and solid-state lighting. A basic scheme of this process is shown in Figure 2-3.

Typically, small luminescent molecules are known to be thermally more stable and easier to control thickness and to have higher luminescence efficiency whereas luminescent polymers have advantages of solution-based processing without any intrinsic device-size limitation. Polymers enables the solution processes, such as spin-coating, ink-jet printing and slot die coating. Large-area and fine-pixel displays could be easily developed in comparison with the vapor deposition process.

For sufficiently volatile and thermally stable small molecules, the fine metal mask (FMM) method is the most common means of creating devices with multiple discrete layers. The FMM method utilizes a precision metal shadow mask to physically block evaporative deposition in undesired regions of the OLED substrate. The need for continual cleaning of residual materials from the mask is another drawback for large-scale manufacturing. Remaining FMM patterning issues include difficulty of fabricating high resolution masks for large-area displays, mask lifetime and cleaning, particle contamination, and thermal expansion effects. In addition, maintaining dimensional stability of the mask while scaling to large format displays on large mother glass may prove to be difficult [8].

The solvent based methods make the construction of multilayer devices difficult since each coated layer must be applied from an orthogonal solvent, otherwise the coating process will disrupt previously deposited layers. I also had to deal with that during this thesis during the spin coating of the Alq_3 small molecules from a solution of toluene and Alq_3 above a triazene layer. However, many devices prepared via solvent based printing have no more than two coated layers – a hole injection layer and an emissive layer because materials re-dissolved during the deposition. Additional common layers may be applied during cathode evaporation.

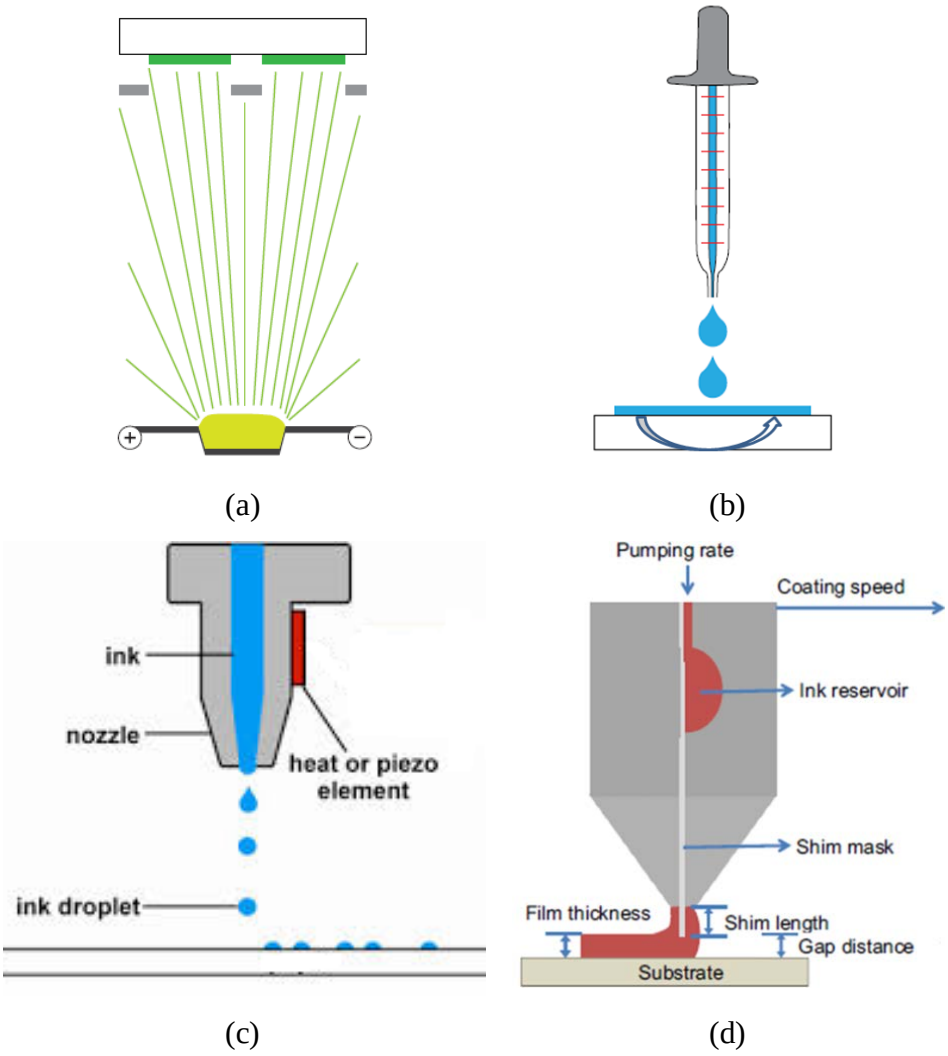

Figure 2-3:Oled deposition technique: (a) Thermal evaporation through a shadow mask,(b) spin coating from a solution, (c) inkjet printing, (d) slot die coating

There is considerable interest today in the development of semiconductor fabrication technologies that do not require photolithographic processing. In order to realize an inexpensive and easy manufacturing process for large-area displays, solution-based processes such as inkjet printing and slot die coating, are highly desirable [21]. As a consequence, many laser-based patterning techniques have been developed which involve sublimation/evaporation of the materials, controlled by a patterned laser beam. Laser-induced forward transfer (LIFT) is a versatile noncontact technique that appears to be an interesting alternative to the conventional patterning techniques, since it avoids the use of expensive photolithographic processes and, thanks to the high focusing power of lasers, presents higher integration scales than spin coating deposition and ink-jet printing [22].That technique also is used in this

thesis for the OLEDs fabrication by transferring locally a thin layer of light emitting material and it is analyzed further in paragraph 2.4.

Conventional thermal printing techniques can also be applied to the patterning of electro-active organic materials. Hot stamp printing, resistive thermal mass transfer printing, and dye diffusion thermal transfer are all examples of conventional thermal printing. They involve the use of a heater, a donor film with a transfer layer, and a receptor. The precoated donor is usually placed in contact with the receptor and heat is applied to the side of the donor opposite the transfer layer. In the case of mass transfer, heating enables the release of the transfer layer from the donor and creates a new interface between the transfer layer and the receptor surface.

Laser thermal printing encompasses a range of technologies that have in common the use of a laser as a heating device. At least five laser thermal transfer methods have been described in the scientific literature. The methods can be broadly characterized as occurring with either release/adhesion or ablative mechanisms. If the mechanism is release/adhesion, then an organic transfer layer remains primarily compact during the process. In an ablative mode, the integrity of an organic transfer layer is often destroyed [8].

2.3 Basic Structures of OLEDs

An organic light-emitting diode (OLED) is a special type of light-emitting diode (LED). OLEDs are heterojunction devices in which organic active layers are incorporated into devices as thin solid films. An OLED is composed of at least one undoped organic layer that is put between two electrodes. Electrons and holes are injected from either side of the electrode, respectively. After applying a voltage, both carriers will drift towards the other side in the applied electrical field. When both electrons and holes meet at the bulk or the interface, they then recombine to form excitons, which will decay to produce light emission.

The first OLED in its basic structure was built in 1987 by Tang and Van Slyke [16]. They produced a thin film device based on aluminium tris(8-hydroxyquinolinate) (Alq_3) as an electron injection/luminescent layer. This structure was created by thermally subliming/evaporating the various layers onto an indium tin

oxide (ITO) coated glass substrate. ITO acts as a transparent anode; on top of this the organic layers were deposited and sandwiched with an Al cathode. This type of design is often referred to as a sandwich structure. [23]

In Figure 2-4 it is shown the schematic of the first thin film OLED based on Alq_3. A small-molecular OLED consists of one organic layer or multiple organic layers between two electrodes. The one organic layer device is called a single layer device (Figure 2-5). Thus, the organic material must serve all the three main functions: electron transport, hole transport and emission. In this case, the injection rates of both carriers should be almost equal for high efficiency. Otherwise, the surplus electrons or holes will not recombine, which results in low operation efficiency.

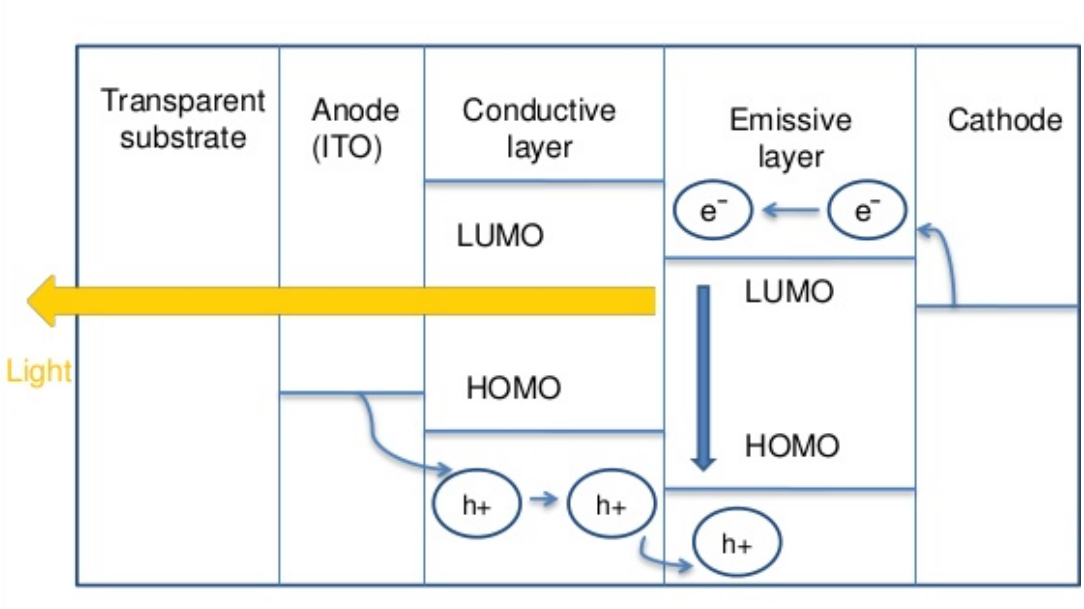

Figure 2-4: Basic schematic of the energy levels of a OLED

However this limitation can be avoided by employing multiple organic layers in the OLED structure. The basic device structure with three layers is shown inFigure 2-5. This structure employs an electron transport layer (ETL), a hole transport layer (HTL) and an emissive layer. The emitter material can be either a layer between ETL and HTL or a dopant in one of these layers, close to the recombination zone. The dopant with a lower exciton energy than its matrix will yield a high luminescent efficiency.

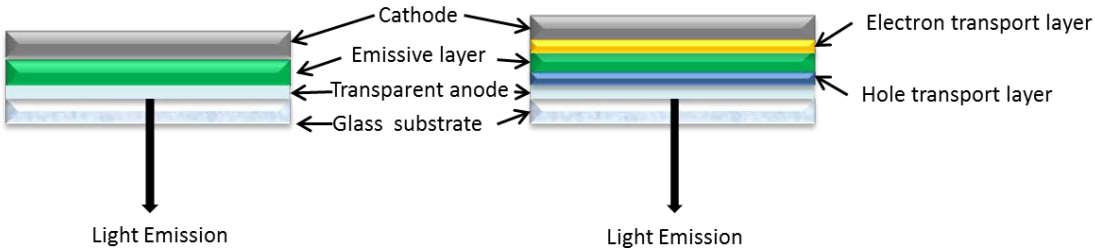

Figure 2-5: Configuration of OLED

The performance of the diode also strongly depends on the materials of electrodes that they employ. Generally, the work function of the cathode should be sufficiently low and the work function of the anode should be sufficiently high in order to have good injection of both carriers, respectively. Furthermore, for the application of the OLEDs, one electrode should be transparent to allow the emission of light from the device.

So far, the most commonly used transparent anode is indium-tin-oxide (ITO), which has a relatively high work function of 4,5-5,1 eV. Since the work function of the cathode should be low enough, the generally used materials for anodes are Al, Ma, Ca, etc. However, these metals will oxidize or corrode in the air. Thus, alloyed electrodes were made for higher stability with relatively low work functions. For example, Mg and Ag alloys are more stable than Mg. Also the fabrication of free-ITO WOLEDs based on multi-cavity architecture has mentioned as a potential method for OLEDs applications [24].

The first reported polymer used in PLEDs was poly(para-phenylene vinylene) (PPV). The chemical structure is shown in Figure 2-1. The device structure of this polymer LED is shown in Figure 2-5, which is almost the same as that of small molecular OLED. PPV has an energy gap of about 2.7eV which emits green light in the region of the spectrum. In forward bias, the injected electrons and holes recombine in the polymer layer and emit light. The polymer layer is about 100nm, to allow efficient charge injection and carriers transport through the layer. The device structure can be also bilayer with an additional conducting polymer layer between the ITO and emissive layer. The conducting polymer layer will improve the hole injection and electron blocking.

2.3.1 White OLEDs (WOLEDS)

In order to realize full color display, two approaches were used. The first is patterning red, green and blue emitters using a selective deposition. Another approach is based on a white-emitting diode, from which the three primary colors could be obtained by micro-patterned color filters.

White organic light-emitting devices (WOLEDs) has been attracting considerable attention recently due to their potential applications as full color displays, backlights for liquid crystal displays, and even paper-thin next-generation light sources. To achieve white emission in organic light emitting devices (OLEDs), an additive mixture of the three primary colors or two complementary colors is required. Various methods have been demonstrated to produce white light emission from organic OLEDs, including mixing of the three primary colors (red, green and blue, RGB) from respective layers in a multilayer structure, doping a single host emissive layer with RGB-emitting materials and mixing a blue host with an appropriate amount of Yellow or orange dopant in a single emissive. [25]

The simplest WOLED architectures that incorporate polymers have several emissive chromophores, which are polymer sand/or small-molecules, blended, into a solution that is coated onto the transparent anode by techniques such as spin-casting, or inkjet printing. After the organic materials are printed or coated onto substrate, metal cathodes are vacuum deposited through a shadow mask. [26]

2.3.1.1 Tandem Devices

In order to increase efficiency of white OLED, some authors presented white OLED with tandem structure. Basically, tandem structure needs higher driving voltage which results in the higher power consumption. Therefore, it seems that tandem structure is not effective for higher efficiency and lower power consumption.

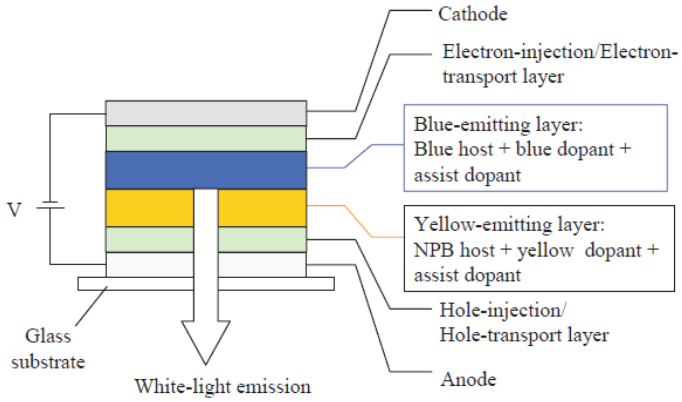

Figure 2-6: Schematic of the two-layer white OLED

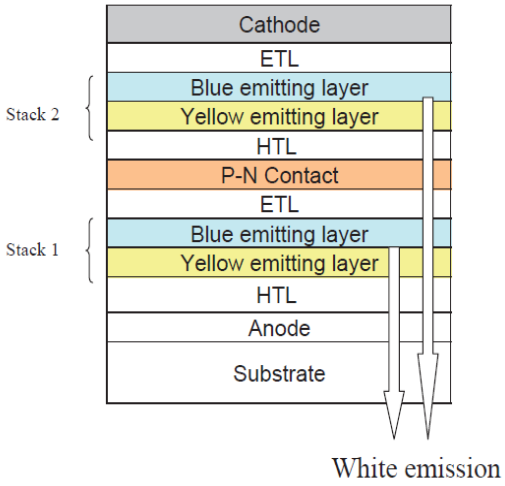

Figure 2-7: Schematic of the 2-stack tandem white OLED

However, in case of practical AMOLED display, it has frailly advantage compared with single layer structure. It is because that double stacked tandem structure, for example, doesn't need double driving voltage because it doesn't need double hole transport layer, and electron transport layer compared with single structure [27].

The white OLED structure based on two-light-emitting layers is shown in Figure 2-6. It is similar to that used for producing monochrome colors, such as blue, green or red, except that it contains two light-emitting layers, Yellow and blue. Both the blue-emitting and Yellow-emitting layers incorporate host and dopant materials.

2.3.1.2 RGB-Side by Side Technology

The goal is the realization of full color displays. White OLEDs are being used for manufacturing micro-displays by micro-patterning above that layer, color filters for the three basic colors side by side. Also the realization of a full color display without a WOLED as a backlight layer is possible. White OLED and color filter method has a disadvantage for emissive efficiency because the color filters cause the efficiency loss of emission of white OLED.

The first patterning technique for defining the R-, G-, and B-emitting pixels is by precision shadow masking as shown in Figure 2-8. It uses a thin metal shadow mask (50μm thick) that is positioned in close contact with the substrate in order to

define depositions within the appropriate regions of the substrate. The mask is aligned appropriately with the electrodes (typically ITO), and red, green and blue emitting layers are deposited. Three separate alignments/depositions are required. This method produces the highest efficiency and good color gamut, but it has significant disadvantages. Some of those disadvantages are process time, thermal expansion of the mask causing misalignment, defect generation caused by necessary contact with the substrate and high cost. It is also difficult to manufacture masks with small apertures and scaling up to large substrate sizes. This technique also becomes impossible for fabricating micro displays where the subpixels are only a few micrometers in size. Another major disadvantage is the differential aging of the R, G, and B pixels. Other techniques to pattern individual R, G, and B emitting are being investigated, such as laser transfer and inkjet printing, but so far these techniques have not been proven to be manufacturable and scaleable.

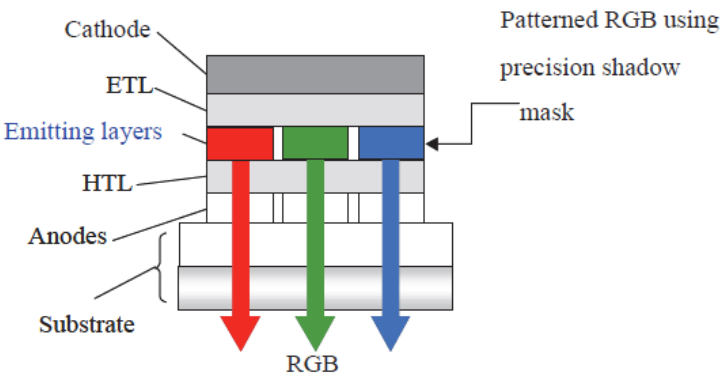

Figure 2-8:Methods of color patterning by R,G,B pixelation

The second method is that of depositing an unpatterned blue-emitting layer and using a color filter array or a color change medium (Figure 2-9). It does not require a precision shadow mask, since blue emission is absorbed through the color conversion layer or color filters and is converted to either green or red light. As mentioned before, blue emitters typically have poor stability and efficiency, which may inhibit the usefulness of this technique, and consequently this approach is significantly disadvantaged for applications requiring high stability.

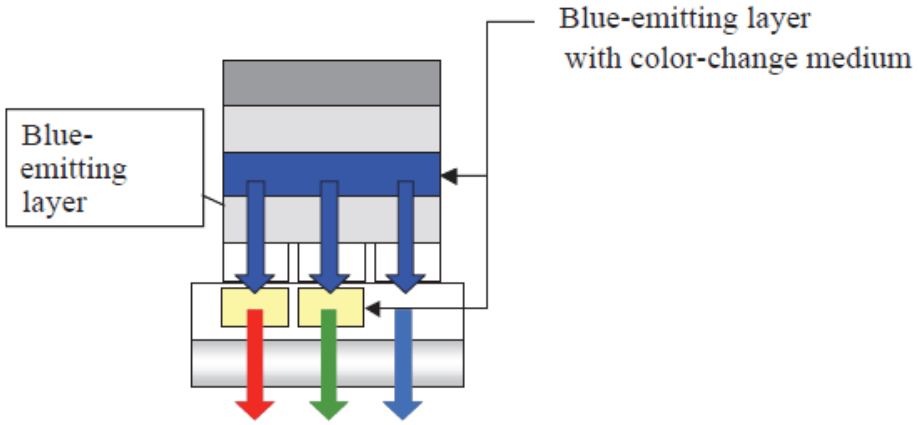

Figure 2-9:Method of color patterning using blue-emitting layer with color change medium

The third method is to provide the R, G and B emissions through the implementation of a white emitter combined with color filters (Figure 2-10). In the case of the white OLED with color filter arrays, it is expected that the manufacturing yield will be higher, and scalability to larger substrate sizes will be possible. Although the color filtering drastically reduces the transmitted light intensity, the high efficiency of the white OLED has led to performance that can be comparable to displays of the first-generation pixelated R, G and B emitters.

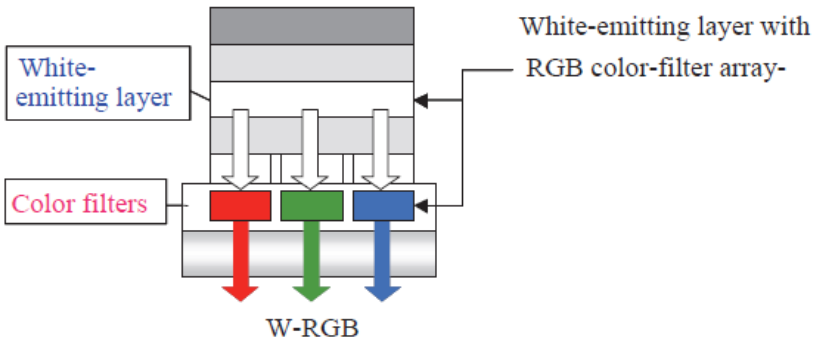

Figure 2-10:Method of color patterning using a white-emitting layer and color filters

2.4 Fabricated OLEDs by Laser transfer Techniques

Laser induced forward transfer of OLEDs is a relatively new topic. The first reference in literature about laser assisted printing of electronic thin films happens in

the 90s [5].It was based on matrix-assisted pulsed laser evaporation (MAPLE). Since then, many various attempts have been made to transfer organic light emitting materials, but only a few have resulted in successful device fabrication. Here are presented some of those attempts.

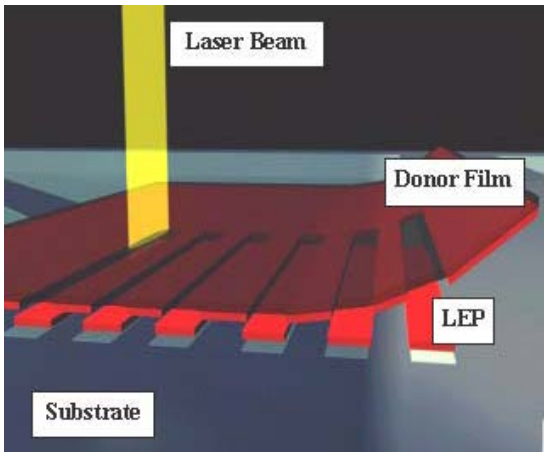

Figure 2-11: Schematic of the LITI Process [28]

LITI has the unique ability to pattern multiple discrete organic layers in a single step. This ability is useful, for example, in the patterning of phosphorescent OLED stacks since their optimal construction frequently requires exciton confinement and, hence, multiple charge blocking and transport layers. Laser Induced Thermal Imaging (LITI) have used for the patterning of active matrix OLED (AMOLED) materials for large format, high resolution displays. The construction of the donor film greatly influences the mode and quality of transfer. The donor sheet is typically constructed of three coated layers: the Light to Heat Conversion Layer (LTHC), the interlayer, and the transfer layer. Samsung SDI has recently used the LITI technique to prepare a series of full color AMOLED demonstration devices. [8], [28], [29]

Also the DRL-LIFT technique was used to fabricate OLEDs. The critical step was the addition of the layer of the Triazene polymer between the transparent substrate and the transfer layer. The transfer layer was a bilayer consisting of the electroluminescent polymer poly[2-methoxy-5-(2-ethylhexyloxy)-1,4-phenylenevinylene] covered with an aluminum electrode onto a receiver substrate. The soft transfer results in laterally well resolved pixels (~500μm), whose fluorescence as well as electroluminescence spectra remain unaltered. [30] Also, Alq_3 “LIFTed” pixels had been fabricated by the DRL-LIFT technique where pixels had

transferred from a stacked layer (donor) to an also stacked layer on the receiver.(Figure 2-12) [31]

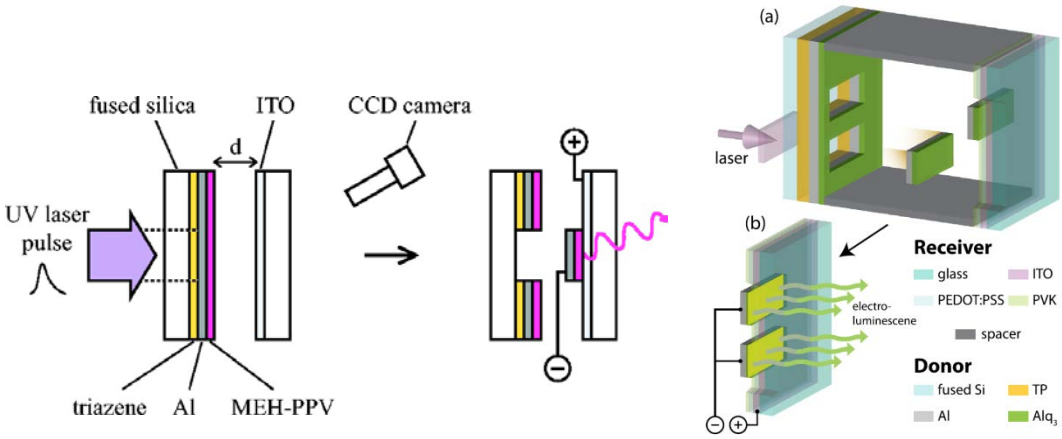

(a) (b)

Figure 2-12: Scheme of the transfer principle for OLED fabrication via DRL-LIFT process

BA-LIFT technique also has been used to transfer electroluminescent inks on a receptor with ITO on the top, from a donor of glass/polyimide/Ink. After the deposition of the ink, the aluminum electrode were deposited by vapor deposition to complete the fabrication process. [6], [32]

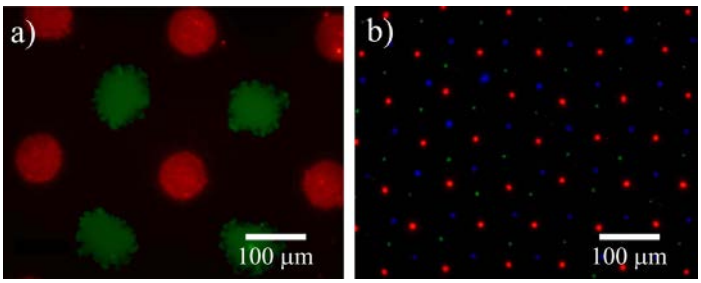

Figure 2-13: "LIFTed" of PEL by BA-LIFT. [6]

Eastman Kodak Company and 3M Corporation developed laser thermal printing. This was meant for high-resolution digital patterning for potential applications, such as patterning OLED emitters, organic thin-film transistors and color

filters. This process is similar to thermal printing where a donor sheet (blanket coated with appropriate emitting material) is placed adjacent to the substrate, and a laser is used to pattern-wise transfer the emitting material from the donor to the substrate.

A schematic representation of the radiation- induced sublimation transfer (RIST) process developed by Boroson et al. (Figure 2-14) [17]. The donor includes a polyimide support (75 mm), a silicon anti-reflection layer (50 nm), a chromium absorption layer (40 nm) and an organic transfer layer (20–60 nm). The total reflectivity of the donor at the laser wavelength is <7% (including the air/polymer interface), resulting in highly efficient conversion of the laser energy to heat to sublime the organic transfer layer. In the RIST process, the organic material is transferred to the substrate by vacuum sublimation. Therefore, the donor and active portion of the substrate are spaced apart within the vacuum system to maintain a transfer gap of 1–10 μm. Radiation is applied only to the areas where material transfer is desired. The organic transfer layer (emissive layer in this example) sublimes and re-condenses on the substrate. Singlet and triplet dopants and hosts, as well as mixtures of multiple dopants and hosts, can be coated onto the donor for transfer by RIST.

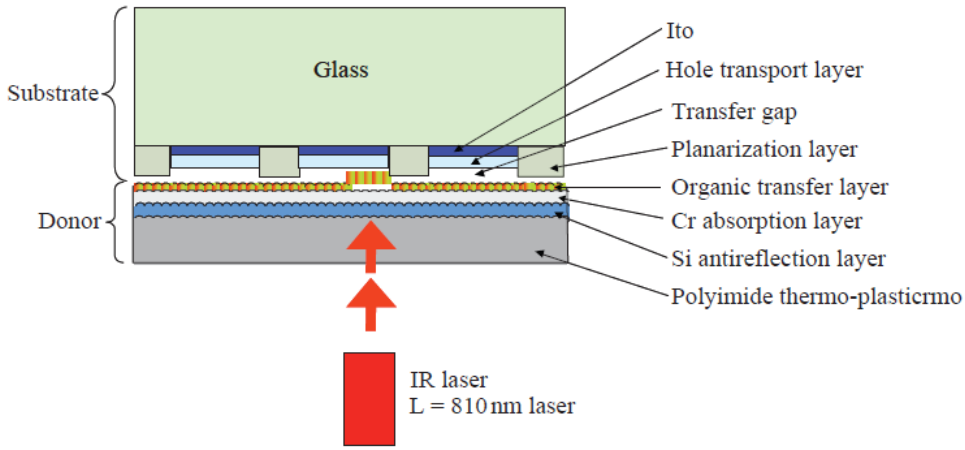

Figure 2-14:Schematic representation of the radiation-induced sublimation transfer (RIST) [17]

This technique eliminates the need to precision shadow mask. However, the operational luminance stability of these devices is lower than those fabricated using conventional thermal evaporation technique. Also some of the luminance materials were found to be degrading during the transfer process, thus limiting the usefulness of this non-contact process.

In LITI process, direct contacts between donor films and the emitting area will degrade the device and transfer quality. Though, RIST is sublimation process without the direct contacts, OLED material will be damaged by gases (H_20, O_2) released from a film donor during laser-heating. In addition they require high precision technique to set flexible film on a large-scale glass substrate uniformly without adhesive agents.

Another technique for OLED displays have been developed from Matsuo et.al. [33]. Laser Induced Pattern-wise Sublimation (LIPS) technology had been developed in order to realize high volume manufacturing and high yield with device performance comparable to evaporated small molecules displays. In Figure 2-15 a schematic representation of the typical LIPS process is shown .

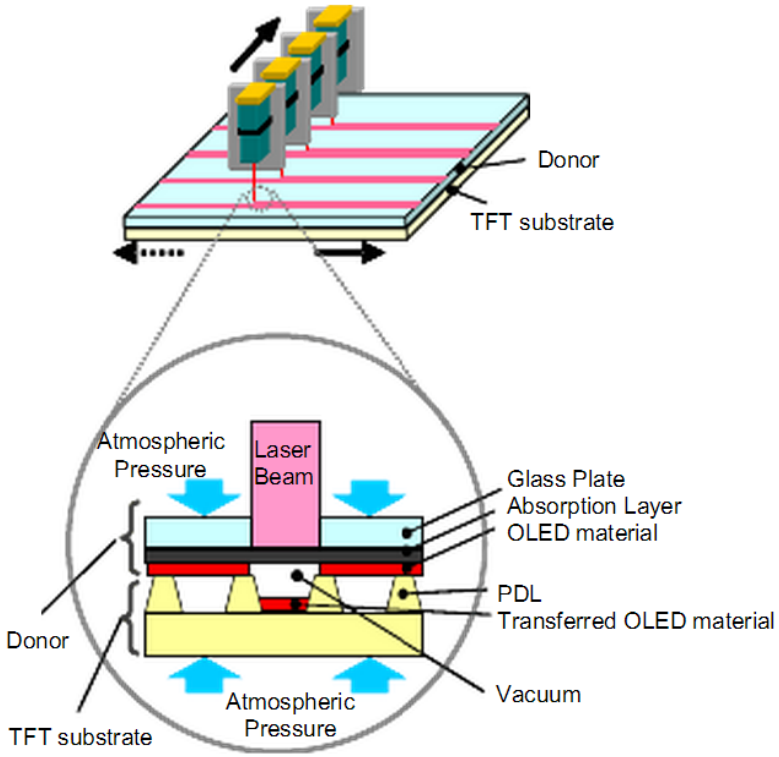

Figure 2-15: Schematic of LIPS process

The donor consisted of a glass plate with a molybdenum layer and an emission layer (EML). The EML is typically deposited by vacuum deposition. The TFT substrate has pixel defined layer (PDL) and organic common layers such as hole injection layer (HIL) and hole transport layer (HTL), which are also vacuum-deposited. Those donor and TFT substrate are put together in a vacuum chamber and

fixed with a clamping frame which has O-rings to prevent organic layers from contamination by ambient gases.

Once donor, TFT substrate and clamping frame are fixed in the vacuum, those are taken out of the chamber and set on the stage of the laser transfer system. As a result, the donor and the TFT substrate contact intimately by the atmospheric pressure while the gap in the pixels is kept by the height of PDL and the rigid donor. Therefore, EML and HTL in the pixels do not contact directly. The vacuum condition in the gap is kept by the clamping frame.

After laser head alignment with the substrate is completed, laser beam starts to scan and heats the designated position of the glass donor and EML material is transferred to the substrate by vacuum sublimation. The patterning process is done for each emission layer. Common layers such as an electron transport layer (ETL) and top electrode are formed on the patterned substrate after removing the donor in inert gas.

3 Experimental

3.1 Sample Preparation

3.1.1 Substrates

The donor and the acceptor substrates were both glass plates (eagle glass). The substrates were subsequently washed with acetone, isopropanol and methanol, and blow dried with nitrogen, before I clean them in the UV-ozone reactor for 10min. When our purpose was to do PL measurements, high quality quartz plates were used instead of common glass to avoid the UV absorption both donor and acceptor.

3.1.2 Film-Forming

The triazene thin layer deposited by the spin coating method from a solution of 1%, 2% or 4% in chlorobenzene and cyclohexanone (1:1, w/w) [Nagel et al (2007)]. After the spin coating of the TP polymer the samples were baked for 1 hour at 70^0C. Various thicknesses of TP ranging from 40 nm to 300 nm was obtained by changing the spin speed from 600 rpm to 3000 rpm.(Table 1 and Table 2)

For transfer experiments the next layer was Alq_3 small molecules, evaporated at low pressure($5\ 10^{-7}$ bar) with a deposition rate at 2 A^0/sec, and the thickness of that layer was 100nm. Also, samples with the same DRL but with a thin vacuum evaporated layer of IMEC'S light emitting layer (LEL) above of 20nm thickness were also used to do LIFT experiments. Furthermore, some experiments have been done with a spin coated layer of Alq_3 upon the triazene layer. The copper layers were made by the vacuum evaporation technique as also the SiN/H and a:Si/H layers in presence of Hydrogen. Furthermore, the thin layers of Super Yellow (SY) were made by the spin coating technique from a solution of Super Yellow dissolved in toluene.

The film quality was checked using a profilometer and an optical microscope. The donors were kept into a glove box when our desire was to get photoluminence measurements. In the Chapter 4, more details are presented about the preparation as also about the experiments each self.

3.2 Laser Set-Ups

3.2.1 Nd:YAG

For the experiments of that thesis the basic tool was a class-4 diode-pumped solid state picosecond-laser. The system has designed as a general-purpose laser micromachining tool for thin-film patterning, cutting, drilling and marking. The system is built on a granite gantry platform supported by special base with vibration isolation legs. The laser(s) and beam delivery optics are enclosed in two optics boxes mounted on the side and top of the gantry. Motion control is achieved using a 3-axis movements structure.

In Figure 3-1 are shown the basic parts of the laser tool which allow us to control it by the CIMITA software. We can control the power of the beam using an external and an internal attenuator.

The possible wavelength which can be achieved with that laser system are 1064nm, 532nm and 355nm. And the power of the beam measured at the laser head for each wavelength is 16W, 8W and 4W. With the XY stage which is able to move to both directions with a resolution of 0,25 μm we can control the movement of the sample based on the XY-stage. In that way the substrate can be move on a computer-controlled translation stage underneath the laser during the experiments. A motion is possible at z axis where is applied the laser camera as also the alignment camera which has the ability to move with a resolution of 0,5 μm. In that way we can control the focus position of each wavelength regarding always the installed lens. Furthermore, by changing the Z-axis position we can control the laser spot diameter and consequently the fluence as also the profile of the Gaussian beam. The theoretical spot diameter for 1064nm in focus is 110μm, for 532nm is 55 μm or 15μm regarding which focus length lens is used, and for 355nm is 35μm.

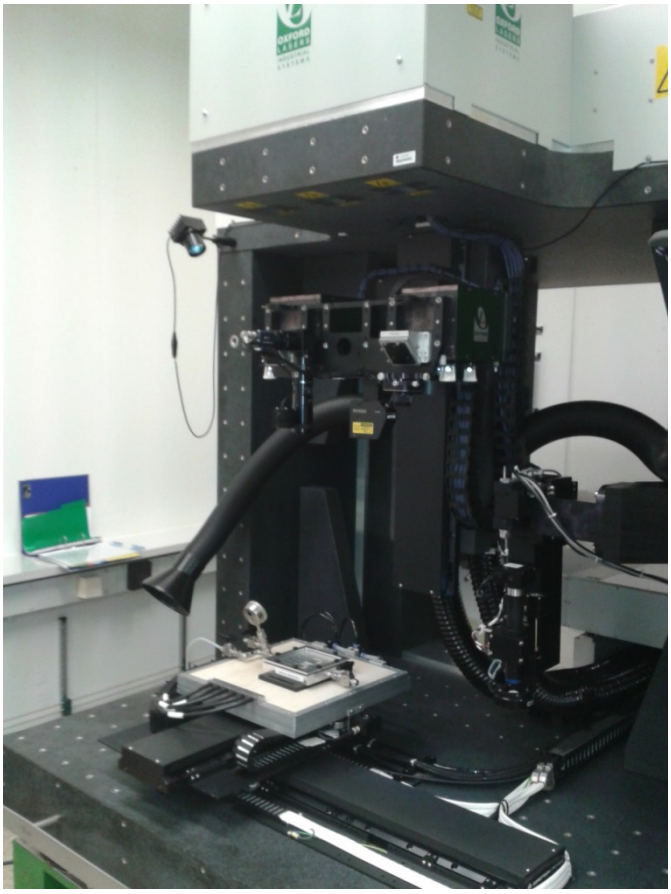

Figure 3-1: Geometric structure of the picosecond-laser system

Finally, there is also a power meter applied on the side of the XY-stage which make possible to measure the power of the laser beam after each experiment in real time.

3.2.2 Excimer

An excimer is a powerful laser which operates in the UV range and generates nanoseconds pulses. The laser system, which were used for my thesis is located in TU/e-Eindhoven and is a class-1 laser system. The amplification medium is Krypton-Fluoride. Its pulse is at 50 nanosecond and it emits at 248nm.

The operation of the system is similar to the Nd:YAG laser system. One important difference between those two laser systems is that the Excimer is equipped with a flat-top beam profile when the Nd:YAG' s laser beam has a finally Gaussian beam profile.

3.3 Environmental Chamber

In order to perform LIFT experiments in a nitrogen environment and vacuum conditions I used a special environmental chamber shown in Figure 3-2. The chamber's dimensions are 147x147x28mm

The window of the chamber is a quartz glass 127x127x6,1mm which perfectly fit it in the box. After the fitting of the glass to the box the exposed area of the glass dimensions are 118x118mm. The chamber has two holes which can be used as entrance and exit for air or nitrogen.

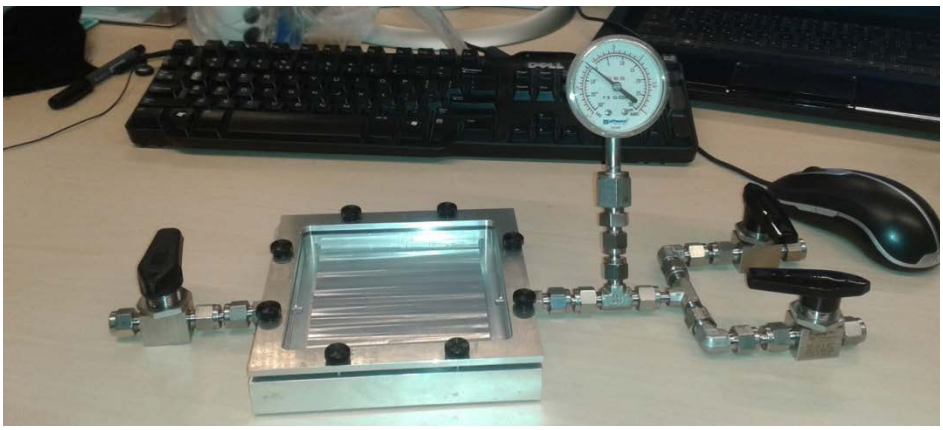

Figure 3-2: Environmental Chamber

In addition it is equipped with a pressure valve and tree switches. Also, I add a safety valve on the box which automatically opens for pressures higher than 1,6bar. Furthermore an o-rig rubber under the quartz window and a flat rubber above certifying the absence of any leakage in the chamber. The chamber after testing is being found to work perfectly also in house vacuum (0,2 bar). Furthermore, the pressure meter which is applied on the box shows the environmental pressure in the chamber and indicate for any leakages.

4 Background Experiments

4.1 Triazene ablation

To prevent heat and light induced damages, an advanced LIFT process has developed using an intermediate sacrificial layer of a UV-absorbing dialkyltriazene polymer. Thin films of this photopolymer are excellent DRLs because they decompose integrally into volatile fragments at very low ablation thresholds. The DRL layer import a mechanical propulsion of the transferred layer without permit to the light energy to destroy the material. The polymers containing the photochemically most active group (triazene) exhibit the lowest threshold of ablation and the highest etch rates, followed by the designed polyesters and then polyimide [4].

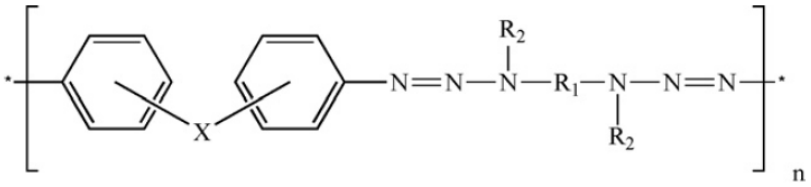

Figure 4-1: Chemical structure of Triazene-Polymer.

Furthermore many studies have been done if the ablation mechanism is dedicated by photothermal or photochemical processes. The answer in that question so far is that the triazene is ablated after irradiation with a UV light by a combination of those mechanisms [34]. However, polymers that show a photochemical ablation behavior at the irradiation wavelength are preferable for structuring, as damage to the surrounding material by thermal processes is minimized and there is less surface modification in the irradiated area. Also a conversion of the polymer into gaseous product is advantageous, as the amount of ablation products that are redeposited on the structured surface is reduced, and additional cleaning procedures are not necessary. Irradiation with the appropriate wavelength can then lead to photochemical decomposition or bond breaking and energy release in the polymer.

From the Beer-Lambert law **1.2** and the equation **1.3** and **1.4**, the Graph 4-1 and Graph 4-2 are produced where you can see the absorbance, the transmittance and the optical penetration for different wavelengths.

The percentage for the absorption of a 100nm thick layer of triazene at 355nm wavelength it has been found at 64%. If there is no scattering of the light we can assume that the transmittance is T=36%.So we can calculate the absorption coefficient which after what we assumed, it should be equal to the extinction coefficient and the optical penetration:

$$a_{(355nm)} = -\frac{log(T)}{x} = -\frac{log(0.36)}{100} nm^{-1} = 0.004470388 nm^{-1} \qquad \textbf{4.1}$$

$$\mathrm{OP} = \frac{1}{\mathrm{a}_{(355\mathrm{nm})}} = 223.69\mathrm{nm} \qquad \textbf{4.2}$$

And the optical depth for 100nm thick layer of triazene should be:

$$\mathrm{OD} = \int_0^{\mathrm{x}} \mathrm{a}_{(355\mathrm{nm})} \mathrm{dx} = 0.447 \qquad \textbf{4.3}$$

After studying those graphs above we can see that the optical penetration for triazene for the wavelength that we use (355nm) is near to 200nm. So we have to choose the most preferable thickness of triazene-DRL when the biggest percentage of the light intensity absorbed by the DRL protecting the transferred layer and the same time the transferring isn't so violent protecting the layer from creating debris and avoiding the spreading of the transferred layer during the transferring.

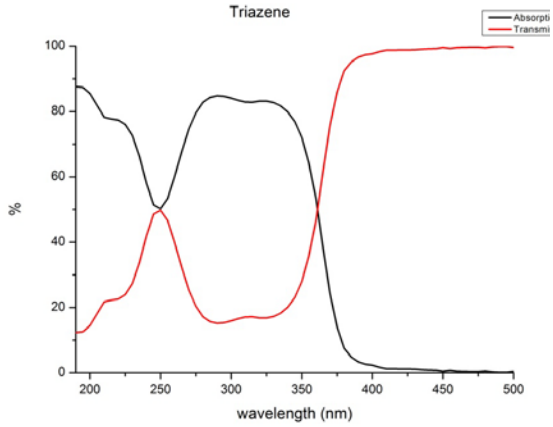

Graph 4-1: Absorbance and transmittance (%) spectrum of a thin layer (100nm) of triazene

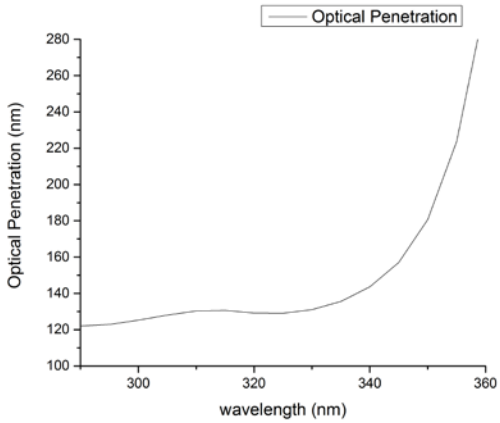

Graph 4-2: Optical penetration of triazene for different wavelengths

However, a linear optical absorption coefficient obtained from UV-Vis spectroscopy is not really applicable to a dynamic ablation process with temporal and spatial changes in the material properties throughout the pulse duration, particularly considering the movement of the solid-gas interface. For this reason an "effective" absorption coefficient (α_{eff}) is considered (**1.6**), an empirical property dependent on the many material properties that may alter during a laser pulse; these include transient and permanent material modification to the film, the different absorption characteristics of the gaseous ablation products, and the movement of the solid-gas interface [35]. This empirical value, derived from frontside ablation data, or it can be calculated from fundamental material properties, as for metals: the linear optical absorption coefficient, of the DRL, the DRL thermal diffusivity, and also the laser pulse length [36].

Furthermore we have to mention that in previous studies it has been shown that, intriguingly, only about 2 % of the input energy is transferred into the flyer, with ~ 30 % going into the shockwave and the rest lost in other processes (these values vary with fluence). Possible loss mechanisms include mechanical strain upon ejection, gaseous leakage lowering the pressure build-up, and thermal loss into the substrate as well as the rest of the TP film [37].

4.2 Spin coating of Triazene

The most used settings for the triazene layer are the settings which are presented in the Table 1 and Table 2. Triazene from two different suppliers were used during this study. For both of them the produced layers had been characterized with the DekTak as far as it concerned its thicknesses. Type A triazene was bought from SYNCOM and type B was supplied from TNO.

Table 1: Thickness of triazene layer for different spin coating settings. (A)

Concentration w/w	Spin coating speed(rpm)	Thickness(±10nm)
2%	2000	80
	1000	90
	800	100
	600	110
4%	1000	230
	800	245
	600	295

Table 2: Thickness of triazene layer for different spin coating settings (B)

Concentration w/w	Spin coating speed(rpm)	Thickness(nm)	Roughness (nm)
0,5%	600	36,6	1
	1000	37,3	1
	1500	25,8	1
	2000	25,1	2
	3000	18,0	1
1%	600	62,5	1
	1500	41,5	3
	2000	35,2	1
	3000	29,2	1
2%	600	224,4	6
	1000	175,7	2
	1500	142,1	1
4%	600	508,4	7
	1000	348,7	1
	1500	285,2	3

At Table 2 are presented the results from the spin coated depositions for various settings of the triazene (B). All the steps for the preparation of the triazene layers were the same. I only change some setting at the spin coater and also I use three different solutions to achieve different thicknesses of layers. Table 1 shows the different settings, as also and the quality of the layer of triazene after spin coating. The roughness in all the samples was less than 8nm.

I have to notice that each time we prepare a new solution of triazene there were caused some variations on the produced layer. Those variations are concerned mostly of the thickness of the triazene layer. But also, some possible impurities into the solvent have forced me to filter the solution before I use it. Those variations were reflected also to our experiments by effecting the threshold fluence for LIFT or the formation of the “LIFTed” pixels.

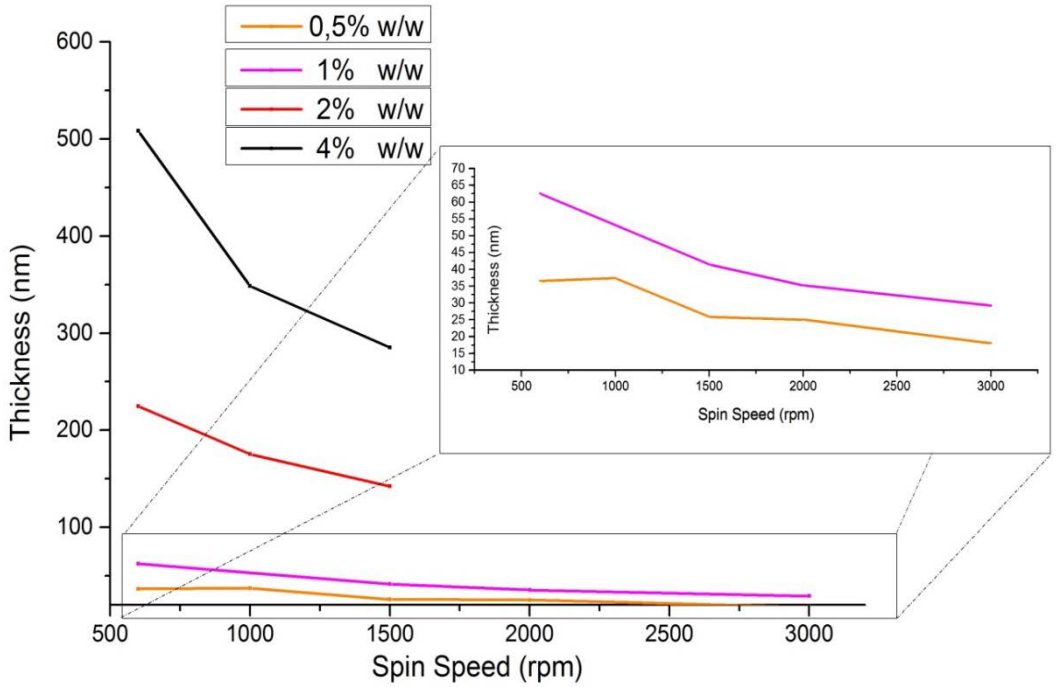

Graph 4-3:Triazene layer thickness for different Spin Speed. (Type B-Triazene)

4.3 Spin coating of Alq_3

The most common method for preparing organic small molecules film is vacuum dry evaporation method because of those materials, for example Alq_3, is usually powder in normal condition. During this thesis in order to find a method to fabricate OLEDs in lower cost I tried to spin coat Alq_3 small molecules on the top of triazene from a solution of chloroform(5mg Alq_3/10ml Chloroform).

The challenge is that a limitation for multilayer stacks of solution-processable materials is solvent compatibility. For depositing Alq_3 from a solution by spin coating, we use chloroform to dissolve Alq_3 and that solution wash out part of the

triazene layer during spin coating. To study the influence of the Alq_3/chloroform solution on the triazene layer during spin coating we spin coated pure chloroform as also Alq_3/chloroform on triazene layers in different concentrations and in different spin coating settings on different triazene thicknesses. Afterwards we measured with a profilometer the thickness of each layer or of stack of layers. To measure the deposited volume of the solution on the sample we used a pipet in order to drop always the same volume of solution with the deposited material on the layer. The data had been acquired are presented in Table 3.

Table 3: Thickness of triazene, Alq_3 or triazene/Alq_3 for different spin coating settings, concentrations

Triazene spin coating settings(baked 1h , 70C^0)	DekTak (nm)		Alq3 and chloroform spin coating settings		DekTak (nm)		
	Thickness	Roughness				Thickness	Roughness
2%,800rpm, 60sec	80,9	2,5	Alq_3	2 steps, 1000rpm, 15sec	center	206,1	3,5
					edge	150,6	3,4
				2 steps, 1000rpm, 5sec	center	190,2	4,7
					edge	188,1	5,1
				1 step, 1000rpm, 15sec	center	160,7	4,2
					edge	134,7	3,4
				1 step, 1000rpm, 5sec	center	215,5	4,3
					edge	224,6	5,2
			chloroform	2 steps, 1000rpm, 15sec	No triazene		
				2 steps, 1000rpm, 5sec			
				1 step, 1000rpm, 15sec			
				1 step, 1000rpm, 5sec			
2%,800rpm, 60sec	117,5	9,7	2 steps, 10^3 rpm, 30sec	Alq_3 on triazene 250microlt 10mg/ml		264,6	13,3
				Alq_3 on triazene 150microlt 10mg/ml		234,1	8,8
				Alq_3 on triazene 150microlt 20mg/ml		228,6	10,1
				Alq_3 on triazene 300microlt 20mg/ml		263,6	6,3
4%,1000rpm, 60sec	240,6	6,1	Chloroform 2 steps, 1000rpm, 15sec		No triazene, it was totally washed out		
4%,800rpm, 60sec	294,3	3,8					
No Triazene			Alq_3 10mg/ml	2 steps, 1000rpm, 30sec	123,4		2,3
			Alq_3 20mg/ml		258,8		3,6
			Alq_3 10mg/ml	2 steps, 1000rpm, 15sec	center	320,8	1,1
					edge	223,2	1,7
				2 steps, 1000rpm, 5sec	center	140,3	1,0
					edge	224,7	1,3
				1 step, 1000rpm, 15sec	center	95,7	0,5
					edge	89,0	0,8
				1 step, 1000rpm, 5sec	center	105,0	0,8
					edge	46,9	1,5

*1 step means that we try to deposit the solution after the spin coater had already gain the speed that referred in the table.

*Spin coating settings: Concentration, spin speed, duration

In every sample with different thickness of triazene on which we try to spin coat pure chloroform the triazene was totally washed out. Even for a really thick layer of triazene (294nm). The 2% concentration of Alq_3 in chloroform gives an enough thick layer of Alq_3. In almost all the samples the layer is thicker in the center than near to the edges. The variation between the thickness of the layer in the center and near to the edges of the sample is about 10nm. In paragraph 5.1.5 the results from this specific experiment are presented. The most promising settings are: 2 steps, 1000rpm, 5 sec which is the sample we also use to make LIFT experiments with the picosecond-Laser.

4.4 Spin coating of Super Yellow

The layers of Super Yellow polymer were made by the spin coating method from a solution of Super Yellow in toluene. The same cleaning procedure were followed as that one for the triazene layers. After the spin coating the samples were cured in a hotplate for 5 min at 60 ^{0}C. In Table 4 the yielded layers for 2 different concentrations of Super Yellow in Toluene and for different spin coating settings are presented.

Table 4: Thickness of Super Yellow layer for different spin coating settings.

concentration	Spin coating speed rpm	Time(sec)	Thickness nm	Roughness nm
5mg/ml	600	15	92,4	1
		30	87,8	2
	800	15	77,2	1
		30	81,4	1
	1000	15	81,8	1
		30	81,7	1

5 LIFT on smOLEDs

Introduction

The aim of this project is to transfer good quality pixels without using a metal and without degrading the light emitting organics in order to achieve multilayer devices by sequential LIFT processes. The current approach for the fabrication of OLEDs is the transferring a bilayer of an organic material on top of a metal cathode from a transparent substrate to a receiver with a deposited layer of ITO on the top [31].

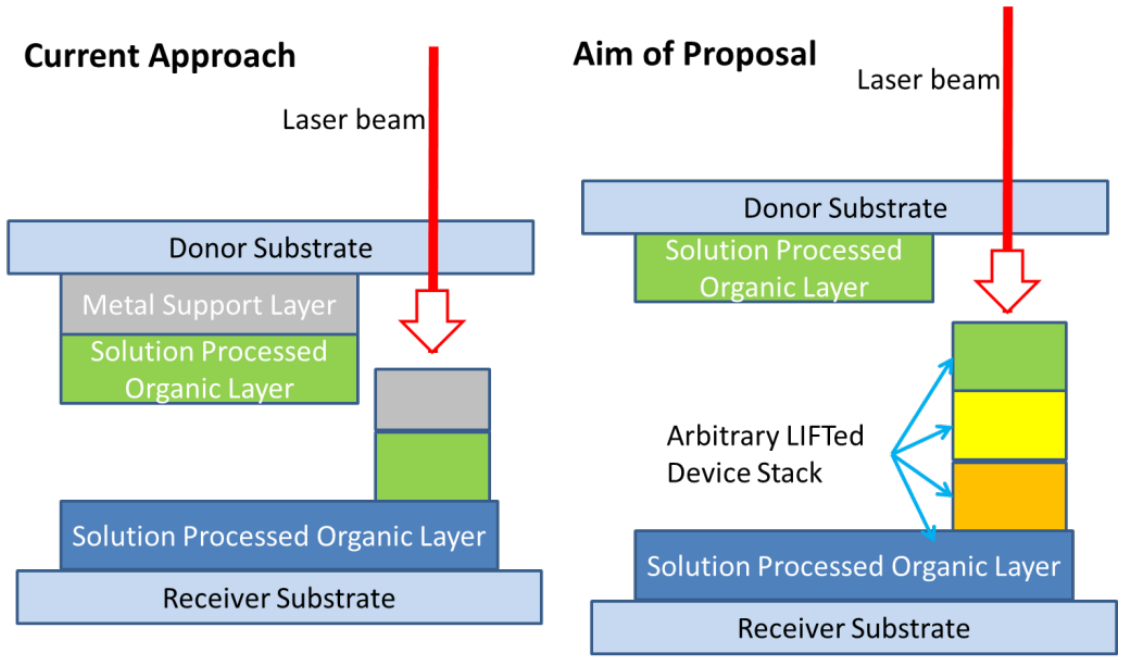

Figure 5-1: Sequential LIFT of different organic layers.

Rapid developments in the organic LED technology promise to deliver thin, lightweight and power-efficient light sources for lighting applications. Laser patterning of OLEDs for display applications has been decently reported the last years. Our aim here is to quantify the potential of picosecond lasers for this application and determine a robust laser process window for large area selective OLED electrode patterning.

5.1 DRL-LIFT on Alq_3

5.1.1 Influence of the thickness of DRL (Triazene)

The Dynamic Release Layer as we mentioned to a previous chapter plays a critical role for the LIFT process. I am using as DRL TP polymer (Triazene). We prepared samples of three different thicknesses of triazene: 100nm, 240nm and 300nm. The triazene layer has deposited on eagle glass samples after cleaning (acetone, methanol, isopropanol-UV plasma) by the spin coating method from a solution of cyclohexanone: chlorobenzene(1:1 w/w)-triazene 2% or 4%. Afterwards I deposited to each sample a 100nm thin layer of Alq_3 on the top of triazene. The LIFT experiment yielded with the picosecond laser (355nm) and the gap between the donor and the acceptor were 13 μm.

In Figure 5-2 we can see the donor for three different thicknesses of triazene with a 100nm layer of Alq_3 above after irradiating with a laser beam (355nm) through the transparent substrate. In Figure 5-2 we can see that the ablation threshold is about the same with a small increase for a 300nm thick layer of triazene. In Graph 5-1 the ablation threshold is presented more detailed. It is also obvious, that thicker layers of triazene give more debris on the surface of the donor.

From Figure 5-3 it's obvious the influence of the DRL layer to the LIFT process where is presented the transferred spots from the donor at Figure 5-2. On the left column the transferred pixels became from a monolayer of Alq_3 without a sacrificial layer. When the DRL was added the formation of the pixels significantly improved, and the deposition was more controllable. Without any DRL the transferred spots have bad shape and the transfer is not homogenous in every spot regarding the extremely thin layer of the Alq_3.

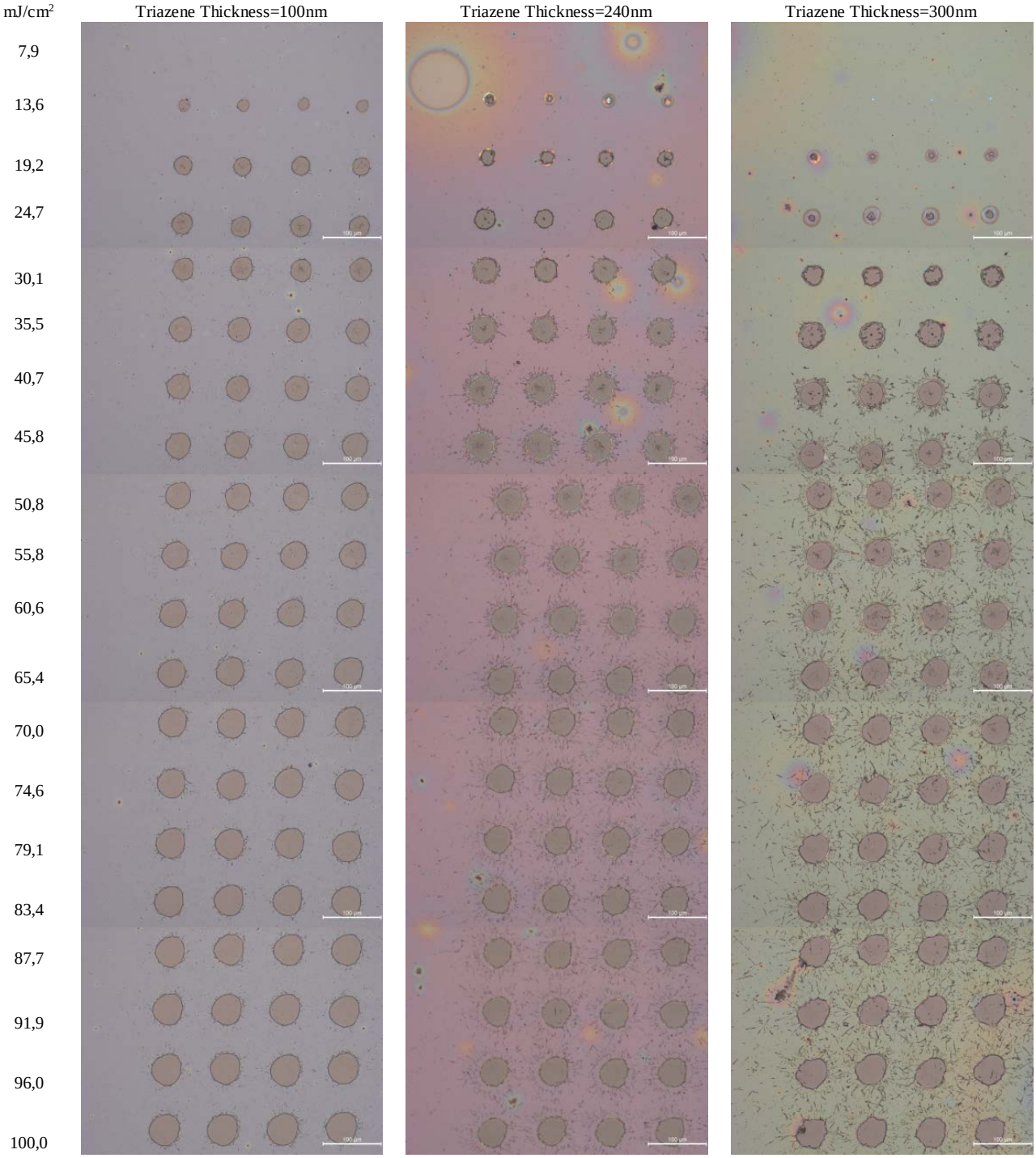

Figure 5-2: Microscope pictures of the donor after Laser-ablation for three different thicknesses of triazene(100nm, 240nm, 300nm) with a layer of 100nm on the top.

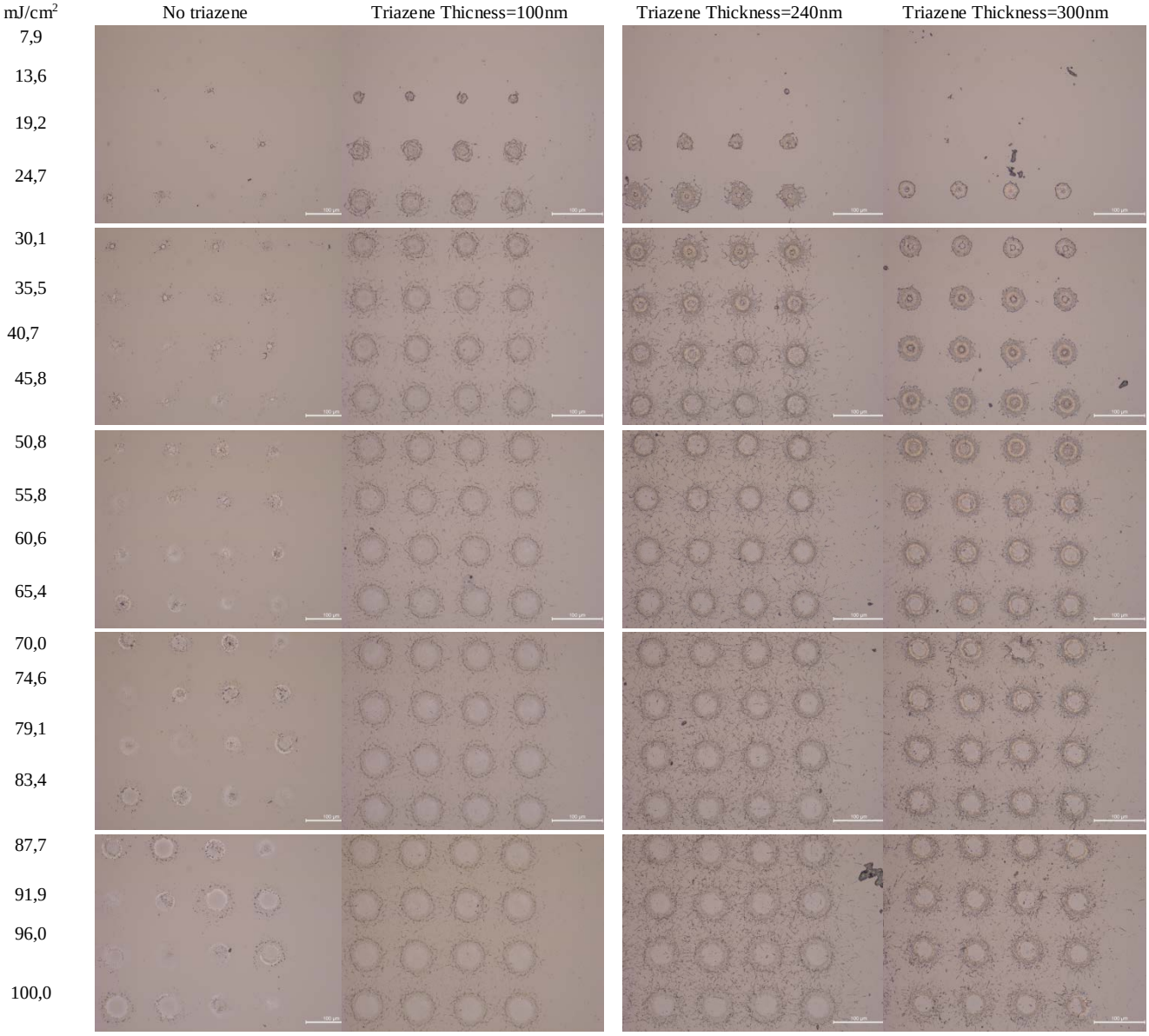

Figure 5-3 : Microscope pictures of the acceptor after 'LIFTing' of a 100nm thick layer of Alq_3 for three different thicknesses of triazene(100nm, 240nm, 300nm) and without triazene.

In Figure 5-3 we can see that when the triazene' s layer getting thicker bigger fluencies are needed to achieve LIFT. The diameter of the transferred spot is bigger when the fluence is higher. It is interesting to notice that we observed a hole in the center of the transferred pixel. One of the reasons for that is the influence from the Gaussian beam of the laser, but for the shame fluencies that effect getting stronger in thicker layers of triazene which is something unexpected. Thicker layer of Triazene means less light pass through it for the same fluence. Probably, the thrust caused by the triazene photo-ablation is the reason for that observation. In the next paragraphs we will explain that effect with more details. Finally we have to mention that better

results has been achieved from samples with a 300nm thickness of triazene (Figure 5-4).

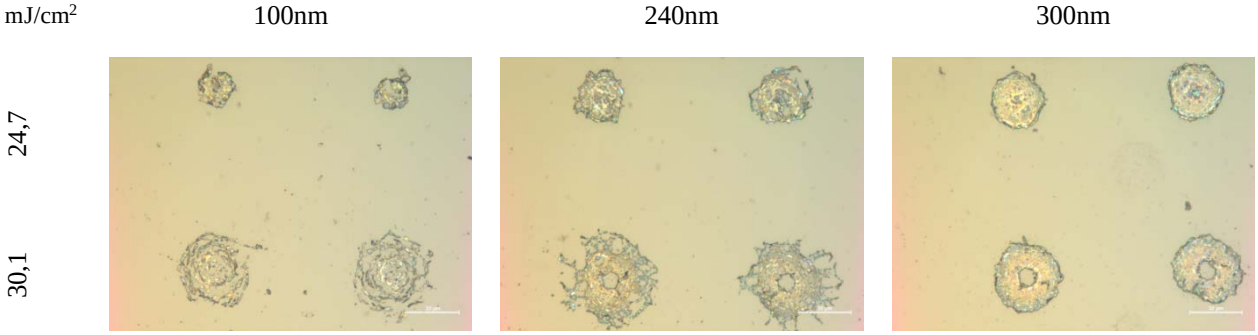

Figure 5-4 : Fabricated pixels from three different thicknesses of triazene(100nm, 240nm, 300nm)

As the thickness of the triazene layer is getting bigger and the pulse as well as the intensity of the laser beam remain the same, which means that the fluence remain the same, the way that the detaching starts became less violent and we have a more gently transference of the layer to the acceptor. So using a thicker layer of triazene and keeping the same fluence and gap we can see that we have less produced debris. Furthermore, the wavelength we use is 355nm and in that wavelength the optical penetration is calculated at 224nm. So a layer around 100nm can be too thin for that wavelength and the UV beam can cause serious effects on the Alq_3 layer.

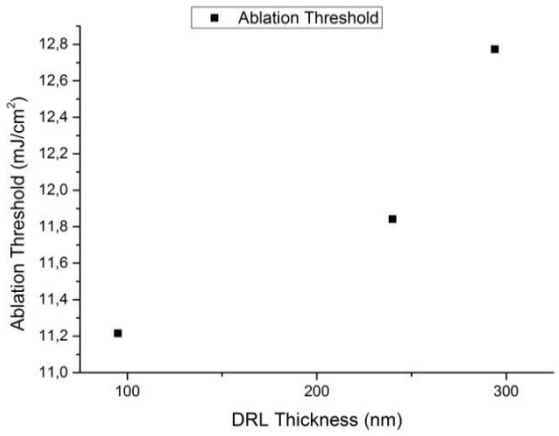

Triazene Thickness (nm)	Threshold ablation (mJ/cm^2)
90±10	11,2
240±10	11,8
300±10	12,7

Graph 5-1: The threshold ablation for three different thicknesses

After calculating the diameter of the ablations holes in each donor I can calculate the ablation threshold for those different thicknesses of triazene. In Graph 5-1 we can see the ablation threshold for different thicknesses of triazene.

Additionally, the ablation threshold for an Alq_3 layer of 100nm was calculated at 13,0 mJ/cm^2.

In the literature is referred that the threshold ablation of the triazene is decreased as the thickness of the layer is decreased. But below a certain thickness the threshold starts increasing because not enough light is absorbed by the triazene. Therefore, the ablation fluence starts to increase again.

The most challenging part is the thin layer we are trying to transfer from a fragile and brittle material. The mechanical properties of the material insert a critical mechanically instability to the layer during transferring. The shock wave that the transferring cause, the gap between the donor and the receiver, the environmental pressure as also the pulse, the wavelength and the shape of the laser beam are some of the parameters we can optimize. In the next pages it will be explained what I was able to observe in the lab using our facilities.

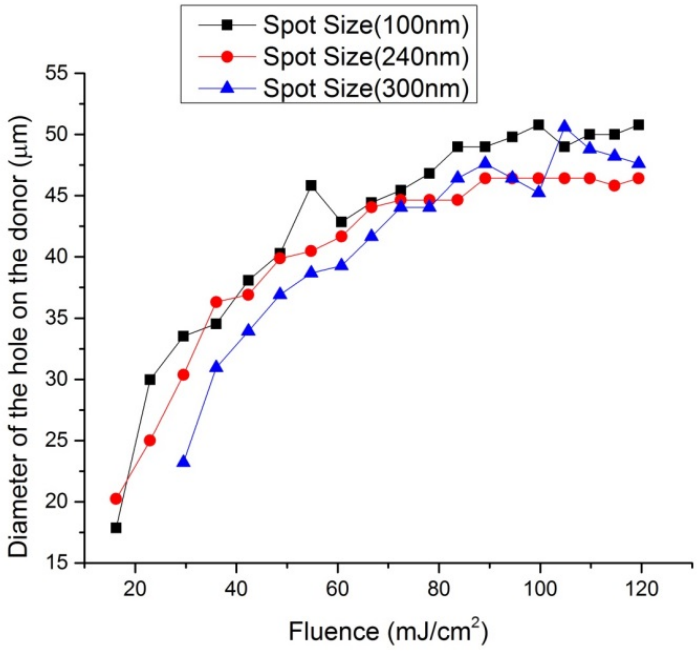

Graph 5-2: Diameter of the ablation hole (donor-355nm) vs fluence for 3 different thicknesses of Triazene

Also in the center of the hole on the donor for some certain fluencies and for each thickness we can noticed that there are some debris from the transferred layer which we are going to investigate further in the next chapter where the shock wave

effect is explained. It has to be mentioned that the size of the transferred pixel differs from the size of the hole on the donor where it came from. In average the transferred pixel's size produced by the samples of 240nm and 300nm of triazene were 20% bigger than the ablation holes on the donor. As far as concerned the samples with 100nm layer of triazene, the transferred pixels were 16% bigger than the ablation holes on the donor. The most preferable is to decrease that difference to 0% in order to avoid the dispersion of the pixel.

In Graph 5-2 is shown the diameter of the ablation holes which had been created after the irradiation of the triazene layer with a 355nm laser beam for three different thicknesses of triazene(100nm-240nm-300nm). It is obvious that, that diameter has a strongly correlation with the fluence of the laser beam as also with the thickness of the triazene layer. As the fluence is increased we can see that the graph it turns to a flat area where the diameter stops increasing with the fluence. That happens because the intensity of the light in all the Gaussian profile became enough to ablate all the thickness of the triazene and the ablation hole became equal to the diameter of the laser beam-spot.

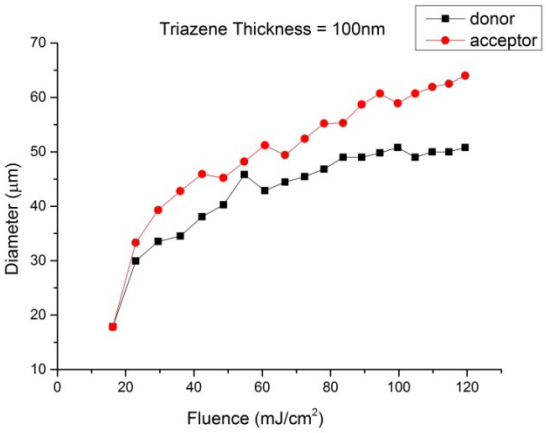

Graph 5-3:Spot size on donor and on the acceptor vs fluence for a triazene thickness at 100nm

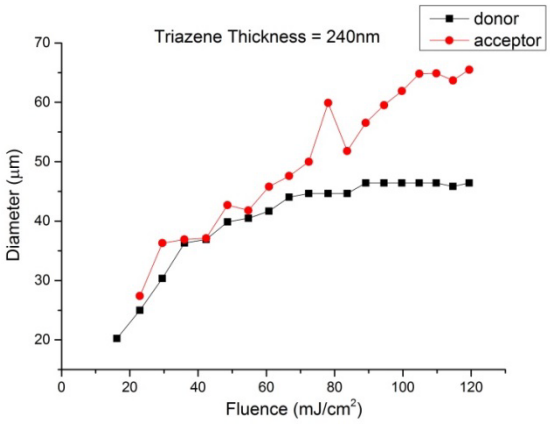

Graph 5-4:Spot size on donor and on the acceptor vs fluence for a triazene thickness at 240nm

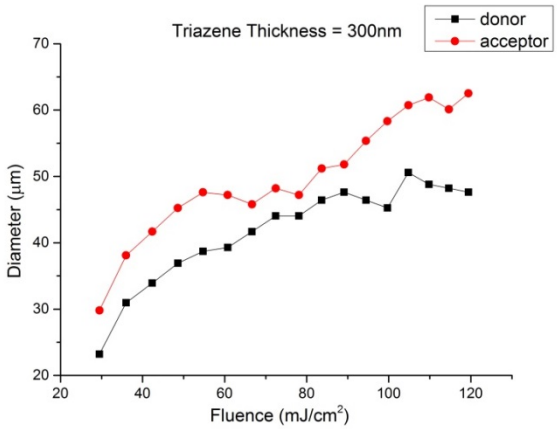

Graph 5-5:Spot size on donor and on the acceptor vs fluence for a triazene thickness at 300nm

The decomposition of the triazene is an exothermic reaction. So we can assume that the input energy comes from two sources: the laser fluence F and the energy from the decomposition reaction of the triazene ΔH_{dec}. There are four energy outputs: the energy in the flyer's kinetic energy, the energy lost in the kinetic energy of the decomposition products, the proportion of input laser energy lost due to reflection, and the energy lost below the minimum energy required for the activation of the decomposing of Triazene. There may be other energy losses in the process, but here it is assumed that they are all included in the reflection. In addition it is assumed that the decomposition enthalpy ΔH_{dec} created by the release of the "potential energy" in the chemical bonds may be dependent on the activation energy of the DRL decomposition. [36]

More energy is produced for less TP ablation, meaning that the flyer is thicker, and greater kinetic energy is required to make the flyer go at the velocity observed experimentally for a lighter flyer. About 10% of the input laser energy is converted into useful flyer kinetic energy. When gaseous kinetic energies are considered this increases to 15–20%.Mechanical loss mechanisms are unlikely to increase with fluence but thermal loss mechanisms are probably the most promising, like thermal loss into the substrate.

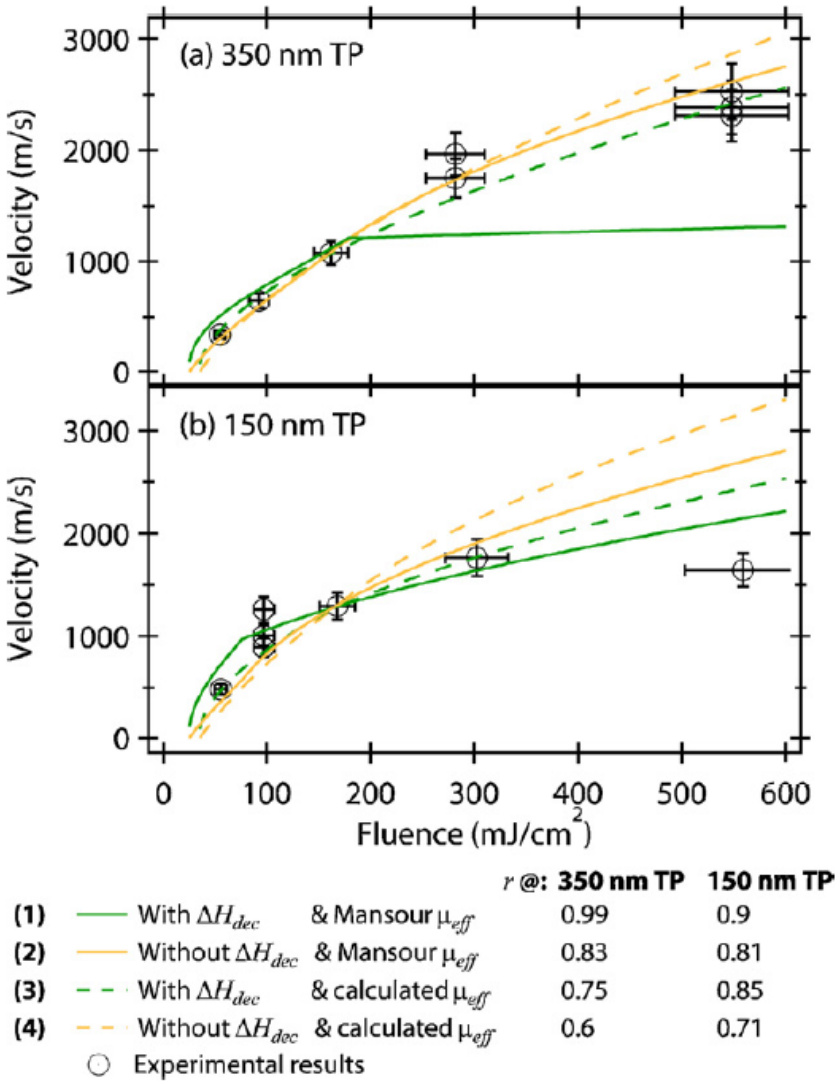

Graph 5-6: Flyer velocity as a function of fluence, comparing a model results with experimental data points for (a) 350 nm TP/80 nm Al and (b) 150 nm TP/80 nm Al. [36]

As you can see in Graph 5-6 for low fluencies which are near to ablation threshold for each thickness of triazene, the produced velocity of the transferred layer is bigger for a thinner layer of triazene. And that happens because of the decomposition energy from the triazene itself.

5.1.2 Influence of the Gap-Shock Wave Effect

The gap between the donor and receiver plays a critical role for the LIFT technique. Especially for our occasion where we try to transfer Alq_3 small molecules there are many parameters we have to optimize because we are trying to transfer a very thin layer from a really sensitive material. The mechanical properties of the material plays also a critical role.

Changing the environmental pressure we change the speed of the transferring. When the pressure is reduced the speed getting higher because there is no air to prevent the increasing of the speed. On the other hand when we get lower pressures, we decrease the shock wave effect.

In addition the Gaussian beam insert a delay parameter for different points on the transferring layer and in combination with the mechanical properties of the material, a curved layer of Alq_3 is created before it detached. That means that the trust which the Gaussian beam causes in the center of the transferring spot is higher than the edges. So the starting speed in the center of the circular spot is different that the starting speed in the edges. Our material is mostly brittle and unlike with an elastic material those small variations can cause fragments in the main area on the transferred spot and folding in the edges.

In Figure 5-5, are presented the transferred pixels which have been yielded for different gaps while the rest of the parameters were the same. Also, the donor substrates are presented in the first three columns. We can see that as the gap getting smaller we have no transfer for lower fluencies. The fluence in each raw is the same but considering the shock wave which is getting bigger when the gap getting smaller, the demanded fluence to achieve LIFT is changed. The experiment happened in atmospheric pressure. The shock wave which is produced and reflected from the receiver surface prevent the transferring of the material. When the gap getting bigger the produced shock wave is the same for same fluence but there is enough space to escape and spread before its reflection on the receiver(Figure 5-6).

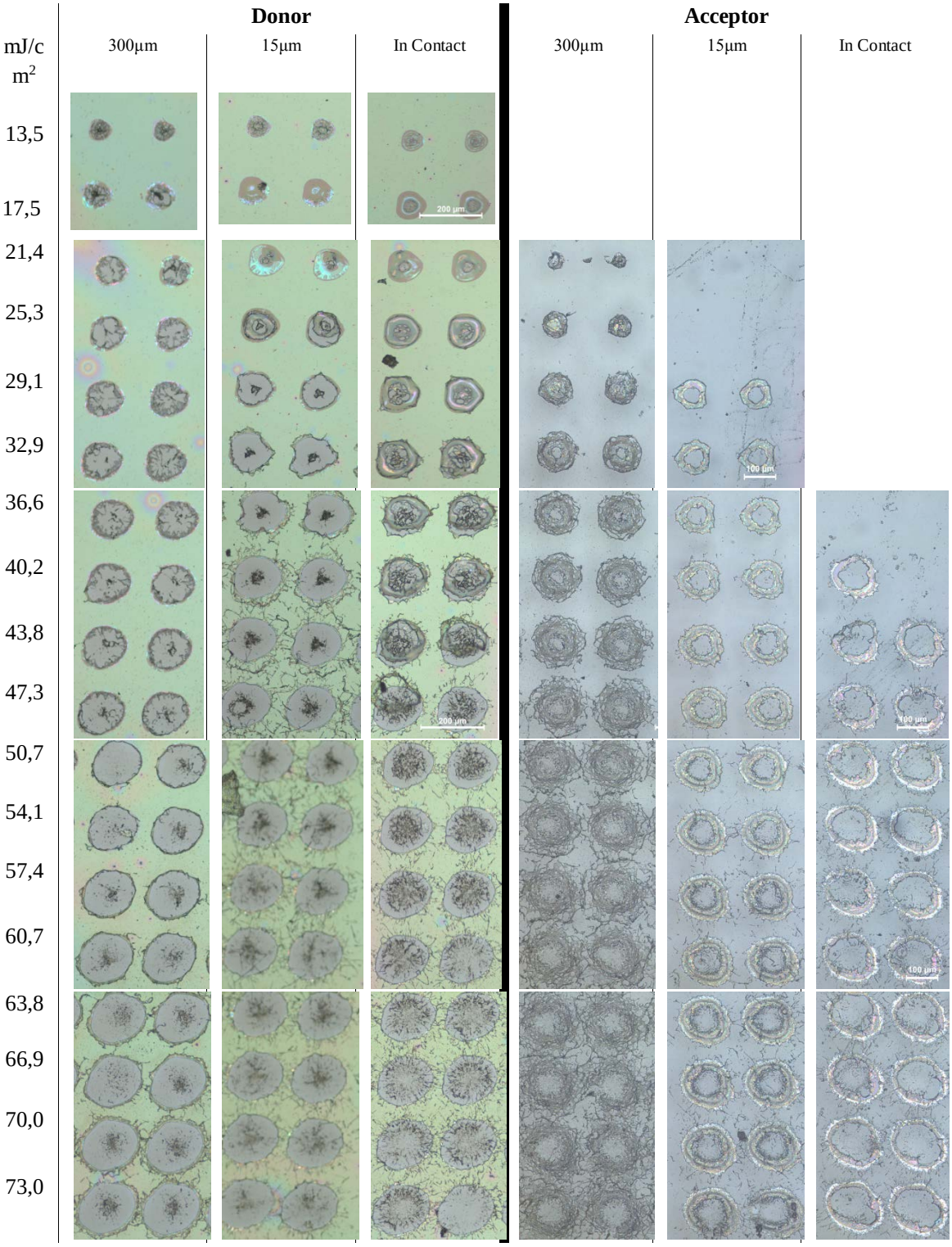

Figure 5-5: Microscope pictures from the donor and the acceptor after LIFT for three different gaps and the same thickness of triazene(300nm)

For a 15µm gap we got pixels which has the shape of a donut. Also the layer which is transferred is smoother. After analyzing the PL pictures we see that the photoluminence properties of the layer is mostly remained. A shape like that is not the preferable shape for screen technology but there are also some other applications

where it can be applicable (plasmonics, microsensors, microresonetors, solid state lasing).

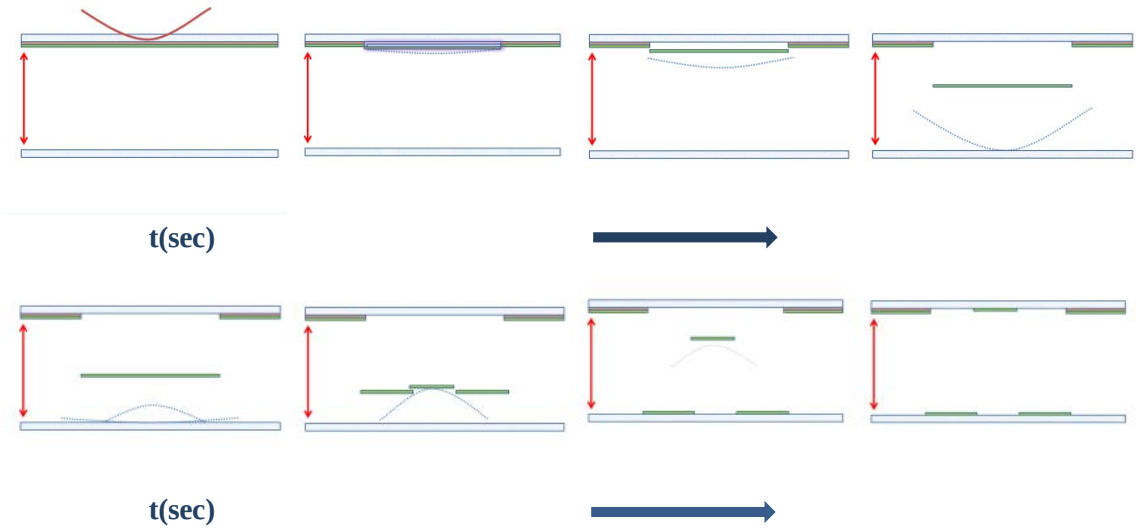

Figure 5-6:Shock wave effect.(Schematics of the shock wave during LIFT)

About the contact mode transfer we see the first transferred layer after the fluence of 40,2mJ/cm^2. That happens because the shock wave bunches back to the acceptor surface and propel the transferred layer back to the donor surface. In really big gap about 300μm we almost avoid the shock wave effect. But then the transferred layer is getting more fragmented because of the big distances (Figure 5-5).

Last we noticed that the hole in the center for each transferred spot is getting bigger when the gap is getting smaller. That also because the shock wave which also follow the shape of the Gaussian beam, is more faster and stronger in the center. What can be assumed is that the center of the spot stops transferring during the transferring when the traveling layer meets the reflected shock wave from the acceptor. Then the shock wave propels that part of the layer to deposit back to the donor surface (Figure 5-7). So we have to consider that the hole in the center of each transferred spot it's not only because the ablation of the Alq_3 layer from the laser beam but also the shock wave plays a very important role for the creation of that hole.

The diameter of each spot is getting bigger as it was expected for higher fluencies and the same gap. Those holes in the center caused by laser ablation. But after comparing the transferred spots for different gaps we can see that we got rid of that hole in the center caused by the shock wave. For example in Figure 5-5 on the

acceptor from 300 μm the donut shape it is almost disappeared but the bigger gap also helps the layer to spread during the transferring.

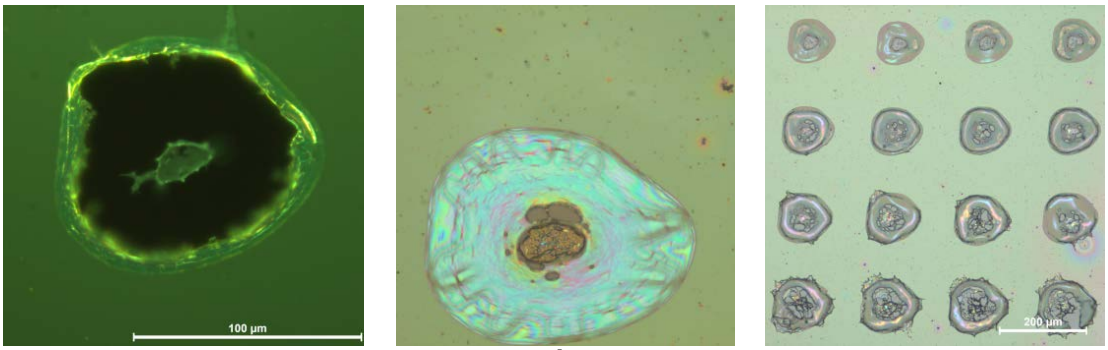

a b c

Figure 5-7: a) We can see how the shock wave propel a part from the center of the transferred layer back to donor, b) The produced shock wave prevents the detaching of the layer from the donor, c) Contact mode – Shock wave effect

After the calculations of the spot size on the donor we calculate the threshold for the triazene ablation with Alq_3 on the top. (We measure the area of each spot which is not totally spherical and afterwards we calculate the diameters for the analogous area of a circle.) A similar value as in focus was expected. Where the results are repeated as the threshold had been found :**12,6mJ/cm^2**.

It's obvious that even in small energies the triazene is ablated but the transferring of the layer stops from the shock wave which is created by the reflection of the initial shock wave on the receiver. In Figure 5-5 we can see the important role of the shock wave. We can see that the laser fluence starts effecting the donor at the same fluence regardless of the gap. But as the gap getting smaller the transferring starts in higher fluencies. The shock wave which travels faster than the layer reflected on the receiver and in certain fluencies it prevents even the detaching of the layer. We know that the triazene should behave with the same way for same fluencies. For example when the gap is 300μm for 21,4mJ/cm^2 the triazene totally ablates and we have a spot transferred on the donor. For the same fluence but for a gap equal to 13μm we can only watch a delamination of the Alq_3 layer and something prevent it from detaching.

At low fluencies the shock wave is strong enough to prevent the detaching of the Alq_3 layer from the triazene layer. In middle fluencies the transfer is happening because the trust from the entrapped gases came from the triazene decomposition is

comparable with the force of backscattered shock wave. But in really higher fluencies, when the reflected shockwave meets the transferring pixel, a violent interaction takes place.

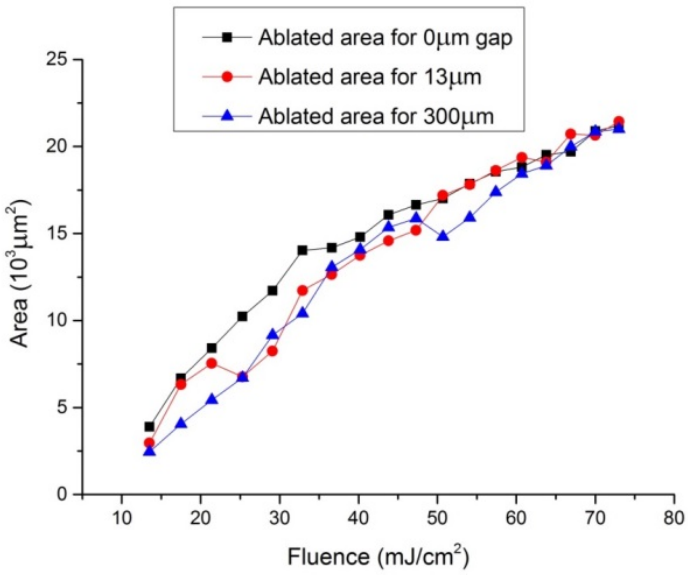

Graph 5-7: The ablated area on the donor for different gaps (0μm, 13μm, 300μm).

The ablated area on the donor remains the same for the same fluence regardless the gap. It depends only from the properties of the laser beam (shape, fluence, pulse) and the properties of the stack of layers on the donor.(Figure 5-5 & Graph 5-7)

That happening because for big gaps we have big dispersion of the transferred spot during transferring but for smaller gaps that is not happening. In contact mode, there is not enough space for the transferred material and the products from the decomposition of triazene to escape and that push the material to bigger diameters. This is one more reason that we have to optimize the gap between the donor and the acceptor (Figure 5-5). The area of the hole in the center is getting bigger as the gap is getting smaller. That happens because the shock wave is getting bigger. Also in contact mode the produced gases from the triazene ablation are trying to find a way to escape. As a result those gases are pushing the transferred material from the center to the edges in a circular symmetry. So, the hole in the center is getting bigger.

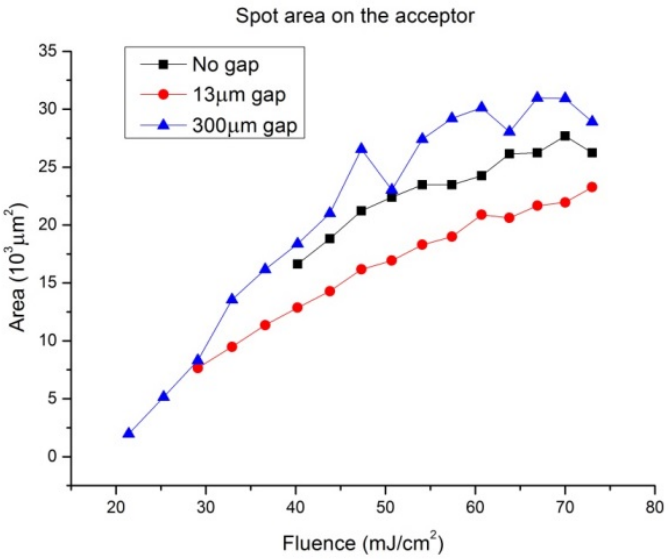

Graph 5-8: Deposited area on the acceptor for different gaps (0μm, 13μm, 300μm).

The total surface area between different gaps is behaving with a different way. As you easily can see in low fluencies the transferred pixel have the same size for the gap between 13 μm and 300 μm (Graph 5-9). But as the fluence getting bigger the transferred pixel from a gap of 300 μm is bigger from the transferred pixel of a gap at 13 μm and in contact mode. The big gap has another disadvantage, may the shock wave effect disappeared but now there is a big distance of traveling which allow to the material to waist with the same way a light beam is dispersed as it travels. The pixels in contact mode are bigger than in 13 μm gap for the same reason that the donut holes are bigger.

In Graph 5-8 is shown the deposited area on the acceptor for different gaps. The biggest spots are yielded for a 300μm gap and the smallest for a 13μm gap. The size is mostly controlled by the distance that the flying layer should travel. In the other hand when the gap is getting really small the entrapped gases produced by the triazene ablation starts to affect a lot on the pixel and increase its size.

In Graph 5-9 is shown the create hole in the center of the transferred spot for different gaps. Similarities are observed for that holes for different fluencies in the presence of a gap. But when we remove the gap that hole increase a lot, because of the entrapped gases produced by the triazene ablation.

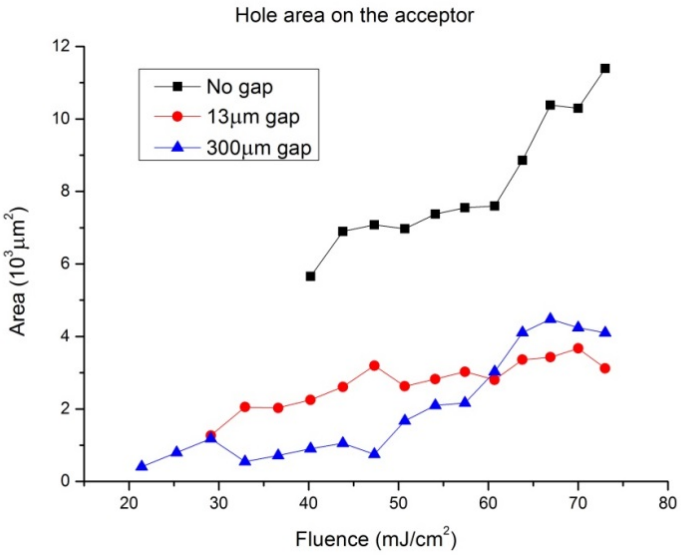

Graph 5-9: The hole in the center from the 'donut shape' transferred pixel on the acceptor for different gaps (0μm, 13μm, 300μm).

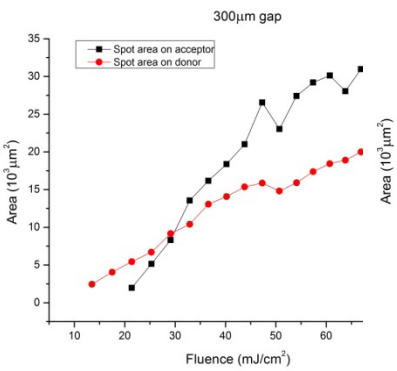

Graph 5-10: Ablated area on the donor VS deposited area on the acceptor for 300μm gap.

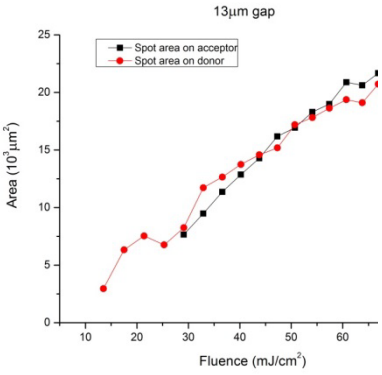

Graph 5-11: Ablated area on the donor VS deposited area on the acceptor for 13μm gap

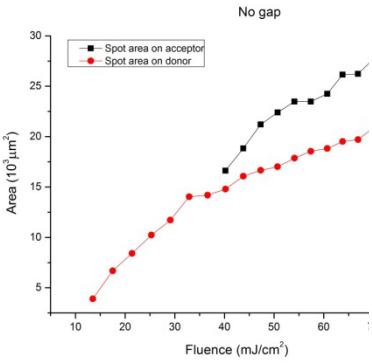

Graph 5-12: Ablated area on the donor VS deposited area on the acceptor for 0μm gap.

After the calculation of the ablated areas on the donor and the deposited pixels on the receivers we can compare them and find the difference between them. For a 300μm gap the pixel's size on the acceptor was 44%±14% bigger than the ablated area on the donor (Graph 5-10), for a 13μm gap the pixel's size on the acceptor was 0%±7% bigger than the ablated area on the donor (Graph 5-11) and for the 0μm gap the pixel's size on the acceptor was 27%±6% bigger than the ablated area on the donor (Graph 5-12).

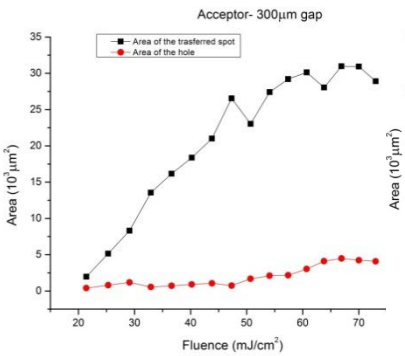

Graph 5-13: Deposited area on the acceptor VS area of the hole in the donut on the acceptor for 300μm gap

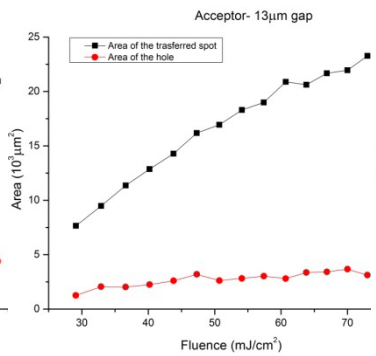

Graph 5-14: Deposited area on the acceptor VS area of the hole in the donut on the acceptor for 13μm gap

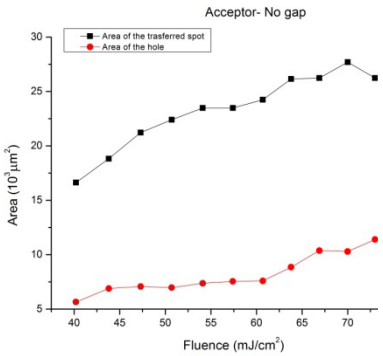

Graph 5-15: Deposited area on the acceptor VS area of the hole in the donut on the acceptor for 0μm gap

In literature also is referred that shorter pulses generates faster flyers and shockwaves than longer pulses. So we have to consider that in our case where we are using a ps-laser the produced shock wave should have more effect on the transferred layer than a produced shock wave from a ns-laser. [35] The speed of the shockwave expansion has been seen to depend only on the laser energy used. No significant influence of an additional TP layer was observed. The speeds of the flyers were also not influenced significantly by a TP layer. More important for the flyer speed is the flyer thickness, i.e. flyer mass. Thinner layers are ejected faster at the same laser fluence [37].

5.1.3 Optimization of the gap (Specific experiment)

In particular, the introduction of a gap between the substrates was viewed as a means to improve the robustness and applicability of the technique. In addition, a gap between substrates is more favorable for implementation of LIFT as an industrial manufacturing process, allowing for a faster turnover of substrates.

For a successful transferring the optimization of the gap is major. In that specific experiment, a linear variation in the gap width from ‘in contact’ to 300μm has been achieved by adding a spacer at one side of the donor-receiver ’sandwich’. In that way we can create a slope to the donor and by doing an fluence scan is possible to optimize the gap.

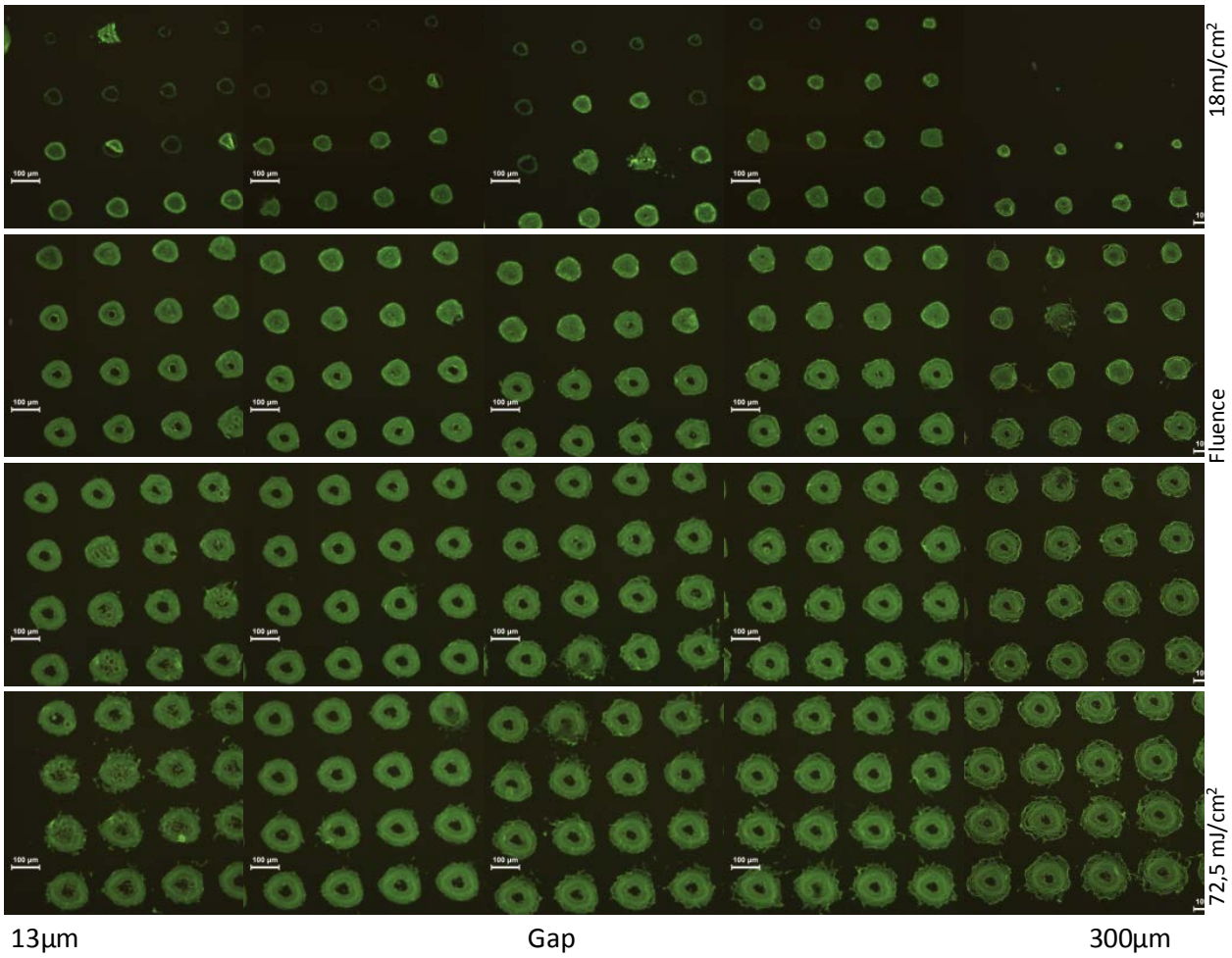

Figure 5-8: PL images for the optimization of the gap (Ambient Environment)

The experiment had repeated also in an ambient environment as also in the environmental chamber at a pressure of 0,2bar. That the lowest pressure which can be achieved using the box and the house vacuum in our lab. The thickness of the triazene for that experiment was 300nm and the thickness of Alq_3 was at 100nm. We see some big difference in the quality of the transferred layers for different gaps , but for a reduced pressure the difference is not so big. Stewart et al. [38] has checked the same transfer for a lower pressure at 0.1 bar and they have found the results much more better in vacuum than in environmental pressure.

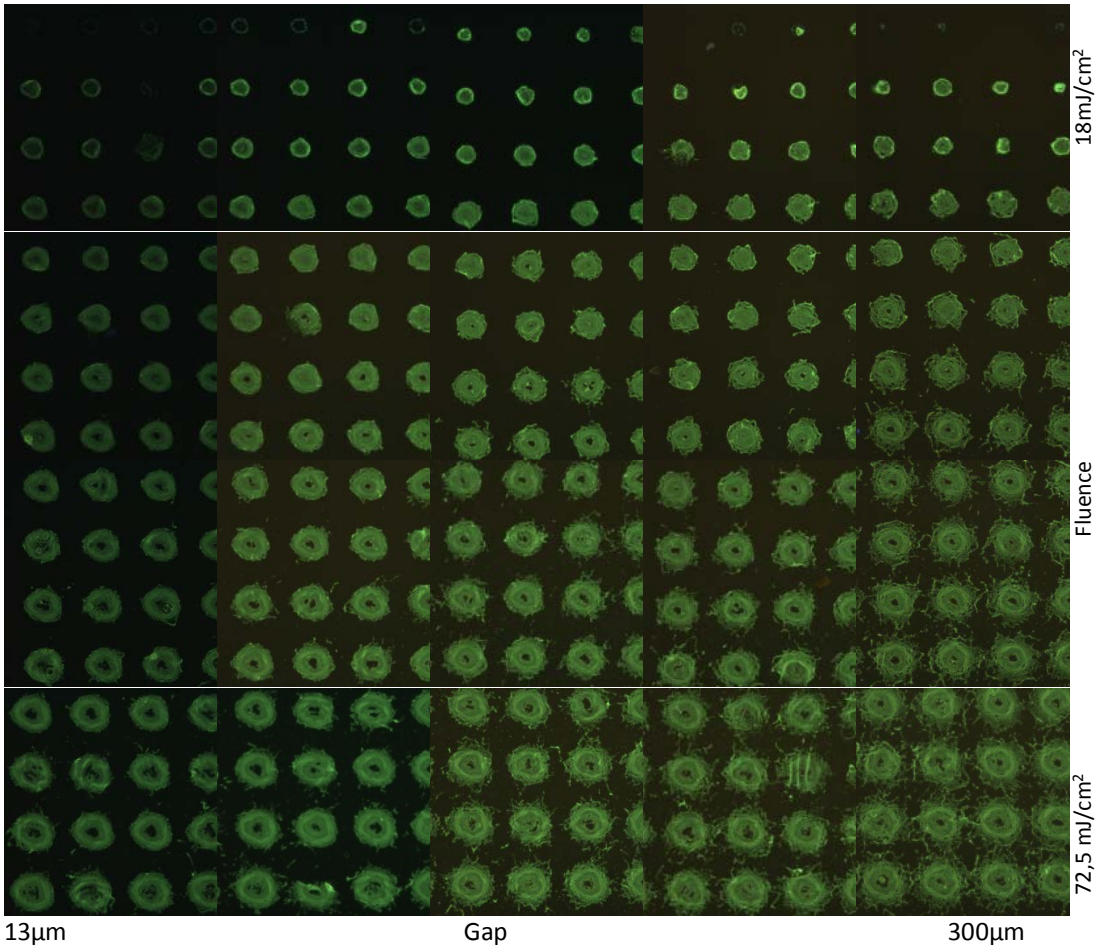

Figure 5-9: PL images for the optimization of the gap (Nitrogen Low Pressure Environment)

In our case the best quality with the best morphology pixels have been achieved for the following settings: gap=40µm, fluence=19,2-21,8mJ/cm^2. In Figure 5-11 the best pixels have been achieved are presented. I have to mention that for every new batch of samples small variations on the optimized fluence were observed.

After the comparison of the yielded pixels in ambient and in a low pressure environment, we can observe in general the following. Transferring can be achieved from lower fluencies in a low pressure environment than in atmospheric pressure. This is again another effect of the shock wave. Reducing the pressure then the produced shockwaves is minimized and because of that the transferred layer can detached form the donor easier. In addition also the hole “donut” shape is reduced for the same reason. In the other hand, the speed that the transferred layer is landing on the acceptor is increased and that has as a result the formation of fragments and inhomogeneities on the surface of the pixel.

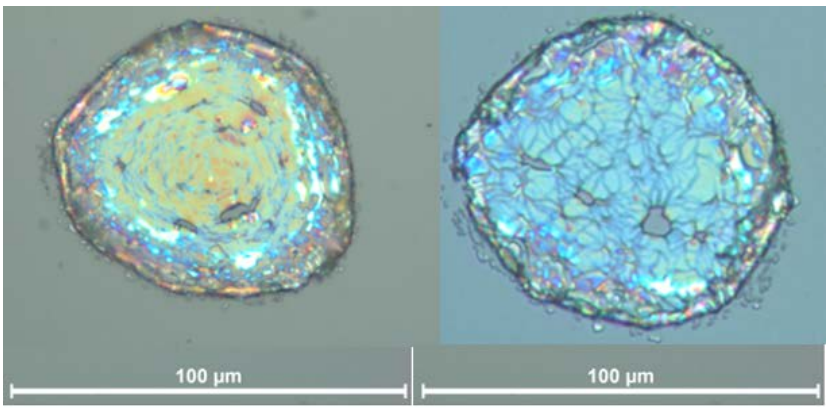

Figure 5-10: Cracks and holes on the transferred spot from the Alq_3 material

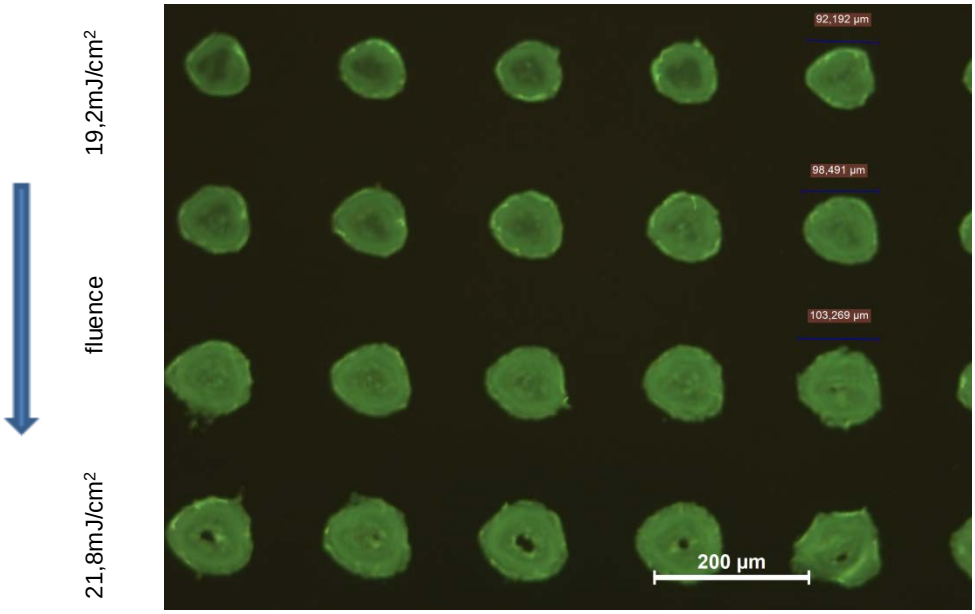

Figure 5-11:PL image of transferred spots after optimization of the gap and the fluence

But as you easily see in Figure 5-10 there as still some issues that should have been solved before these pixels are suitable for OLEDs applications. There are some holes and cracks on the surface of the pixel. The surface roughness obviously is high. In the center a bleaching effect can be observed, and furthermore we can notice some folding at the edges which is probably caused by mechanical causes.

5.1.4 Excimer Laser

The first attempt of transferring a monolayer of a 100nm Alq_3 by LIFT technique was done using an excimer laser which emits at 248nm with a 50ns pulse. The deposited pixels are shown in Figure 5-12. The donor consisted from a stack layer of triazene and Alq_3 small molecules (100nm/100nm). The substrate for the stack of the layers was quartz slides in order to be transparent to the 248nm wavelength. The applied gap between the donor and the acceptor was 15 μm. Transferring is possible but the yielded pixels suffer from a big surface roughness. They mostly transferred as a powder than a compact layer. That makes the results inappropriate for OLEDs applications.

The ablation threshold in excimer laser is higher than the ablation threshold in pico-laser. That means that the thermal damage of the material can be kept low in a picosecond laser. Also previous studies has shown that([35]) the difference in timescales of photochemical reactions (≤ ps) vs photothermal reactions (ns) may have important implications for the kinetics of the ablation process. In conclusion the results confirm that theory, considering the thermal effect on the Alq_3 layer by the ns-pulse.

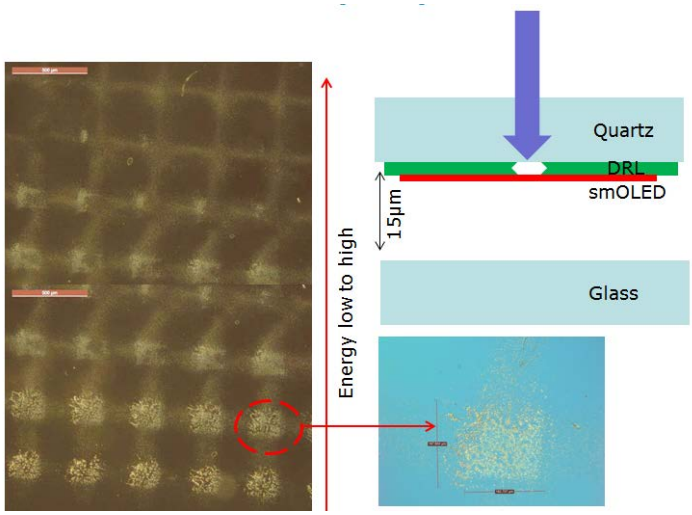

Figure 5-12: Optical micrograph of LIFTed small molecules on glass substrate at various laser fluencies

The greater effective absorptivity need only be linked to the shorter pulse length; a reduction in thermal diffusion may be one explanation for this, but it is by no means the only one. The shorter pulse time means that the movement of the solid-gas

interface will be kept to a minimum by the kinetics of the ablation and this means that an extension of the optical penetration depth, expected for nanosecond pulses by the interface movement during the pulse, would not be as prevalent. Another effect, which can occur at picosecond timescales, is possible two-photon and multiple-photon absorption which would increase the effective absorptivity of the triazene [39]. Overall, the higher TP absorption for picosecond pulses points to higher energy gaseous products, possibly smaller fragments with higher kinetic energy, generated over a shorter time, along with reduced energy losses.

Considering the Gaussian beam profile of the Nd:YAG and the flat-top nature beam profile from the excimer laser, the flyer quality should decrease as a result of a combination of poorer beam energy homogeneity of the Nd:YAG laser than the excimer and the explosive ablation at the picosecond pulse lengths. But here is not the case, probably because the effect of the pulse is much more important than the beam profile.

Using picosecond pulse lengths to irradiate TP films causes significant changes to the ablation process when compared to the more commonly studied nanosecond pulse ablation. The shorter pulse length decreases the ablation threshold, ablates a shallower depth per pulse above a critical fluence, propels the shockwave and flyer faster, and appears to create a more fragmented flyer. These effects, except for the latter, are all mainly the result of the picosecond laser's pulse length timescale which creates higher energy ablation products by increasing the effective absorption of the triazene polymer and reduces losses due to the whole process happening faster [35]. In the next chapters we are going to analyze better the influence of the triazene thickness and how is that correlated with our results.

5.1.5 LIFT on a spin coated Alq_3 layer (Specific Experiment)

The deposition of the Alq_3 layer on the triazene layer by the spin coating method could introduce a much more inexpensive technique for the production of the donor. Subsequently, a potential application in industry could reduce the products which demands micro-fabrication processes.

For the LIFT experiment single pulses from a Nd:Yag laser (λ=355nm, τ=15ps) have been used The goal of this study is to transfer Alq_3 small molecules with

the picosecond-Laser in order to fabricate smOLEDs. The donor's structure was Triazene/Alq_3. The thin layer of the small molecules were deposited by spin coating, from a solution of (Alq_3:chloroform-10mg:ml), above a 100nm thick layer of triazene. The spin coating settings were 1000rpm for 15sec. The final thickness of the triazene-Alq_3 layer was 160±10nm.

From Figure 5-13 it seems that for a thicker layer of Alq_3 we could have better results. Better formation and a smoother layer can be transferred when the transferred spot is thicker than 100nm. Although a thicker layer than 100nm is too thick for OLED applications.

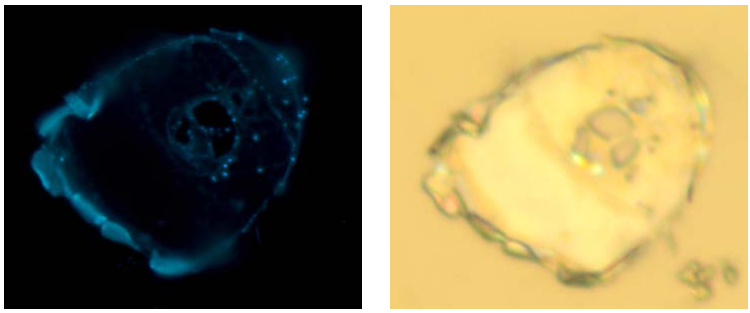

Figure 5-13: Transferred spot by LIFT (on the left-dark and on the right-bright field microscope pictures) at 26,2 mJ/cm^2

That pixel in Figure 5-13 came from a thicker part of the layer because of the waviness of the Alq_3-layer which was caused during the spin coating deposition of Alq_3. The transferred layer has no cracks, although folding effects are viewed as also a hole in the center where the material has ablated because of the peak of the light intensity in the Gaussian beam. Even though, the emitted light from the spot is not as much as some other spots emit which you can see in next paragraphs. Which probably happened due to the blending of the Alq_3 small molecules with the triazene or/and the interaction with the UV laser beam.

We can easily see in Figure 5-14 that there are some variations, in how the stack of the layers react to the irradiation of the laser beam, even in really small distances between the spots. That probably caused by the different thickness of the triazene layer in different areas on the sample. There are variations in the thickness of the layer of Alq_3 on the triazene layer and also in the thickness of the Alq_3 layer itself. We can also reach to the same results from the data are presented in the Table 3. The

thickness of the layers in the center differs from the thickness of the layers at the edges.

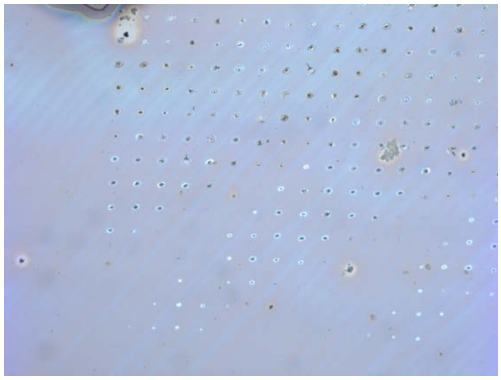

Figure 5-14: Microscope picture from a donor of stack (triazene/spin coated Alq_3) layer after laser ablation.

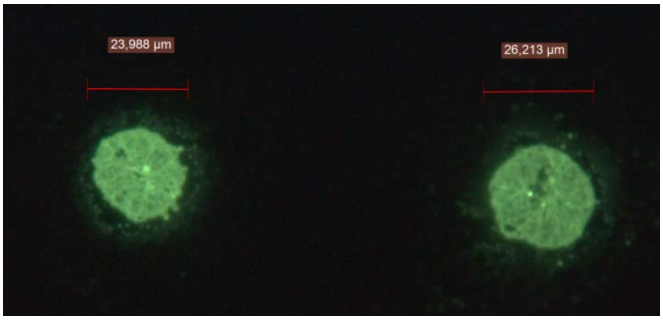

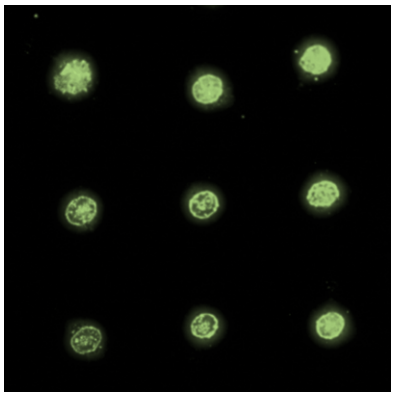

Figure 5-15: PL images of transferred pixels from a solution-processed Alq_3 layer(fluence: 16,2 - 29.5 mJ/cm^2 *~in focus)*

In Figure 5-15, you can see the transferred pixels. As it has already mentioned It is very difficult to use the spin coating method to deposit the Alq_3 layer because the chloroform which we are using as a solvent to dissolve the Alq_3 small molecules is dissolving the triazene layer during deposition. On the other hand the transferred spots had not been degraded but it is difficult to reproduce the same results for the same settings. The method we had used, does not allow us to totally control the results.

5.1.6 Reproducibility & ITO-Receiver

The reproducibility often is a big problem, especially when the human factor plays a critical role. For example during the preparations of the solutions, small differences in the concentration can create big variations in the final thickness of the final deposited layer. As each time a new solution of triazene were prepared, new

thickness measurements were yielded in order to determine the thickness of the produced layer of triazene for different spin coating settings.

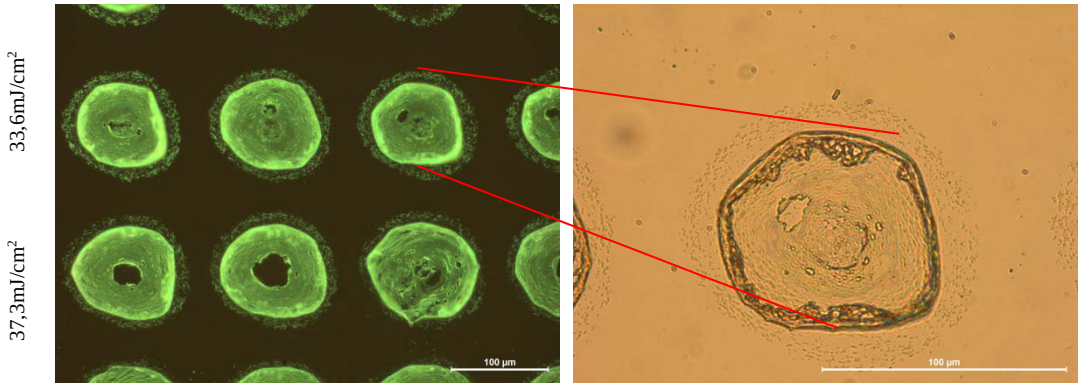

Figure 5-16: PL Image for LIFT of 100nm Alq_3 layer

We were able to achieve similar results and to reproduce pixels with the same quality but in different fluence. Also the ablation threshold in that case is different. That is mostly caused because of a different thickness at the dynamic release layer (Triazene). We used a new solution with triazene for the spin coating deposition, which probably create a thicker layer of triazene.

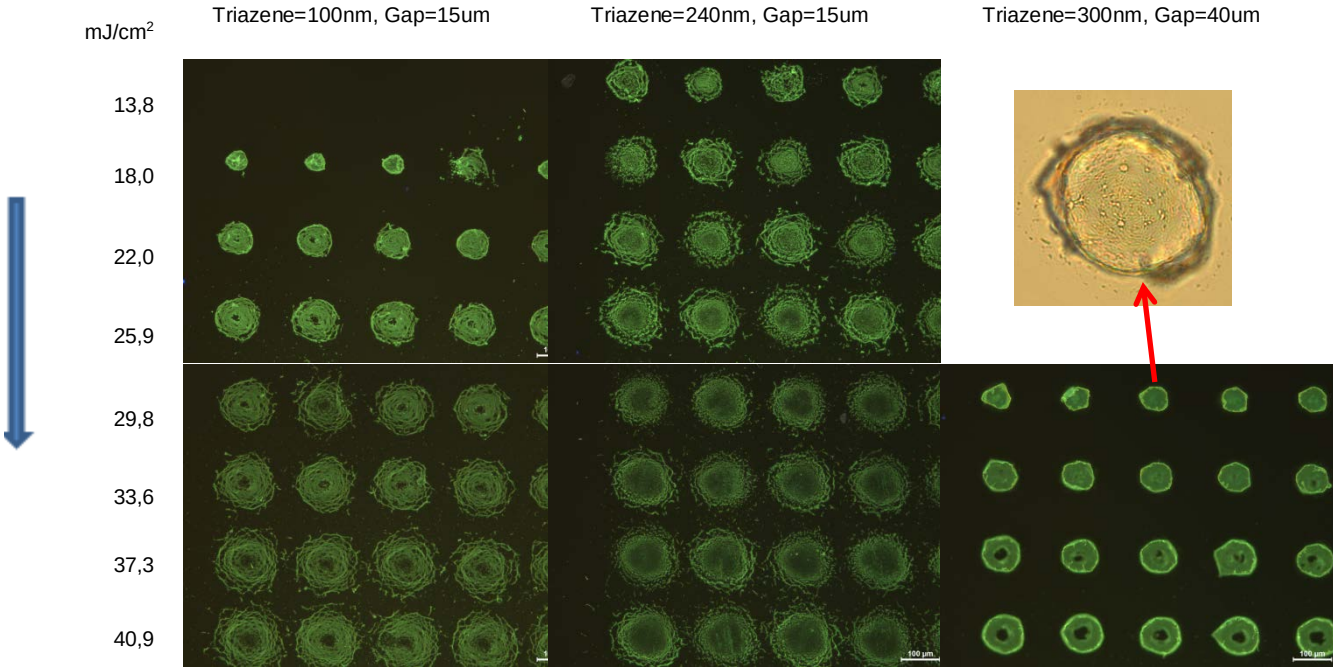

Figure 5-17: (PL Images) LIFT of 100nm Alq_3 layer on ITO layer for three different thicknesses of triazene after optimization. (out of focus)

The adhesive properties of the receiver could sometimes play a critical role. In our case the most preferable receiver is an ITO layer on a glass substrate regarding the

aim of that thesis. In Figure 5-17 are presented the deposited pixels of Alq_3 from donor of triazene/Alq_3 for the optimum settings for three different thicknesses of triazene.

The results are similar as when the Alq_3 small molecules were deposited on a glass substrates without the ITO layer. The different formation of the transferred pixels regarding the different thicknesses of the triazene layer have already described in paragraph 5.1.1.

5.1.7 Optimization of the pitch

During that study I also notice that the shock wave produced from a transferred pixel can also effect the previous transferred pixels which have already deposited on the acceptor creating folding at the edges of the pixels.

In Figure 5-19 is shown a pattern of Alq_3 small molecules by DRL-LIFT technique. The donor was a stack of triazene (300nm) and Alq_3 (100nm) on a glass substrate. When the distance between the "LIFTed" pixels is decreased, the produced shock wave from the transferred pixel propels away and cause partly a folding at the edges at the previous "LIFTed" pixels. To achieve the best patterning each time for a different laser beam diameter and average pixel size, we have to certify the smallest distance between the pixels were the shock wave does not affect the previous pixels. As the shock wave is the cause of those formations, all the parameters that the shock wave be depends on, have to be considered. Laser characteristics, environmental pressure, gap between donor and acceptor, thickness of the transferred layer, thickness of the DRL are some of the factors we have to consider. In addition a correlation also between that effect and the diameter of the transferred pixel is obvious.

On patterning, another effect during that process was observed. When the distance between the spots is too small, the flyer drift with it the left overs of the material on the donor. Probably, the adhesive forces between the molecules of the same material are bigger than the force that keep the material stick on the glass surface. Also the mechanical shock during detaching could be one more reason for that or a combination of those two above.

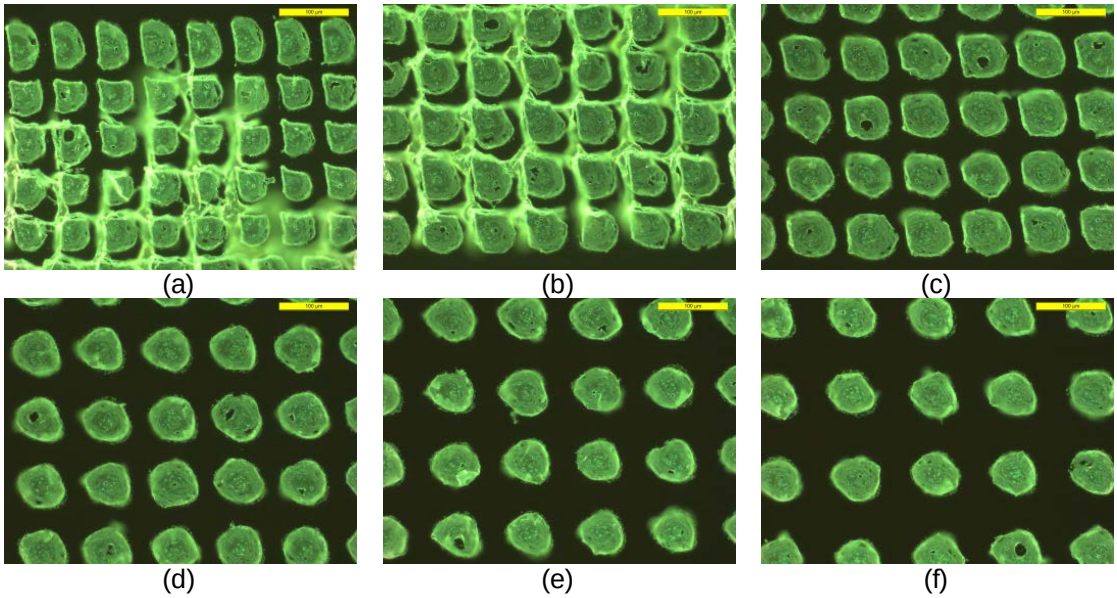

Figure 5-18: (PL Images) Patterning for different distances between the pixels for an average size pixel of 65 μm., (a): distance=65μm, (b):distance=65μm, (c): distance=85μm, (d): distance=95μm, (e): distance=105μm, (f): distance=115μm.

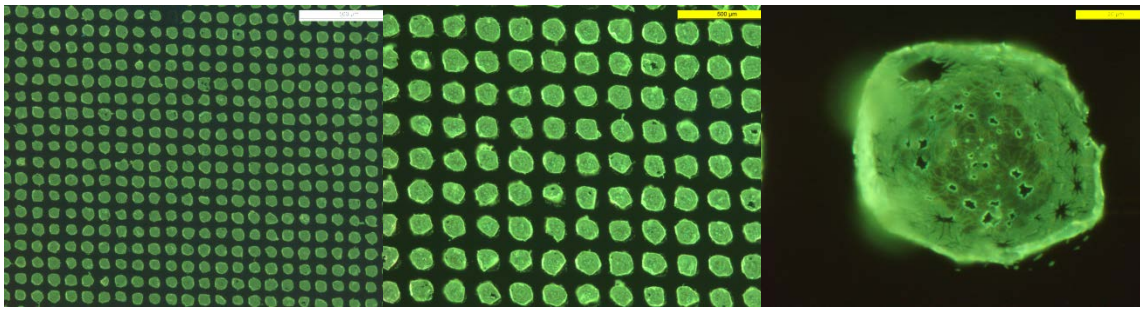

Figure 5-19: (PL Images) (a,b): Patterning a big area of Alq_3 small molecules with the LIFT technique. (c):The average diameter of the transferred pixels is 65 μm.

5.2 DRL-LIFT on IMEC'S Light Emissive Layer

During this thesis some experiments of LIFT had been done with IMEC'S LEL small molecules as the transfer layer (20nm). The DRL was triazene polymer. Experiments for two different thicknesses of triazene had been done (100nm and 300nm). The laser beam produced from the Nd:YAG picosecond-laser at the wavelength of 355nm (15ps). In Figure 5-20 the transferred pixels are shown after patterning with the LIFT technique at 0,75 J/cm^2. The average size of the transferred spots was 60 μm and the average spot size of the beam on the donor was 87 μm.

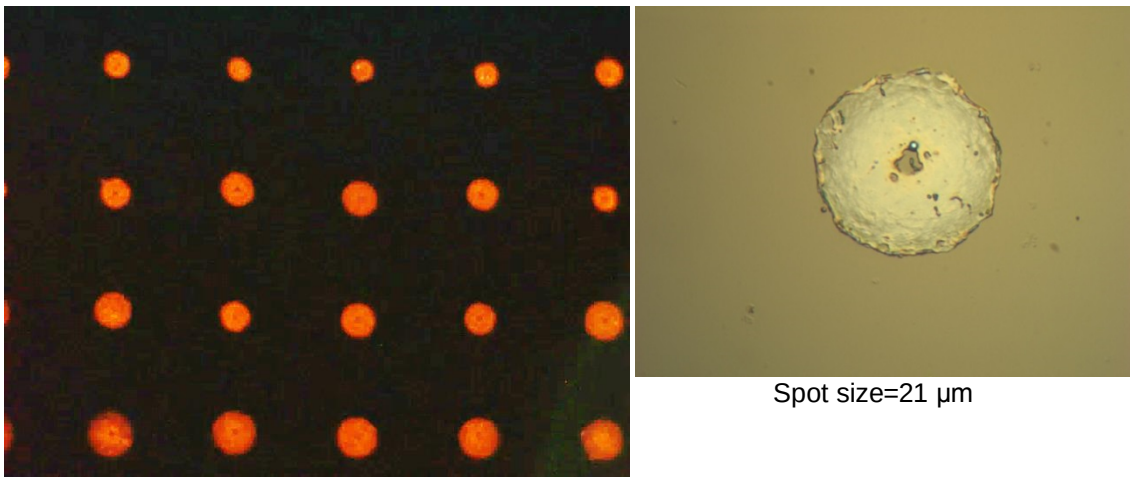

Figure 5-20: Photo-luminescent microscope pictures of the IMEC'S LEL LIFTed pixels

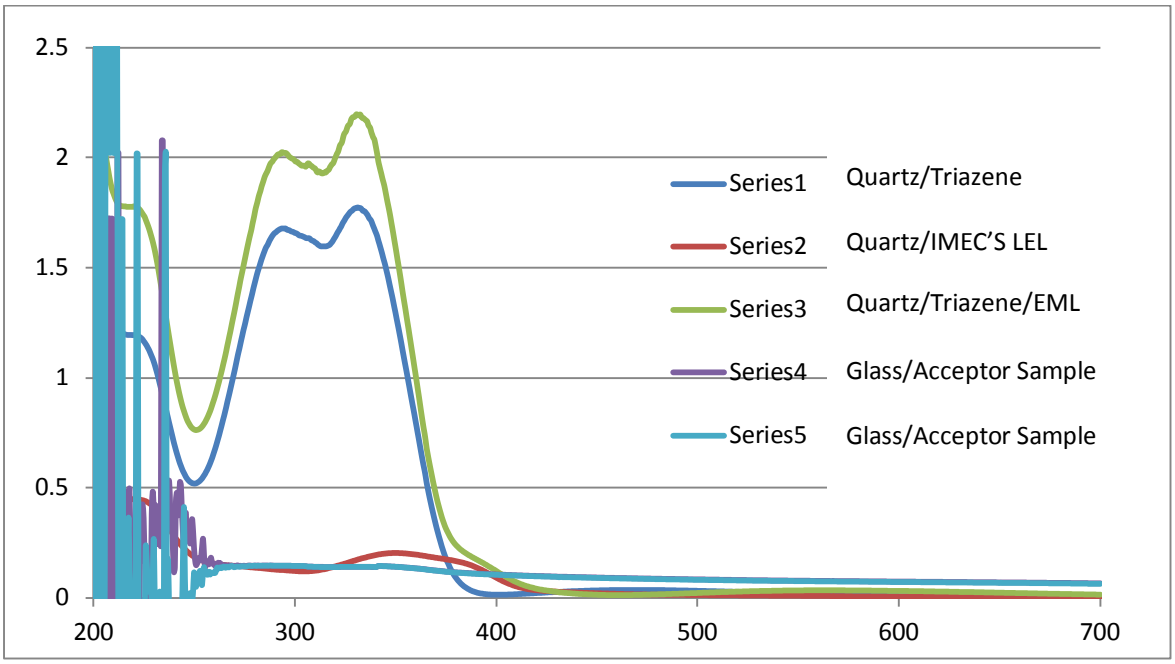

Graph 5-16: UV-Vis measurements for the donors and the acceptor before and after the LIFT process in ambient environment.

Better results yielded after increase the thickness of the triazene layer to 300nm. The optimization of the transferred pixels had been done in ambient environment and the final patterning had been done in the environmental chamber. To achieve an inert environment into the environmental chamber we fill it up with nitrogen and we plug in the vacuum valve several times. In Figure 5-20 are shown the yielded pixels which had been transferred by the LIFT technique. The structure of the donor consisted from a stack of layers: 100nm Triazene/20nmIMEC'S LEL. The

triazene layer was spin coated on a quartz plate before the IMEC'S LEL was thermally evaporated above.

In Graph 5-16, UV-Vis measurements for the donors as also for the acceptors are presented after the LIFT in ambient environment. Those measurements indicate the presence of a dead layer on the acceptor. Photo-oxidation, thermal effects, H_2O and O_2 are some of the reasons that the material degrades after the transfer. The same experiment repeated, but this time the environmental chamber were used in rder to achieve the LIFT process in an inert environment of vacuum or N_2. The donor were kept in the glove box before and after the LIFT process and only touch the air during the set-up of the experiment. The acceptor, also have been kept in the glove box after the LIFT process and afterwards, both of them sent for photoluminescence measurements.

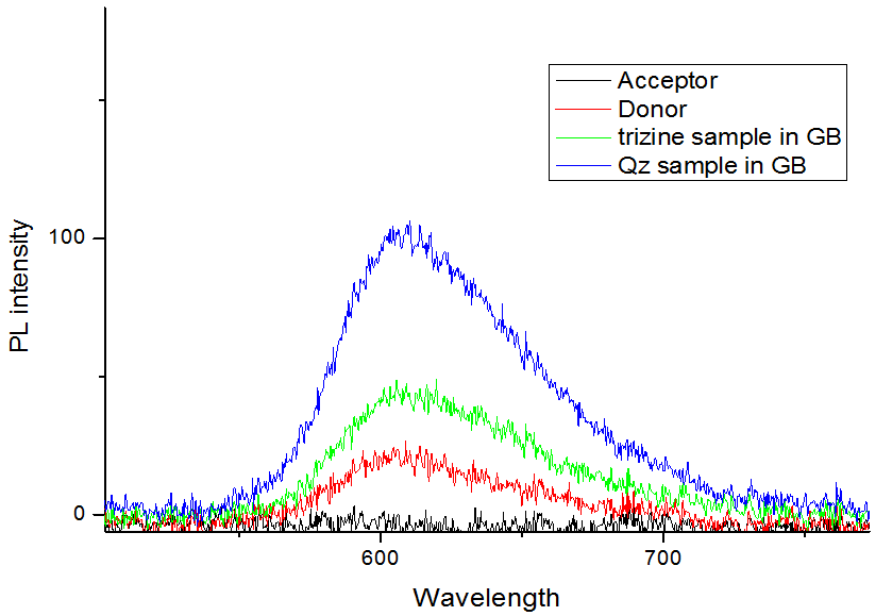

Graph 5-17: PL measurements for the donor and the acceptor before and after the LIFT process in inert environment.

The microscopy pictures(Figure 5-20) indicate a still alive layer of the light emitting material, but the PL measurements do not. Considering that the LIFT happened in an inert environment, we have to study further the effect of the light from the laser beam and the temperature diffusion on the transfer layer during the LIFT. On the other hand , the material seems not to have degraded on the donor sample. (Graph 5-17)

5.3 Hydrogen Assisted-LIFT on Alq_3

The main goal of that experiment is to transfer Alq_3 small molecules by light induced forward transfer straight to a receiver substrate. The spots should have a nice formation and the small molecules should not be degraded. In order to achieve that goal we had also used different dynamic release layers(DRLs). One of those layers was a SiN layer, which after irradiation release hydrogen which propels the layer to deposit on the donor. The technique has already been described in the paragraph 1.2.5

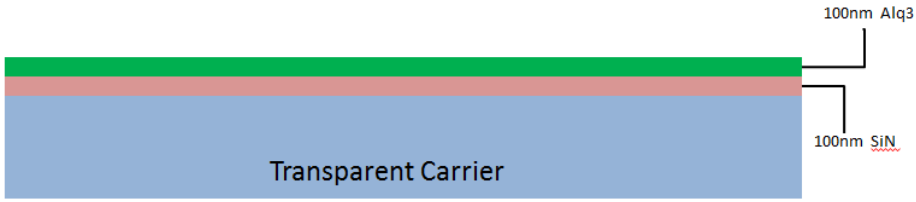

Figure 5-21: Schematic of the donor for the HA-LIFT

Some attempts of patterning small molecules had been done by using that technique. The donors were SiN:Alq_3/200nm:100nm (Figure 5-21). It was used the pico-laser system (10ps) at the wavelength of 1064nm and 355nm and the Excimer laser as well. The pixels, which were deposited, had not a smooth surface. The small molecules transferred mostly like a powder and not as compact layer.

In Figure 5-22 the same structure of donor were used, but the experiments made by a different system of laser. An excimer laser at the wavelength of 248nm was used. Similar results had been achieved with the transferred pixels of the Alq_3 small molecules being rough. The “LIFTed” pixels which had been fabricated by the picosecond-Laser at a wavelength of 355nm are shown in Figure 5-23. The settings of the experiment were kept the same and we only changed the wavelength of the laser beam as also the gap.

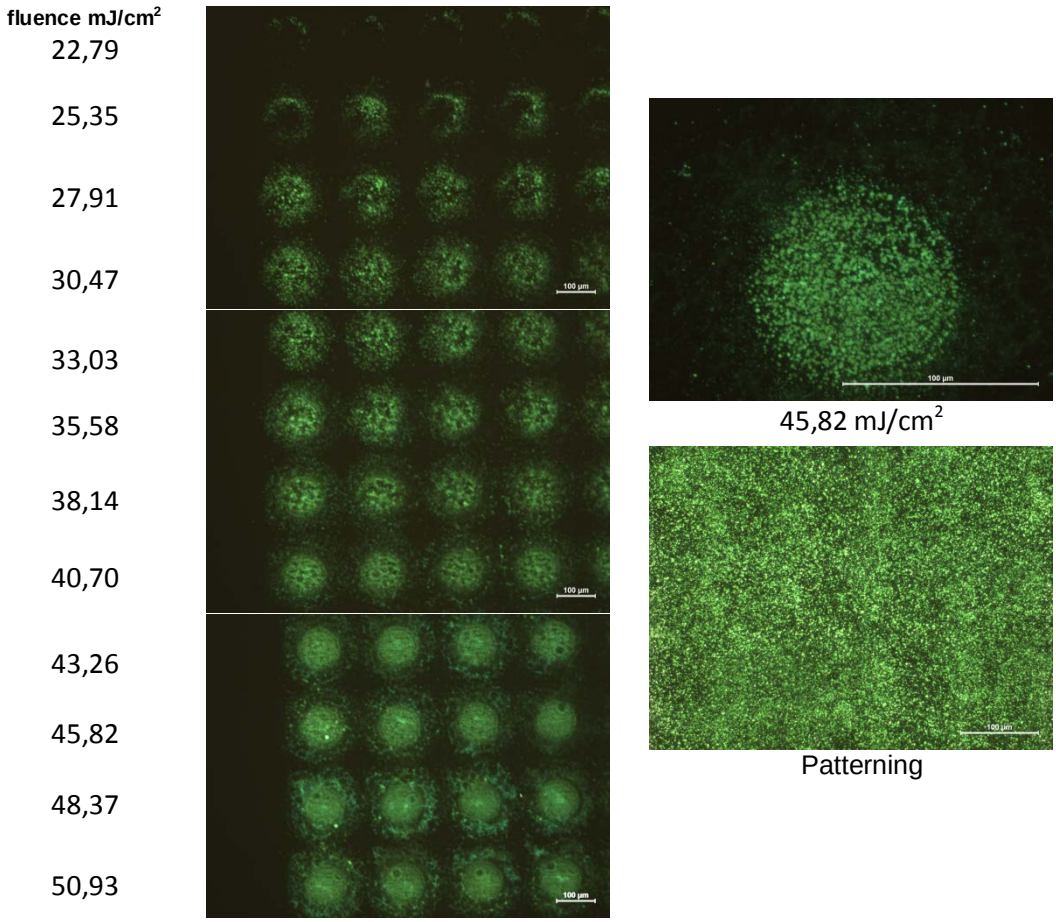

Figure 5-22: LIFT of evaporated Alq_3 using SiN as DRL.(excimer laser- TU/e ~248nm ~40μm gap)

The hydrogen which is released during the transferring procedure propels the Alq_3 layer to the donor. The quality of the transferred pixels was not good enough for OLEDs fabrications. Mostly agglomerations of Alq_3 had been transferred instead of a compactness layer. That probably happens because the produced gases during the transferring entering into the sintered Alq_3 layer. The porosity of the Alq_3 layer combined with the absence of sacrificial layer which allows the total defoliation of the layer led to those results. However, the photoluminence properties of the small molecules did not degrade (Fluorescence microscopy).

The same experiment repeated using the picosecond laser and the 1064nm wavelength, but the results were the same as before.

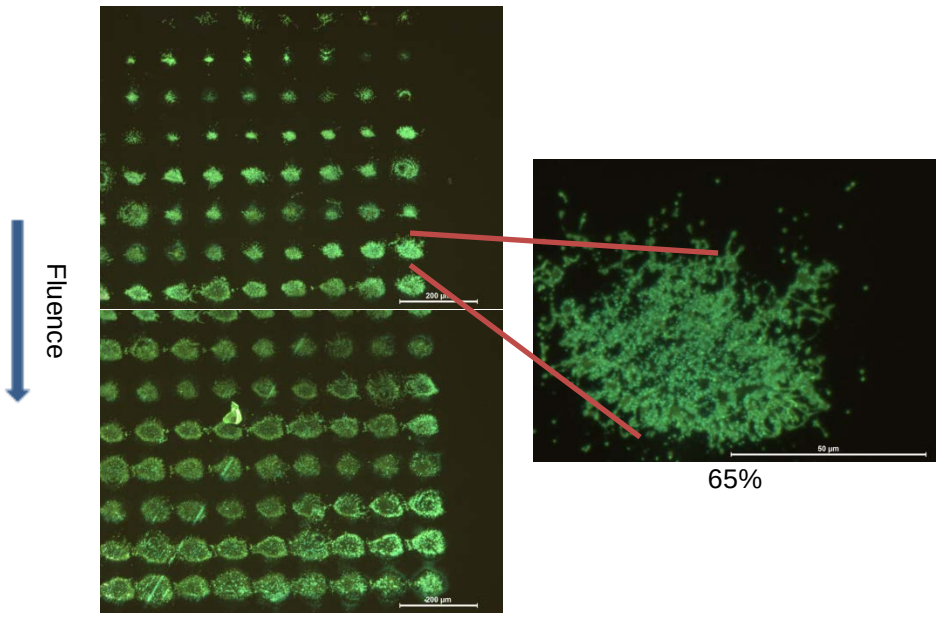

Figure 5-23: LIFT of evaporated Alq_3 using H/SiN as DRL.(Pico-Laser ~355nm~15 μm gap)

5.4 Novel Use of Triazene-DRL (Copper ablation)

The complex mechanism of polymer ablation has been extensively looked at elsewhere, but still has many unanswered questions. TP ablation clearly has a photochemical element to it, in the direct photocleavage of the aryl-triazene chromophores. However, observations have shown that purely thermal decomposition of TP yields almost identical ablation products [40], epitomizing the extent that chemical and thermal decomposition of triazene polymers are intertwined.

Based on that, a new idea of a different use of the triazene came up during that project. The thickness of triazene is one of the main factors for a smooth transfer of the as transferred layer. But as already had been referred there are other factors that effect a good quality transfer. A thin layer of triazene needs more energy to be totally decomposed below a certain thickness. We have also get the best of our results for thicknesses around 300nm. The challenge then, is to ablate a thin layer of triazene without leave the correlating factors to effect the transferred layer.

Taking advantage of the potential thermal decomposition of the triazene we can use an interlayer between the substrate and the triazene layer to play the role of the light to heat conversion layer(LTHC). We name that technique Direct Release

Layer-Light induced Thermal Imaging (DRL-LITI) technique to point out the combination of the DRL and the use of the thermal decomposition. Thermal decomposition of the triazene happens around $230C^0$.

The idea is to use a very thin layer of triazene as a DRL. Triazene 's ablation is very explosive and cause a strong trust to the transferred layer. A thinner layer of triazene could push the Alq_3 layer more gently. But higher fluencies will be required to ablate such a thin layer. Which means that even more energy will reach the Alq_3 layer. After adding a light to heat conversion layer beneath the triazene, we could cause thermal ablation to the triazene instead of photo-thermal ablation.

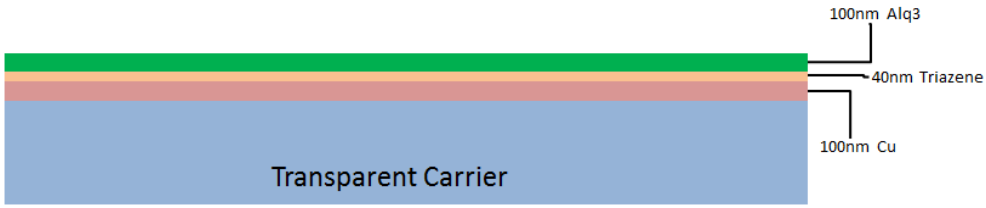

Figure 5-24: Schematic of the donor for the DRL-LITI

The preparation of the samples was similar to the preparation for the donors with triazene and Alq_3. The difference now is that we also add one more step before the spin coating of the triazene, where we deposit by vacuum evaporation an thin layer of Cu. The same laser set-up was used during those experiments. In Figure 5-24 is shown the stack layer of the donor.

The layer of the copper is a strong block layer of the 355nm wavelength (Graph 5-18). Considering that the optical penetration of the copper for the 355nm wavelength is 14,7nm that means that with a 100nm layer of copper before the triazene layer almost no light reach the triazene layer. Off course we have to make sure that the layer of the copper remain untouched from the laser beam which means that we have to work with fluencies lower than the threshold ablation of the copper layer.

During our experiments we have also calculate the ablation threshold of a copper layer-100nm thick, which is the thickness we also use.

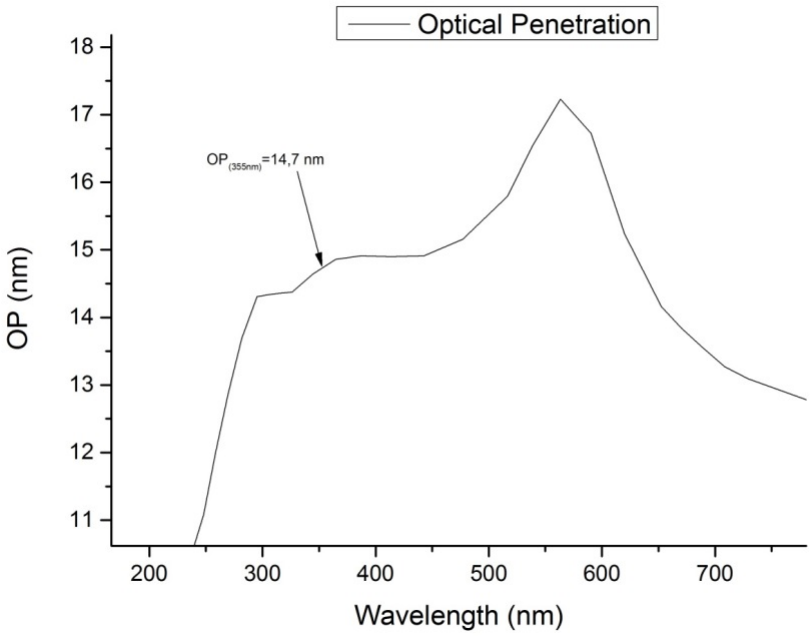

Graph 5-18: Optical penetration Copper for different wavelengths

5.4.1 Optimization of the fabricated pixels

The first attempts were promising. But the biggest problem we had to deal with during that part of experiments was the lack of the homogeneity to the fabricated pixels. The process window in that technique is very narrow, and when we have to work near to the threshold ablation, issues like inhomogeneity are always present. The different donors had been checked was:

- 100nm Cu/ 140nm TP/ 100nm Alq_3
- 200nm Cu/ 140nm TP/ 100nm Alq_3
- 100nm Cu/ 60nm TP/ 100nm Alq_3
- 200nm Cu/ 60nm TP/ 100nm Alq_3

After the characterization with the microscope of the fabricated results a thinner layer of copper and a thinner layer of triazene is preferred. By using thinner layers of Copper and triazene the process window become wider. We now can observe homogeneity.

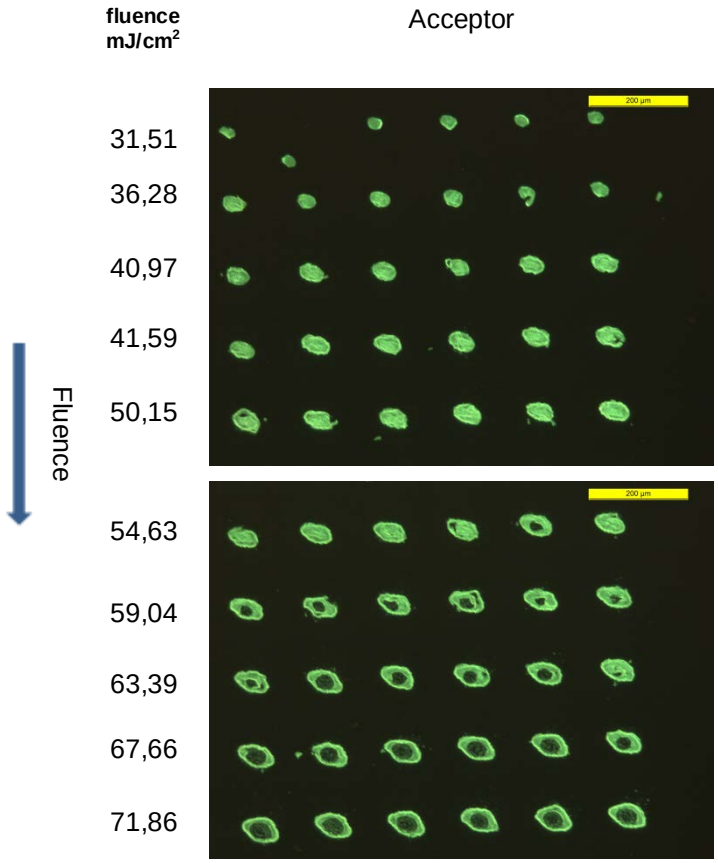

Figure 5-25: (PL Images) Receiver after the LIFT of an Alq_3 (100nm) layer using Copper-Triazene(100nm-40nm) as DRL.

Finally we have to mention that after checking different gaps between the donor and the receiver, we decide to choose the contact mode for that technique. By using contact mode we decrease the transfer threshold. That probably happens because the adhesive forces between the Alq_3 layer and the receiver surface which in combination with the irradiation with the laser beam, they cooperate to release the layer of the Alq_3.

In Figure 5-25 is shown the receiver from fluence scan of the donor and the fabricated pixels. What in general had observed is that we can define in that case two basic steps by increasing the fluence of the laser. In low fluencies the Alq_3 starts transferring without the lase fluence effect the copper layer. The second step is when the copper starts also to be ablated which means that the laser fluence is higher from the ablation threshold of the copper layer. In that case after 31,51mJ/cm^2 we can see that we have LIFT but the copper starts to ablate after 54,63mJ/cm^2.

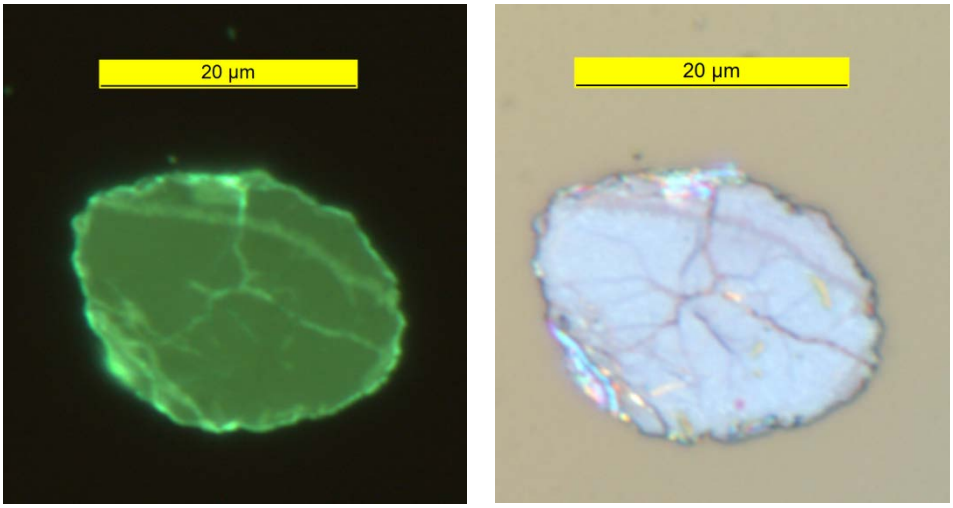

Figure 5-26:Fabricated pixels using copper-triazene as a DRL(right: PL img, left: Bright field microscope img)

As you can see in Figure 5-26 where are presented the fabricated pixels from a Cu/triazene/Alq_3 donor. Those pixels after the characterization with the optical microscope seems to have a really good surface and do not have any more holes or fragments. Furthermore the folding effect had almost totally reduced. Only a few cracks exist. Furthermore the deposited pixels do not lose their photoluminence properties.

The fact that we are not using a gap helps to achieve a more gently deposition of the transferred layer. We decrease a lot the shock wave effect, and we achieve a smoother transfer. On the fabricated pixels there are no folding at the edges or holes and cracks on the surface. The surface had studied further in the next chapter. Furthermore, in that case we can also reduce the pitch limit or even make it extinct.

5.5 Characterization

5.5.1 Surface characterization

The characterization of the surface if the fabricated pixels by using the optical microscope is not enough to conclude our results. That the reason we got for some AFM measurements and also for some photoluminescence measurements. In the next paragraphs I will present you what are the results from the AFM measurements.

5.5.1.1 Triazene-Alq_3

As we already mention the “LIFTed” pixels, has still some surface imperfections, which do not allow to continue further for the fabrication of an OLED device. With the optical microscope we can see some cracks, holes and folding on the edges. To certify even more are assumptions about the surface we made some AFM measurements at one random pixel at the optimum settings as those had mentioned in paragraph 5.1.3.

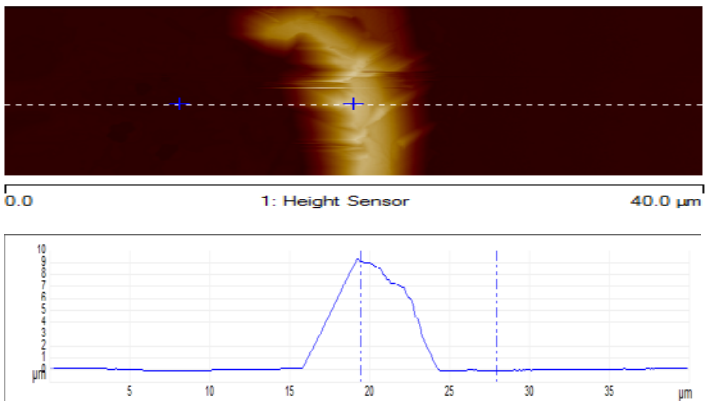

Graph 5-19: AFM Measurements at the edges of a LIFTed pixel.

At the edges, it had been measured a step height of 8,5 µm (Graph 5-19). That declares the folding at the edges. Furthermore, in all the surface area except the roughness there is also, a waviness and it seems to be because the lifted pixel is not touching the glass surface all-over its surface. From that we can also assume that the adhesion will also be low.

Furthermore in Graph 5-20 we can see that waveness and some holes but also we can see that the transferred layer is about of 300nm which is not agree with the initial assumptions for the transferred layer. The thickness of the Alq_3 is only 100nm but this is not seem in these results. Those peaks could be debris from the triazene, but if those were debris the height variations should were sharper. Last, one more explanation for that could be that part of triazene did not ablate during the irradiation of the donor and deposit on the receptor above the Alq_3 layer.

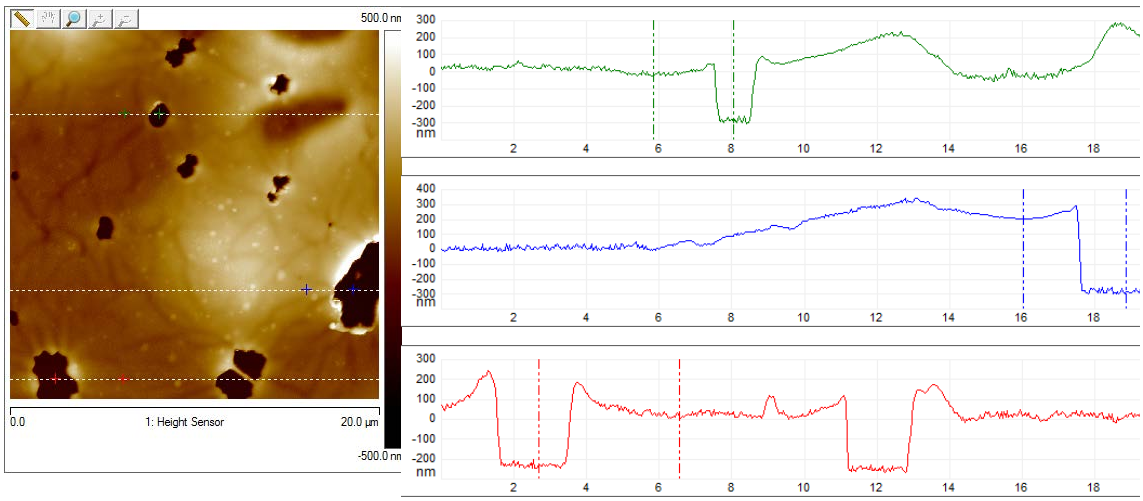

Graph 5-20: AFM Measurements of a LIFTed pixel.

5.5.1.2 Copper-Triazene-Alq$_3$

The transferred pixels came from the triazene-copper DRL looks really promising. In general in Graph 5-21 you can easily see that the roughness of the surface had really improved. There are no holes or cracks, neither waviness on the surface. In some parts there are some step-heights which could possibly be some impurities on the surface. The folding effect has reduced a lot. But the height of the pixel is about 180nm which declares that also the triazene layer has transferred with the layer of the Alq$_3$. So we transferred a bilayer of triazene(60nm±10nm) and Alq$_3$(100nm±10nm). In reality, the copper layer is thermally shocked from the laser beam and that cause the detaching of the bilayer of triazene/Alq$_3$ from the copper. Nonetheless, this technique could further be optimized and it other variations could be applied to different cases.

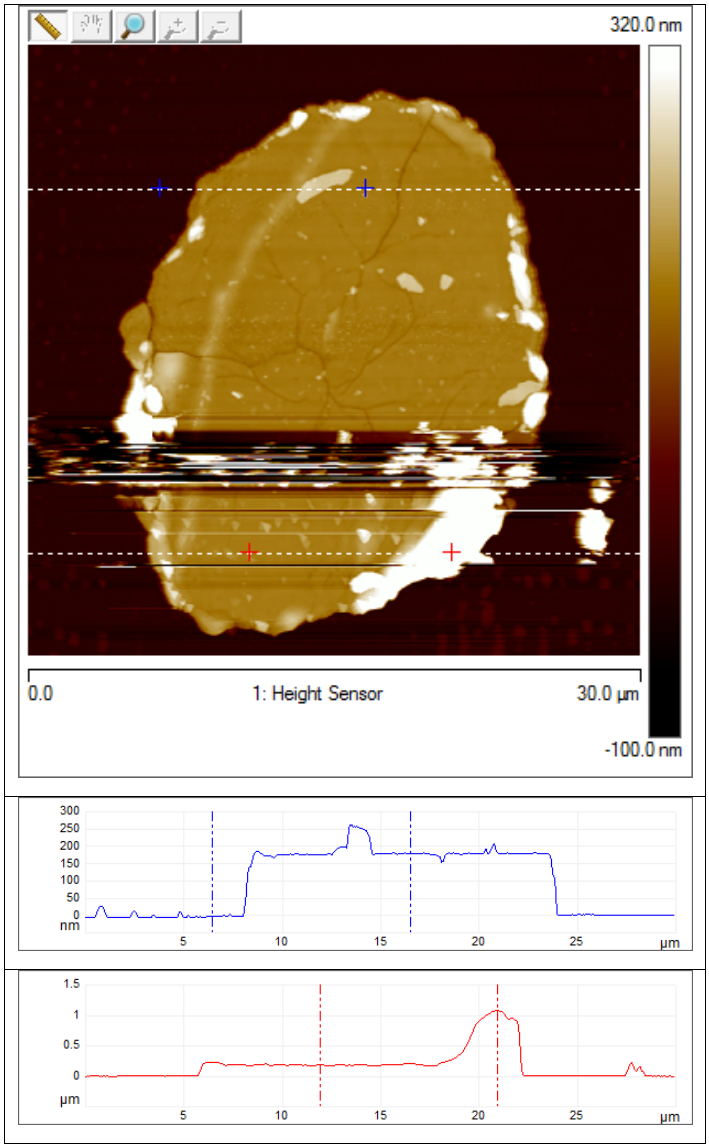

Graph 5-21: AFM measurements of a LIFTed pixel by Copper-Triazene technique

5.5.2 Photoluminescence measurements

Crucial for an functional OLED device is to preserve the photo-emitting properties of the materials. In our case the most used material was Alq_3 small molecules. Alq_3 small molecules according to previous studies does not degrade so fast in comparison with other materials. To investigate further if the LIFT procedure destroys those properties of the Alq_3 we made some measurements of the Photoluminescence properties of the material before and after the LIFT process.

The donor was a stack layer of 300nm triazene and 100nm Alq_3 on a quartz plate. The acceptor was also a quartz plate and one more sample with only Alq_3 was used as the control sample.

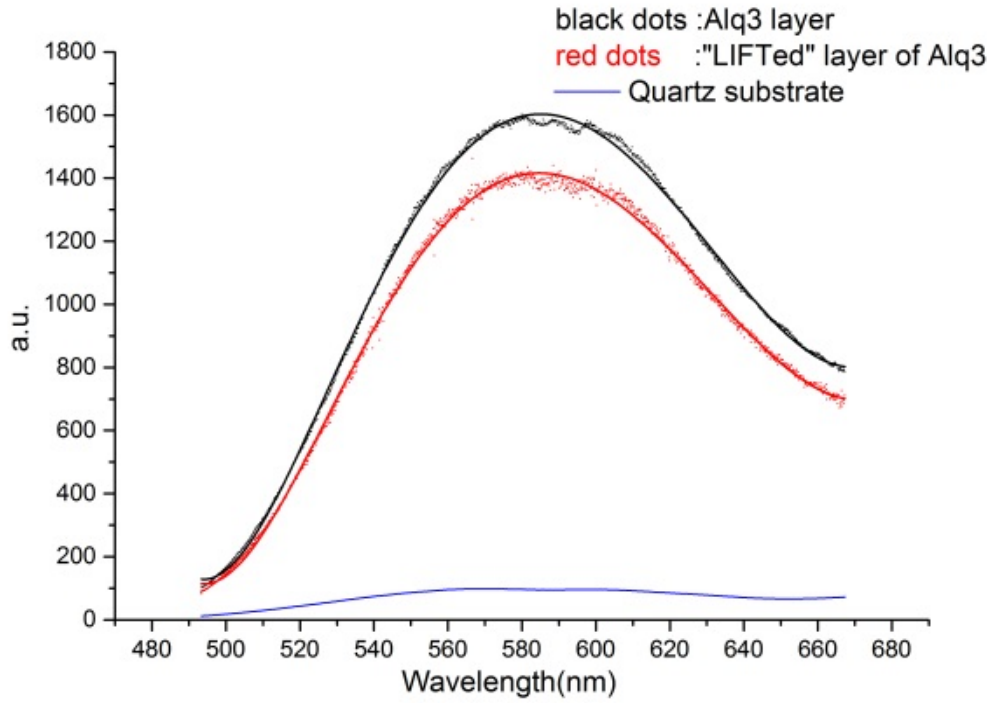

Graph 5-22: Photoluminescence measurements

In Graph 5-22 the results from the photoluminescence measurements are presented. For all the measurements the excitation wavelength was 457nm. The blue line is originate by the quartz substrate which is the background for our samples. The red line is the photoluminescence photons came from the fabricated pixels after the patterning of them by the LIFT process, and the black line is representing the photoluminescence properties of an Alq_3 layer without any other interference on it. All the samples were kept in the glove box and they were exposed in the ambient environment only during the LIFT process and curing the photoluminescence measurements. The scale of the degradation remains in low levels. The pattern of the transferred pixels on the acceptor keeps almost all the photoluminescence properties of the evaporated Alq_3 layer.

5.6 Vapor healing of Alq_3 pixels

During this thesis some experiments about founding a way to heal the layer of Alq_3 were yielded. The transferred pixels of Alq_3 are not in a very good quality. Some ideas is to try an annealing method to make the layer smoother and change the quality

in such a way that it would be possible to deposit on the top a metal cathode without injecting in the fragments of the layer. First we tried by leaving the sample with the transferred pixels on a hot plate. We baked the samples overnight on a hotplate in 70^0C.(Figure 5-27) After the hot plate we were not able to notice any difference on the surface of Alq_3 by using the microscope.

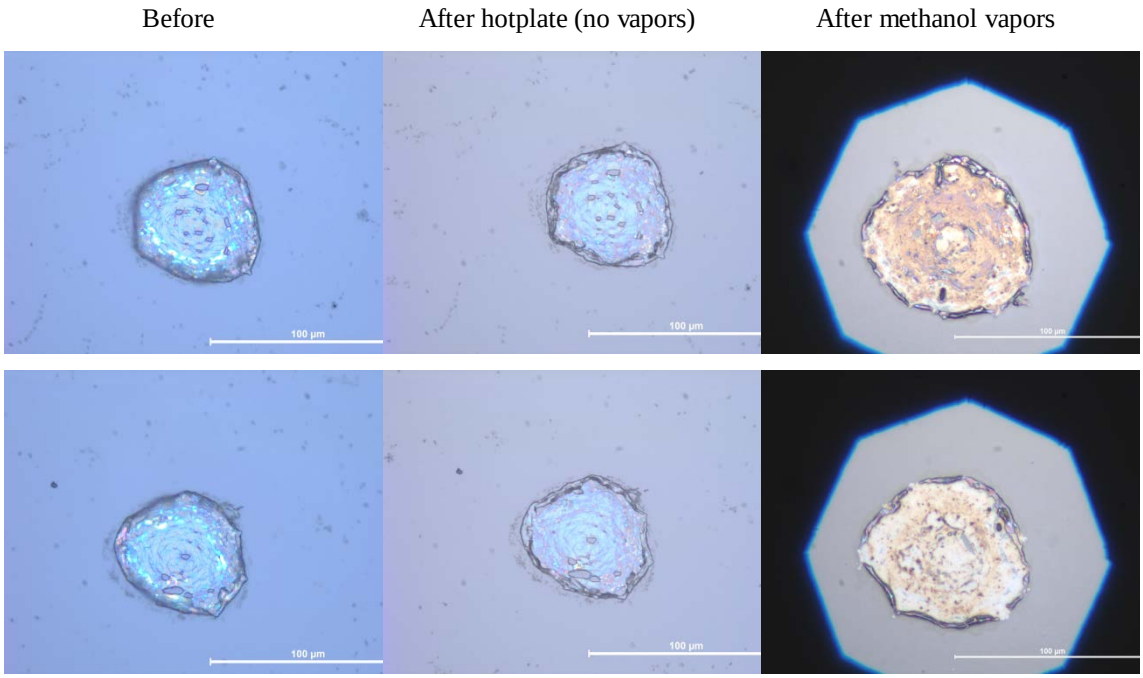

Figure 5-27: Alq3 annealing

Furthermore, some vapors of methanol were used to heal the Alq_3 layer. The vapor healing had been done by adding some methanol vapors in the same box which is used for the LIFT experiments. The results are presented in Figure 5-27.

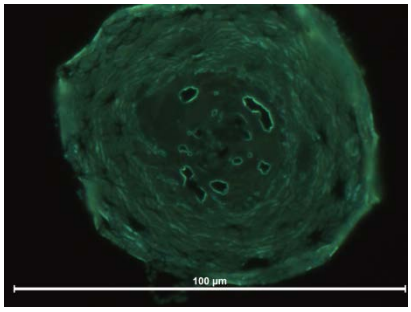

Figure 5-28: PL microscope picture after hot plate without methanol vapors

After vapor healing in a static pressure environment (1atm) with high concentration of methanol vapors, where the sample with the transferred spots of Alq_3

has been installed inside the environmental chamber before we poor methanol in it (ambient environment). The sample was left in the box for a night (18h). It's obvious that there is an important influence on the formation as also on the fragments of the surface on the Alq_3 layer. Furthermore the diameter of the spot increased almost 28%. Potentially that technique can be used to heal the surface of the transferred pixels of Alq_3, but it will needed more investigation to determine the right parameters for the best results.

On the other hand we noticed that the photoluminence properties of the layer after vapor annealing are disappeared unlike what had happened after hot plate annealing. (In Figure 5-28 we can see that there is still photoluminence after hot plate annealing). During our experiments we just create an environment of methanol vapors and atmospheric air which means that O_2 and H_2O remains in the box where we install the sample. One of the possible explanations is that the methanol vapors may change the surface but also allow to those molecules to diffuse into the layer and cause its degradation.

Further experiments had been done, but this time, all the procedure had happened in a glove box in order to avoid the presence of the harmful gases into the box during the vapor healing. The results are similar and a big degradation on the photoluminescence properties of the Alq_3 is noticed. Thar means that a kind of a chemical degradation happens when the Alq_3 small molecules are exposed to the methanol vapors.

On the other hand in the second experiment what was observed is that the surface of the transferred pixels had altered a lot after their exposure to the methanol vapors. These time the change was not a preferable alteration. The material starts to create droplet-formations, but this do not happen all over the surface of the material. We have to consider also the interface of the glass slide and the material. According to the AFM measurements the layer when is landing after the transfer creates some blisters on the surface creating in some areas of the pixel gaps between the Alq_3 layer and the glass slide. Maybe in that parts the methanol vapors fill up the gap and create that formations after the vapor exposure.

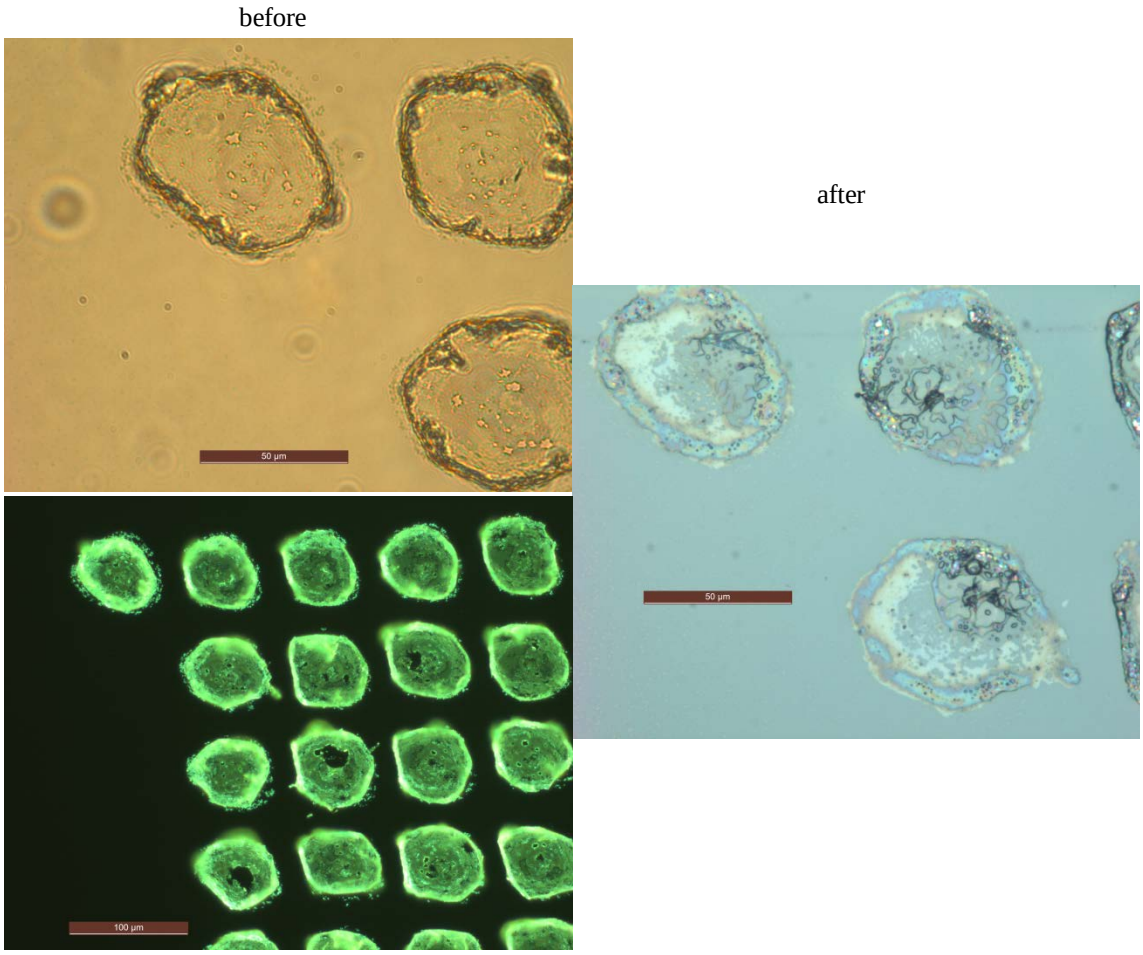

Figure 5-29: Alq_3 annealing in the glove box (nitrogen environment)

6 Additional experiments

6.1 LIFT on Super Yellow Polymer

In order to achieve the fabrication of OLEDs by the LIFT technique in the first part of that thesis small molecules were used as the organic material. But the unstable mechanical properties and the sensitivity of those materials were a big obstacle to achieve our aim. We also used an other material as organic emitting layer. Super Yellow was used, which is a polymer. The advantages of it in compare with the small molecules is that a polymer has more mechanical stability and it is also easily spin-coatable.

The approach will be similar to that used with the small molecules. So the idea was to pattern the Super Yellow on a substrate by LIFT technique. The PEL is spin coatable but the spin coating on a triazene layer will be tricky because the solvent we are using to dissolve Super Yellow is toluene which dissolve also the triazene. Furthermore, Super Yellow cannot be evaporated. So, it is necessary to find another DRL which can easily accept the SY above. Some options is to use a light to heat conversion layer or a hydrogenated a:Si layer. Those two techniques has already described in Chapter 1 (LITI and HA-LIFT). Furthermore the SY is possible to be transferable without the use of any DRL because of its properties.

6.1.1 HA-LIFT on Super Yellow

Our first attempt to pattern the Super Yellow polymer was by using the HA-LIFT technique. The DRL was a 100nm a:Si layer. During the evaporation of this layer in the presence of H_2 molecules of hydrogen was captured in the layer of a:Si and after the irradiation with the laser those molecules escape causing a thrust on the SY layer. The SY had been spin coated on the a:Si layer making a 80 nm thick layer of SY.

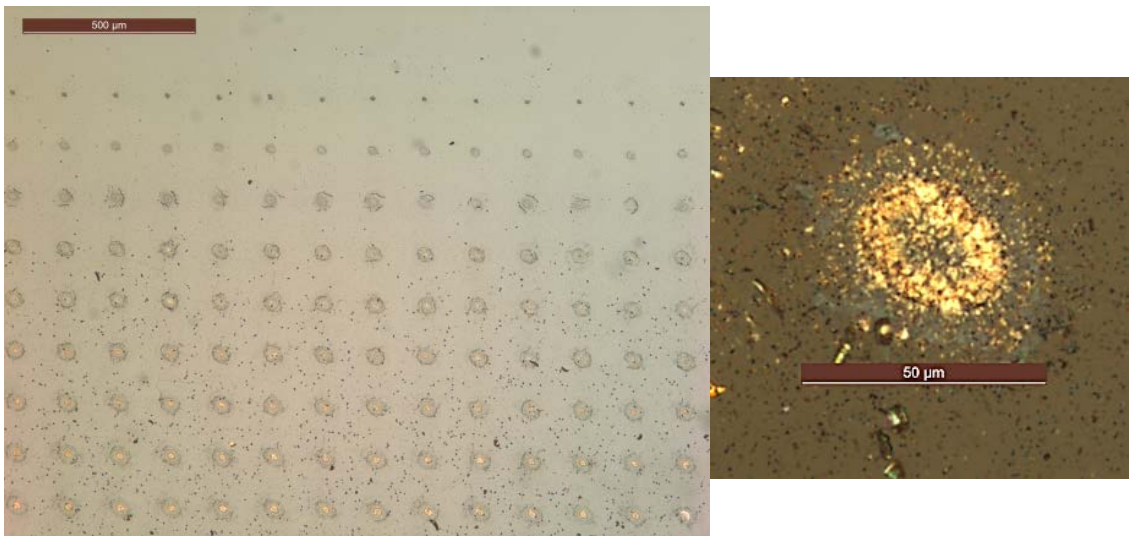

Figure 6-1: (left):Patterning for increasing fluence with Super Yellow on the acceptor, (right):Transferred pixel of Super Yellow by HA-LIFT technique

The result patterns formation was similar with the patterns which came from the same technique but for an Alq_3 small molecules layer. The “LIFTed” pixels had more transferred like a powder than a compact layer. In Figure 6-1 on the left corner is shown the yielded pixels on the acceptor made with that technique with the Super Yellow. On the left of Figure 6-1 is shown the yielded pixels for increasing fluencies and on the right is shown the best of the transferred pixels. As you can easily see there is homogeneity but the fabricated pixels is not acceptable for OLEDs applications.

6.1.2 LITI on Super Yellow

One more attempt with the Super Yellow had been made. This time the DRL was a Light to Heat Conversion (LTHC) layer. The donor consisted from a 100nm Copper layer and a spin coated layer of SY with 80 nm thickness. Afterwards during the experiments the Nd:YAG picosecond laser was used to do the LIFT process

In Figure 6-2a we can see a fluence on the donor of the Super Yellow. There is homogeneity as the fluence increase. We can see two basic effects of the laser beam on the donor. Initially, the laser beam cause only some thermal effects on the interface between the Super Yellow and the copper (Figure 6-2b). As the fluence increase, we exceed the ablation threshold of the Copper and the layer of the copper starts melting. For fluencies higher than that threshold we can see patterns on the acceptor.

The process window should be for fluencies lower than the threshold ablation of the copper, because otherwise the PEL will be destroyed during the ablation of the copper. The Super Yellow layer seems to have strong adhesion to the copper surface. As a result we do not have transfer at all before the Copper ablation threshold.

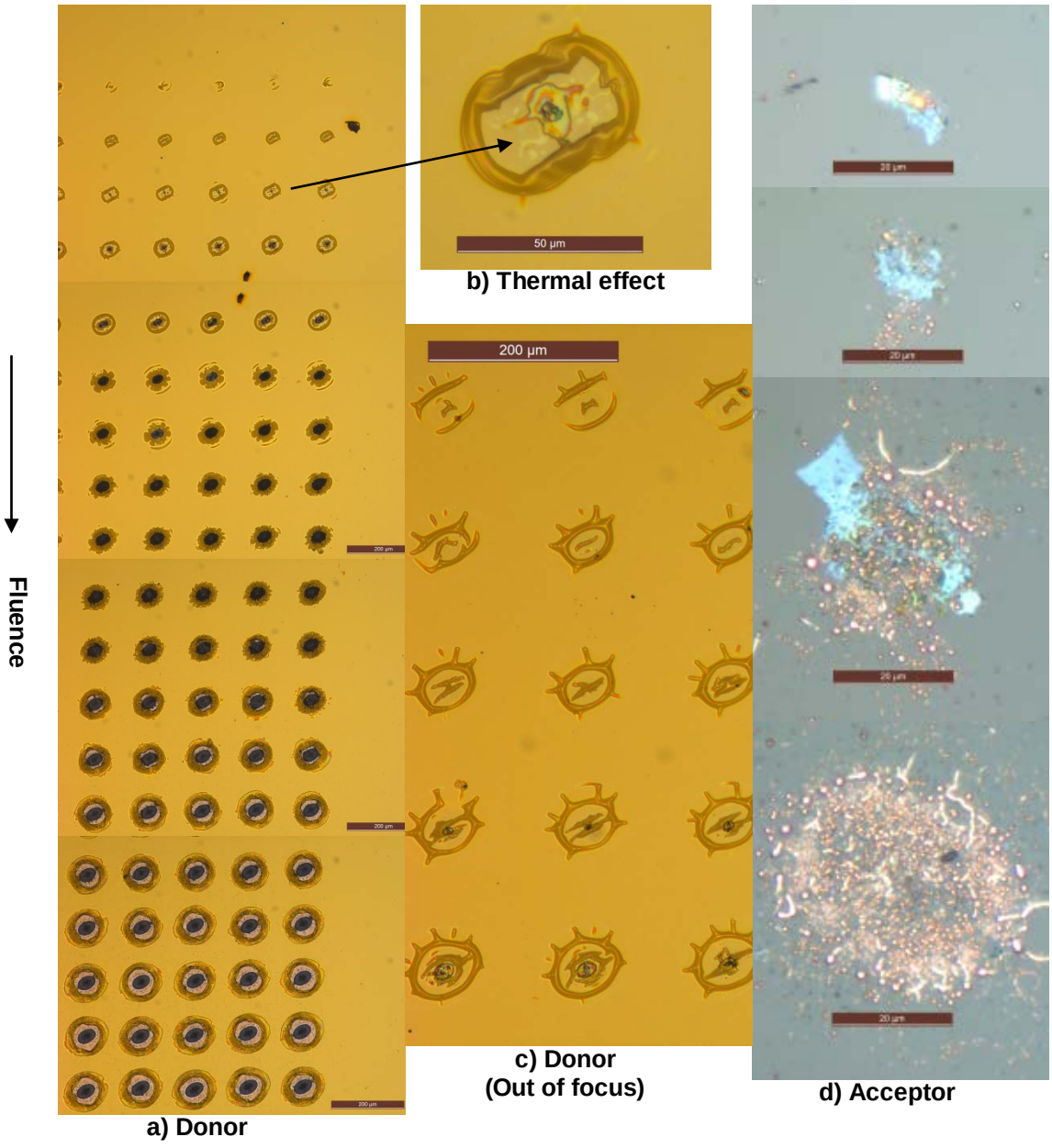

Figure 6-2: a) A fluence scan on the donor (Copper-Super Yellow) b) c) Thermal effect on the Super Yellow layer d) Transferred pixels of Super Yellow

6.2 LITI on Alq_3

After the first results from the experiments where the donor was consisting of a bilayer of copper an triazene we find out by the AFM measurement that not only the Alq_3 layer was transferring but also the triazene layer above.

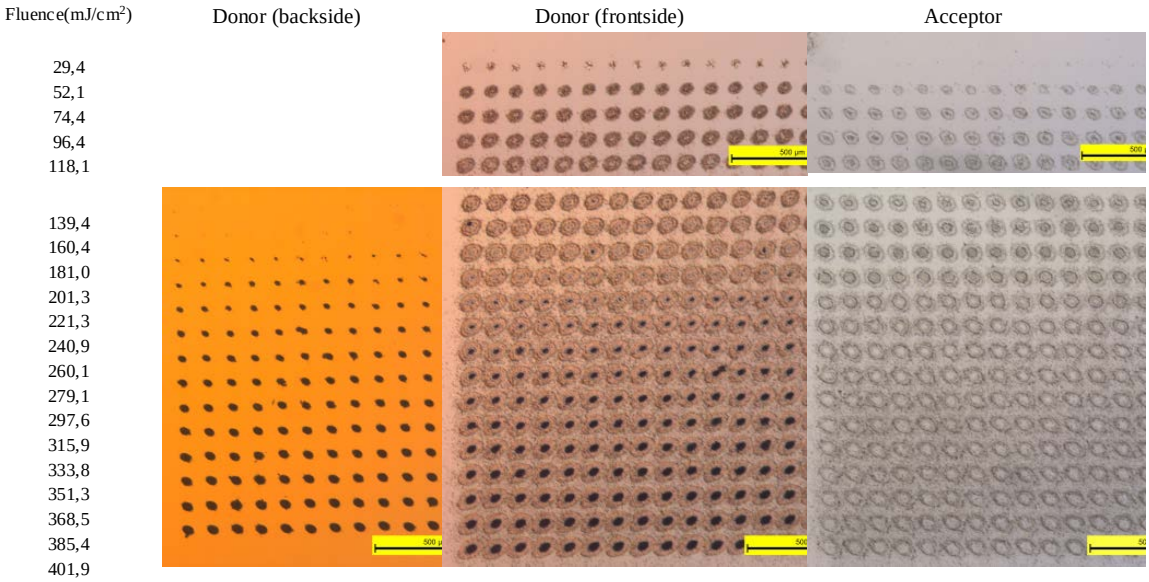

Figure 6-3: Microscope pictures of the donor and the acceptor after Laser-irradiation for a donor of Copper/Alq_3:100nm/100nm.

We repeat the experiments, but in that case without the interlayer of the triazene between the copper and the Alq_3 layer. We used some donors with a stack of a 100nm thick layer of copper and 100nm thick layer of Alq_3 and donors with the same thickness for the LTHL but with a thicker layer of 250nm Alq_3 above.

Transfer procedure was observed even fluencies with values a lot of lower from the ablation threshold of copper. In Figure 6-3 is shown the microscope pictures from the backside of the donor (direct to the copper side through the substrate), the frontside of the donor (direct to the lq3 side) and from the acceptor. As you can easily see, fluencies higher than 0,201 J/cm^2 is needed, to ablate the copper layer but the Alq_3 layer is affected for lower fluencies (0,029 J/cm^2). And transfer is observed for fluencies higher than 0,052 J/cm^2.

With higher magnitude microscope pictures, which are presented in Figure 6-4 we can study further the process.

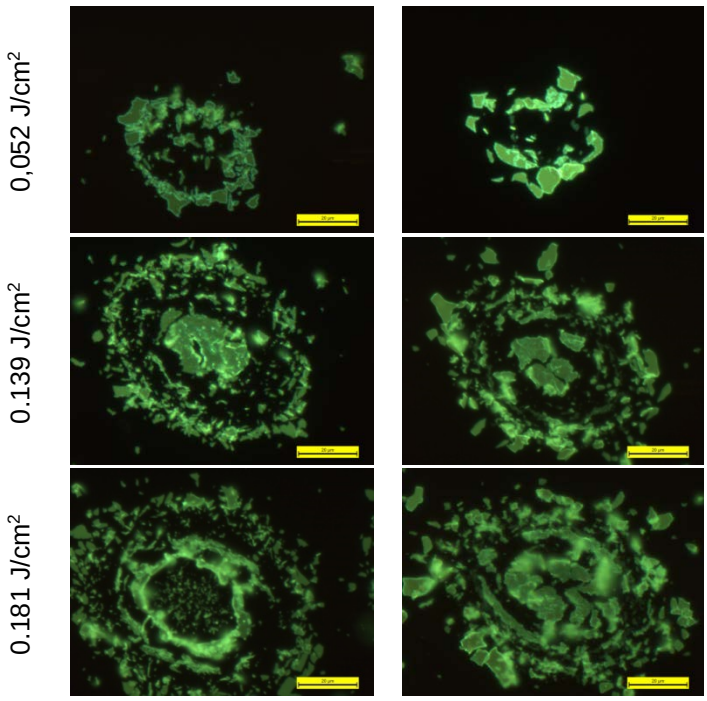

Figure 6-4: (PL Images) Microscope pictures of the patterns by LITI process from a bilayer of 100nm Copper/100nm Alq_3 on the left and from a bilayer of 100nm Copper/250nm Alq_3 on the right.

In the Figure 6-4 in the first row are shown the patterns made for the less needed energy and in the last for higher energies but lower form the ablation threshold of the Copper. In the left column the pictures concerns a 100nm layer of Alq_3 and in the right a layer of 250nm of Alq_3. As you can see the layer had transferred totally in fragments and no process window is noticed even after optimization of the settings.

7 Conclusion and outlook

The main aim of this project was to investigate the fabrication of a multilayer OLED by stacking sequentially light emitting organic materials by the LIFT process with the perspective of a mass and cheap production. To this purpose, first it is important to understand the laser material interaction with different pulse lengths and the dependence of optical properties of material on wavelength and temperature. Secondly, a good understanding of the working principle of LIFT is required to evaluate the obtained results. It is observed from experiments and various journal publications that LIFT is a very promising technique for micro-fabrications. Many experiments have been done and a lot of experience had been acquired from that project. In the next paragraphs we will attempt to write down the conclusions we had reach as also some recommendations about the next steps in that specific project.

7.1 Conclusions

Experiments with a Pico-laser as also with an Nano-laser had been done. The pulse of the laser beam effects our results a lot. The material we are using is very sensitive to heat as also the transfer process is very different when we are using different pulses. A shorter pulse length results in faster heating which ultimately results in a high temperature at the donor layer-substrate interface but longer pulse duration results in longer diffusion length and is capable of melting a thicker volume of the donor material which can also effect the as transferred material. A nanosecond pulse can melt a donor layer of few microns thickness while the picosecond pulse is limited by its shorter thermal penetration depth. The outcome of this work concludes that, picosecond system has more advantages on transferring such sensitive materials, like small molecules than a nanosecond laser.

The IMEC'S LEL small molecules are very sensitive to the ambient environment and in combination with the transfer process we are using, IMEC'S LEL is totally degraded after the transferring. On the other hand the Alq_3 small molecules are more stable, when we are referred on their light emitting activity and are more

promising to be the chosen for a technique like that. Alq_3 seems to maintain its photoluminescence properties for more than a week in ambient environment even after the LIFT process.

The spin coating method which is more preferable for the preparation of the layers has one big disadvantage. The solution which are using to deposit the layers should be compatible each other or else the deposition is not possible or is not controllable. In our case the deposition of an Alq_3 layer above a triazene layer was not possible because the Chloroform were dissolve part of the triazene and created mixtures of triazene and Alq_3 in different parts of the layers. Those variations did not allow us to control our results. As far as it concerns the spin coating method, I should add that I conclude that every time I was preparing a new solution, the solution were remained untouched only for a while. In general, I should certify the thickness of the produced layers before each experiment again. The solvents, I was using were very volatile and the concentration of the solvents were changed after a while.

Four different techniques were used to achieve our aim: Dynamic Release Layer-LIFT, Hydrogen Assisted-LIFT, Light Induced Thermal Imaging and the copper-triazene method. For all the those techniques, it is needed optimization for many parameters. Gap between donor and acceptor, the thicknesses of the layers which consist the donors, the geometrical set-up of the experiment (focus and beam profile), as also parameters which concern the kind of the materials we are using.

The HA-LIFT did not gave us good results because the material wes transferring more like a powder than a compact layer. Similar results for that technique had been acquired from the picosecond laser and from the nanosecond laser as well.

The other two techniques was given us more promising results. The DRL-LIFT involve the direct exposure of the triazene layer to the light and the transfer happens with less energy but the as transferred layer is still more effected in the laser beam. The best pixels had been acquired have on their surface still some roughness, cracks, holes and foldings on the edges. The method where it was attempted to thermo-ablate a thin layer of triazene initially was seemed to have promising results. After the AFM measurements is was proved that the surface of the pixel was

acceptable, but unfortunately also the layer of triazene was transferred with the layer of the Alq_3 and it was contaminating the fabricated pixels. We should add that AFM measurements declare that there are some adhesion weaknesses between the donor substrate and the transferred layer.

Finally after all those experiments, the conclusion is that the most promising technique for the fabrication of OLEDs by an ALq_3 layer with a laser technique is the DRL-LIFT, without rejecting and some other cases or techniques which with some variations could be optimized, but we will present those proposals in the next chapter. In that case some PL measurements has shown that the Alq_3 layer keeps its properties even after the LIFT process. Those, are very satisfied results, because the patterns built in an ambient environment. That means that there is in the future, the perspective for optimization of the quality of the pixels and for some potential applications.

The size of the fabricated pixel in general plays a critical role. The bigger area, which is transferred, become the worse quality pixels we fabricate. This is, probably because of the mechanical vibrations on the transferred layers. Their effect getting bigger as the diameter of the transferred layer getting bigger.

Super Yellow is a polymer. We were expecting the mechanical properties of that material to be the solution to the quality of the pixels. But the spin coating method, in that case is not possible. Different technique was mobilized to achieve the desirable results. LITI was that technique but the Super Yellow proved to have high adhesion on the surface of the LTHL (Copper) and no process window was observed before the transfer of the copper layer.

7.2 Future Recommendations

The case of the DRL-LIFT technique is a lot promising technique. But there are a lot of things that should be done to optimize even more the technique for the fabrication of a good quality pixels with unaltered photoluminescence properties.

One of the parameters which can be seriously affect the results are the optical set-up. Flat-top optics could be the next step for the optimization. Also, it can be checked the effect of an even shorter pulse to the triazene. In that study we saw that

the gap between the donor and the acceptor can play a critical role to that procedure. The produced shock could potentially controlled in such way than it can help to a smoother transfer of the material. As far as concerns the shock wave, the gap, the atmospheric pressure, the thickness of the transfer layer, the beam profile, the pulse duration as also the thickness of the dynamic release layer are affecting it. So, a right combination of those parameters could give a desirable result. More detailed it will be nice for the next step to study the effect of the shock wave to the patterns, for different thicknesses of DRL, gaps and for different environmental conditions (pressure). Extent study of the shockwave effect, for the above cases could give very important information and illuminate us in the process.

One more important factor in our case is the diameter of the transferred pixel. The bigger is the diameter of the pixel the worse quality pixels we fabricate. Possible, the mechanical vibrations on the flyer in combination with absence of the elasticity to the materials we were using, create those fragments and cracks on the surface of the "LIFTed" pixels. To avoid some of those effects we were mention we can focus on techniques that employ in contact procedures. Additionally, it can be tried multiple depositions of the material with an overlap to the laser beam diameter to keep the transferred pixel always in short lengths. This will employ also some needs for alignment.

The method where we use the copper/triazene/Alq_3 was shown to be one of the potential techniques. As also the case with the copper work as a light to heat conversion layer. The fabricated pixels with the first technique were having a nice surface quality and also the method is reproducible. But unfortunately, the layer of the triazene was transferred with the layer of the Alq_3 contaminating the fabricated pixels. That fact does not allow us to continue to the fabrication of a final device. For that reason we have to incorporate one more step before the final one. Some kind of a clean process for the acceptors. Some options are the photo-curing of the triazene layer. Also, the potential of that technique will be helped a lot by using an even thinner layer of triazene. Furthermore, maybe the use of another material instead of triazene will also help, or even could that material will be desirable for the final device.

In the case of the copper/Alq_3 the results was not good. In that case the principal is the same but the Alq_3 is more sticky to the copper layer than the triazene. Maybe that is because of the mechanical properties of the triazene or the attracting forces between the two surfaces. It's possible, by passivating the copper layer before the deposition of the Alq_3 to have a better technique. In our case the samples of the copper were stay a few days in the ambient environment which means that the surface were have been oxidized before the evaporation of the Alq_3. I propose to repeat the experiments by keeping the donors-samples for the all process of preparation in an inert environment.

About the characterization more measurements can be done. Also optical interferometry could be a potential in that case for the surface characterization of the acceptors after the evaporation of a thin layer of Gold or Silver. To make sure about the existence of contaminations on the acceptors some FTIR measurements will be needed.

8 Summary in Greek – Σύνοψη

Εισαγωγή

Η παρακάτω σύντομη μετάφραση του παραπάνω κειμένου στα Ελληνικά αφορά την διπλωματική μου εργασία στα πλαίσια του μεταπτυχιακού Μικροσυστήματα και Νανοδιατάξεις στη σχολή των Εφαρμοσμένων Μαθηματικών και Φυσικών Επιστημών στο Εθνικό Μετσόβιο Πολυτεχνείο Αθηνών. Η εργασία αυτή χρηματοδοτήθηκε από την TNO και πραγματοποιήθηκε στο Holst Center στο High Tech Campus , στο Eindhoven της Ολλανδίας το ακαδημαϊκό έτος 2013-2014.

8.1 Τεχνική LIFT

Η τεχνική Laser Induced Forward Transfer (LIFT), προτάθηκε αρχικά το 1986 από τον Bohandy et. al. Έπειτα από 20 και πλέον χρόνια η συγκεκριμένη τεχνική έχει κερδίσει έδαφος στην πίτα της έρευνας όσον αφορά στο τομέα της νανοτεχνολογίας. Η απλότητα και η προσαρμοστικότητα της τεχνικής αυτής οδήγησε στην εναπόθεση πολλών διαφορετικών υλικών όπως: μεταλλικών υμενίων, μελάνων, πηκτωμάτων (gel), ημιαγωγών, οξειδίων, διηλεκτρικών και βιομορίων. Πολλές παράμετροι όμως απαιτούν περαιτέρω βελτιστοποίηση πριν μπει επιτυχώς στην αγορά. Πολλές παραλλαγές της τεχνικής αυτής έχουν μελετηθεί όπως: Laser Induced Thermal Imaging (LITI), Dynamic release Layer-LIFT (DRL-LIFT), Matrix Assisted Pulsed Laser Evaporation-LIFT (MAPLE-LIFT) κτλ. Στην εργασία αυτή μελετάται η εφαρμογή της τεχνικής LIFT και κάποιων παραλλαγών της με έμφαση στην τεχνική Dynamic Release Layer-LIFT για την κατασκευή οργανικών φωτοδιόδων (OLEDs).

Η βασική αρχή λειτουργίας της τεχνικής είναι η τοπική εναπόθεση του προς μεταφορά υλικού από ένα δότη σε έναν αποδέκτη με την χρήση δέσμης laser. Το προς μεταφορά υλικό (πηγή) φέρεται επάνω σε ένα διαφανές υπόστρωμα στο μήκος κύματος της ακτινοβολίας που χρησιμοποιείται σε κάθε περίπτωση. Στη συνέχεια ο δότης (πηγή) ακτινοβολείται με την δέσμη laser και μέσω αλλαγών (εξάχνωση, εξάτμιση) της θερμοδυναμικής φάσης του υλικού προκαλείται η ελεγχόμενη μικρο-εναπόθεση του υλικού σε ένα υπόστρωμα αποδέκτη.

Dynamic Release Layer - LIFT (DRL-LIFT)

Στη συγκεκριμένη τεχνική χρησιμοποιείται ένα επιπλέον στρώμα ενός άλλου υλικού ανάμεσα από το διαφανές υπόστρωμα και το προς μεταφορά υλικό το οποίο συναντάται στη βιβλιογραφία με το όνομα Dynamic Release Layer (DRL), το οποίο δεν προορίζεται για εναπόθεση. Το στρώμα αυτό προστατεύει επιπλέον το προς μεταφορά υλικό από την ακτινοβολία όπως και από θερμικά φαινόμενα. Επιπλέον προκαλεί μέσω των αερίων παραγωγών του, κατά την αποδόμηση του, την ώθηση του υλικού προς εναπόθεση.

Matrix-Assisted Pulsed Laser Evaporation-Direct Write (MAPLE-DW)

Σε αυτή την περίπτωση ένα επιπλέον υλικό το οποίο δεν προορίζεται για εναπόθεση αναμιγνύεται με το προς μεταφορά υλικό. Με την έκθεση του στην ακτινοβολία του laser η εξάχνωση του επιπλέον υλικού (μήτρα) επιτρέπει την εναπόθεση του προς μεταφορά υλικού στον αποδέκτη.

Blister Actuated Laser Induced Forward Transfer (BA-LIFT)

Σε αυτή την τεχνική, βασική προϋπόθεση είναι οι μηχανικές ιδιότητες του προς μεταφορά υλικού (ημίρρευστα υλικά). Ο δότης καλύπτεται συνήθως από ένα πολυμερές και τοποθετείται σε καθορισμένη απόσταση από τον αποδέκτη. Μετά την έκθεση του στην ακτινοβολία η εν μέρει εξάτμιση του υλικού επιτρέπει την εναπόθεση μικρο-σταγόνων στον αποδέκτη με την στιγμιαία δημιουργία μικρό-σταλαγμιτών, του προς μεταφορά υλικού κυρίως μέσω θερμικών φαινομένων.

Laser Induced Thermal Imaging (LITI)

Στη τεχνική LITI χρησιμοποιείται, ένα επιπλέον στρώμα ανάμεσα από το διαφανές υπόστρωμα και το προς μεταφορά υλικό. Στην συγκεκριμένη περίπτωση στόχος είναι η πλήρης απορρόφηση της φωτεινής ακτινοβολίας από το επιπλέον στρώμα και την πρόκληση της εναπόθεσης του υλικού μέσω θερμικών φαινομένων. Στη συγκεκριμένη τεχνική ο δότης και ο αποδέκτης βρίσκονται σε επαφή και η ακτινοβολούμενη περιοχή παραμένει εκτυπωμένη στον αποδέκτη μετά την απομάκρυνση του δότη.

Hydrogen Assisted LIFT (HA-LIFT)

Το επιπλέον στρώμα μπορεί να είναι άμορφο πυρίτιο (a:Si) ή SiN. Η έκθεση στην ακτινοβολία, προκαλεί την έκλυση μορίων υδρογόνου ανάμεσα από το προς μεταφορά υλικό και τον δότη, με αποτέλεσμα την ώθηση μικροποσοτήτων του υλικού στην επιφάνεια του αποδέκτη.

8.2 Οργανικοί Φωτοδίοδοι

Η βιομηχανία φωτισμού είναι μία από της παλαιότερες βιομηχανίες και απασχολούν μεγάλο κομμάτι της παγκόσμιας αγοράς. Οι οργανικές φωτοδιόδοι αποτελούν μία από τις δυνητικά ιδανικότερες επιλογές για επίπεδες οθόνες ή για επίπεδες συσκευές φωτισμού, λόγω της αυθόρμητης εκπομπής φωτός, μεγάλη ανάλυσης, μεγάλη ένταση ακτινοβολίας, μεγάλη γωνία αντίληψης, μικρή κατανάλωση ενέργειας, και της δυνητικά φθηνής παραγωγής τους. Σημαντικό πρόβλημα παραμένει ο μικρός χρόνος ζωής τους λόγω της μεγάλης ευαισθησίας τους στην υγρασία, στο οξυγόνο, στο φως και στις υψηλές θερμοκρασίες.

Οργανικοί ημιαγωγοί

Οι δύο κύριες κατηγορίες των οργανικών ημιαγωγών με εφαρμογή σε φωτοδιόδους, χωρίζονται στα μικρό-μοριακά και στα πολυμερή υλικά. Συνεπώς και τα οργανικά υλικά εκπομπής φωτός χωρίζονται στις δύο αυτές κατηγορίες δημιουργώντας τις οργανικές φωτοδιόδους μικρο-μοριακών-μεταλλο-πολυμερικών συμπλεγμάτων, (Small Molecules OLEDs: SMOLEDs) και στις οργανικές φωτοδιόδους πολυμερών, (Polymer OLEDs: POLEDs).

Συμβατικές τεχνικές παρασκευής οργανικών φωτοδιόδων

Οι τεχνικές παρασκευής των οργανικών φωτοδιόδων μπορούν να χωριστούν σε δύο μεγάλες κατηγορίες:

- Εναπόθεση υλικών μέσω εξάχνωσης (ξηρή εναπόθεση)
- Εναπόθεση υλικών μέσω διαλυμάτων (υγρή εναπόθεση)

Η ξηρή εναπόθεση απαιτεί την ύπαρξη μάσκας που σε συνδυασμό με τις απαιτούμενες τεχνικές κενού καθιστά απαγορευτική την μείωση του κόστους τις παρασκευής ή την εφαρμογή για ταχεία και μεγάλης κλίμακας γραμμής παραγωγής. Η συγκεκριμένη τεχνική προτιμάται για υλικά οργανικών μεταλλικών συμπλεγμάτων.

Οι υγρές τεχνικές προτιμούνται για τα πολυμερικά υλικά (spin-coating, ink-jet printing, slot die-coating). Σε αντίθεση με τις τεχνικές ξηρής εναπόθεσης βρίσκουν εφαρμογή σε μεγάλη κλίμακα αλλά η ύπαρξη διαλυμάτων καθιστά δύσκολη την εναπόθεση πολλαπλών στρωμάτων.

Σήμερα υπάρχει μεγάλο ενδιαφέρον στη ανάπτυξη τεχνολογιών για την ανάπτυξη ημιαγώγιμων διατάξεων χωρίς την χρήση φωτολιθογραφίας. Μία από τις πολλά υποσχόμενες τεχνικές, είναι η τεχνική LIFT που λόγω της δυνατότητας για απ' ευθείας εκτύπωση πολλαπλών στρωμάτων χωρίς την αναγκαιότητα της χρήσης μάσκας την καθιστά ως μία από τις πιθανές εναλλακτικές τεχνικές για τις σύγχρονες ανάγκες τις μικροηλεκτρονικής βιομηχανίας.

Βασική αρχιτεκτονική φωτοδιόδων

Η βασική διαφορά των οργανικών φωτοδιόδων με τις συμβατικές φωτοδιόδους είναι ότι το ενεργό στρώμα εκπομπής ακτινοβολίας είναι από οργανικό πολυμερές ή από οργανικό-μεταλλικό σύμπλεγμα. Μία οργανική φωτοδίοδος αποτελείται από τουλάχιστον ένα στρώμα οργανικού υλικού ανάμεσα από δύο ηλεκτρόδια. Η εφαρμογή τάσης στα ηλεκτρόδια προκαλεί την εκπομπή ακτινοβολίας μετά την επανασύνδεση οπών και ηλεκτρονίων. Η παραπάνω διάταξη αναπτύσσεται στην επιφάνεια ενός διαφανούς συνήθως υποστρώματος και το ένα τουλάχιστον ηλεκτρόδιο είναι διαφανές στο οπτικό φάσμα (π.χ. Indium Tin Oxide). Επιπλέον στρώματα μπορεί να προστεθούν για την καλύτερη λειτουργία της συσκευής, όπως στρώματα έγχυσης οπών ή ηλεκτρονίων.

Η επίδοση μίας συσκευής εξαρτάται σημαντικά από την αρχιτεκτονική της δομή και από τα υλικά τα οποία έχουν χρησιμοποιηθεί. Γενικώς, το έργο εξόδου της καθόδου θα πρέπει να είναι αποτελεσματικά χαμηλό και της ανόδου αποτελεσματικά υψηλό.

Οι φωτοδιόδοι μπορεί να είναι μονοχρωματικές ή πολυχρωματικές. Οι μονοχρωματικές φωτοδίοδοι αποτελούνται από ένα μόνο ενεργό στρώμα. Οργανικές φωτοδίοδοι λευκού φωτός δημιουργούνται από τον συνδυασμό δύο τουλάχιστον ενεργών στρωμάτων.

Πολυχρωματικές φωτοδιόδοι μπορούν να αποτελούνται από τρία ενεργά στρώματα σε σειρά ή παράλληλα όσον αφορά στην αρχιτεκτονική τους διάταξη. Επιπλέον, η εφαρμογή οπτικών φίλτρων επίπεδης τεχνολογίας έχει ως αποτέλεσμα την δημιουργία πολυχρωματικών φωτοδιόδων που ήδη βρίσκουν εφαρμογή στην τεχνολογία οθονών.

8.3 Πειραματικό Μέρος

Τα υποστρώματα που έφεραν τα υπό εξέταση στρώματα ήταν quartz ή πολύ καλής ποιότητας γυαλί. Στα υποστρώματα πριν την εναπόθεση οποιουδήποτε στρώματος έγινε σχολαστικός καθαρισμός, διαδοχικά με ακετόνη, ισοπροπανόλη και μεθανόλη. Στα ενδιάμεσα στάδια του καθαρισμού η αφαίρεση των έντονα πτητικών διαλυμάτων επιτυγχανόταν με την εφαρμογή αέριου αζώτου υψηλής πίεσης.

Το στρώμα της τριαζήνης αναπτυσσόταν με την τεχνική spin-coating από διάλυμα τριαζήνης σε χλωροβενζόλιο και κυκλο-εξανόνη με αναλογία 1:1 κατά βάρος. Η εναπόθεση στρωμάτων από 30nm έως 300nm επιτεύχθηκε αλλάζοντας την ταχύτητα περιστροφής από 600 στροφές έως 3000 στροφές το λεπτό από διαλύματα με πυκνότητα 0,5%, 1%, 2% και 4% κατά βάρος. Μετά την εναπόθεση της τριαζήνης τα δείγματα τοποθετόντουσαν σε θερμαντική πλάκα με σταθερή θερμοκρασία στους 70^0C για μία ώρα, ώστε να εξατμιστούν οι διαλύτες.

Η τριαζήνη είναι ένα πολυμερές που απορρόφα έντονα στο υπεριώδες φάσμα και φωτο-αποδομείται μέσω εξώθερμης αντίδρασης. Αξίζει να σημειώσουμε εδώ πως το μήκος κύματος το οποίο είχαμε στη διάθεση μας ήταν στα 355nm ενώ το προτιμότερο θα ήταν στα 248nm λόγω του υψηλότερου δείκτη απορρόφησης της τριαζήνης.

Η εναπόθεση του Alq_3 έγινε μέσω ξηρής εναπόθεσης κενού και spin coating και του πολυμερούς Super Yellow με την τεχνική του spin coating. Η εναπόθεση του

Alq_3 με την τεχνική του spin coating είναι αδύνατη επάνω από το στρώμα της τριαζήνης. Το χλωροφόρμιο το οποίο χρησιμοποιούμαι ως διαλύτη για το Alq_3 διαβρώνει το στρώμα της τριαζήνης το οποίο δημιουργεί σημαντικές επιφανειακές ανωμαλίες που επηρεάζουν σημαντικά τα αποτελέσματα μας και καθιστούν αδύνατη την επαναληψιμότητα των πειραμάτων. Η ποιότητα και το πάχος των στρωμάτων χαρακτηρίσθηκε μέσω οπτικής μικροσκοπίας, κατατομετρίας (profilometry) και οπτικής συμβολόμετρίας.

Το βασικότερο εργαλείο στην μελέτη αυτή ήταν ένα παλμικό laser με παλμό 15ps. Το σύστημα έχει σχεδιαστεί ως μηχάνημα μικρο-μηχανικής, και είναι εξοπλισμένο με μία βάση με δυνατότητα κίνησης στις δύο διευθύνσεις με υψηλή ακρίβεια. Κατά τον κάθετο άξονα μπορεί να κινηθεί η κάμερα του laser αλλάζοντας έτσι την εστίαση της δέσμης στο στόχο. Το laser είναι ένα Nd:YaG laser με δυνατότητα εκπομπής στα 1064nm, 532nm και 355nm.

Επιπλέον για την διεκπεραίωση κάποιων πειραμάτων σε συνθήκες κενού σχεδιάστηκε και κατασκευάστηκε ένας θάλαμος κενού εξοπλισμένος με ένα βαρόμετρο και με 3 αντλίες που αναλόγως των απαιτήσεων μπορούσαν να χρησιμοποιηθούν ως έξοδοι ή είσοδοι αερίων ή κενού.

8.4 DRL-LIFT σε υμένια μικρο-μοριακών οργανικών

Ο στόχος της εργασίας αυτής είναι η εναπόθεση πολλαπλών στρωμάτων μέσω διαδοχικών τεχνικών LIFT . Η μέχρι τώρα προσέγγιση στην κατασκευή OLEDs μέσω της τεχνικής LIFT απαιτούσε την ύπαρξη ενός μεταλλικού στρώματος που παίζει υποστηρικτικό ρόλο στη μηχανική σταθερότητα του ενεργού στρώματος κατά την διαδικασία εκτύπωσης. Η παρουσία του μεταλλικού αυτού στρώματος καθιστά αδύνατη την εναπόθεση επιπλέον στρωμάτων και για αυτό ακριβώς το λόγο επιθυμείτε να απομακρυνθεί.

Επίδραση του πάχους της τριαζήνης

Το πάχος του DRL επηρεάζει άμεσα και σημαντικά την διαδικασία καθώς και το αποτέλεσμα. Όσο το πάχος του στρώματος της τριαζήνης μεγαλώνει, χρειάζονται και υψηλότερες ροές ενέργειας για να επιτευχτεί πλήρης αποδόμηση του συνολικού

πάχους της τριαζήνης και εκτύπωση του προς μεταφορά υλικού. Επιπλέον, τα παχύτερα στρώματα, προστατεύουν πιο αποτελεσματικά το προς μεταφορά υλικό από την φωτεινή ακτινοβολία και τα θερμικά φαινόμενα που εισάγει έμμεσα η αλλαγή θερμοδυναμικής φάσης της τριαζήνης, λόγω της επίδρασης της φωτεινής ακτινοβολίας από το laser αλλά και άμεσα η δέσμη laser. Τελικά τα παχύτερα στρώματα τριαζήνης έχουν ως αποτέλεσμα, την εκτύπωση καλύτερης ποιότητας και μορφολογίας pixel στην επιφάνεια του υποστρώματος-αποδέκτη.

Επίδραση της απόστασης δότη-αποδέκτη

Επιπλέον το κενό μεταξύ του δότη και του αποδέκτη παίζει σημαντικό ρόλο για τον έλεγχο της διαδικασίας. Αυτό οφείλεται κυρίως στο παραγόμενο ωστικό κύμα μετά την φωτο-αποδόμηση της τριαζήνης. Το ωστικό αυτό κύμα μπορεί να ελεγχθεί είτε αλλάζοντας τις συνθήκες ατμοσφαιρικής πίεσης είτε αλλάζοντας την απόσταση μεταξύ δότη και αποδέκτη.

Όταν το κενό μεγαλώνει η διασπορά του ωστικού κύματος επιτυγχάνεται πριν αυτό συναντήσει την επιφάνεια του αποδέκτη με αποτέλεσμα να μειώνεται η αρνητική του επίδραση. Επιπλέον όμως η ποιότητα των pixel μειώνεται αφού ταξιδεύουν μεγαλύτερη απόσταση πριν εναποτεθούν στο υπόστρωμα και κυρίως λόγω μηχανικών διαταραχών, αναπτύσσουν ανεπιθύμητη μορφολογία.

Σε συνθήκες μειωμένης ατμοσφαιρικής πίεσης επιτυγχάνεται πάλι η μείωση της επίδρασης του ωστικού κύματος λόγω της μικρότερης ισχύς του. Παρ' όλα αυτά, η ταχύτητα προσέγγισης του μεταφερόμενου στρώματος κατά την εναπόθεση του είναι ιδιαίτερα μεγάλη με αποτέλεσμα να είναι καταστροφική για τα pixel.

Επιπλέον, ιδιαίτερα ενδιαφέρων παρατήρηση που αξίζει να σημειωθεί είναι η καταγραφή δημιουργίας pixel σε σχήμα δακτυλίου. Η επικρατέστερη εξήγηση είναι ότι η επίδραση του ωστικού κύματος το οποίο μετά την αντανάκλαση του από το αποδέκτη, παρασύρει μέρος από το κέντρο του μεταφερόμενου δίσκου του υλικού και προκαλεί την εναπόθεση του πίσω στο δότη.

Η αύξηση της ατμοσφαιρικής πίεσης, ενισχύει την επίδραση του ωστικού κύματος αυξάνοντας έτσι την ελάχιστη απαιτούμενη ενέργεια για να επιτευχθεί

εκτύπωση. Ενώ δεν επιδρά καθόλου στην ελάχιστη απαιτούμενη ενέργεια για την πλήρη φωτο-αποδόμηση της τριαζήνης.

Για την συγκεκριμένη τεχνική επιπλέον η επαφή των δύο υποστρωμάτων κατά την διαδικασία κρίνεται απαγορευτική εφ' όσον τα αέρια παράγωγα από την φωτο-αποδόμηση της τριαζήνης έχουν καταστροφικές συνέπειες στο προς μεταφορά υλικό αναζητώντας διεξόδους διαφυγής.

Επιπλέον όσο αυξάνουμε το διάστημα μεταξύ δότη και αποδέκτη αυξάνεται και η διάμετρος των pixel λόγω της μεγαλύτερης διασποράς που εισάγεται από την μεγαλύτερη διαδρομή των pixel κατά την εκτύπωση. Ενώ η διάμετρος των οπών στο δότη από την φωτο-αποδόμηση της τριαζήνης παραμένει σταθερή.

Βελτιστοποίηση της απόστασης δότη-αποδέκτη

Η βελτιστοποίηση της απόστασης του δότη από τον αποδέκτη κρίνεται αναγκαία για την επίτευξη pixel καλής ποιότητα και καλής μορφολογίας. Κατά την βελτιστοποίηση τοποθετήσαμε τον δότη με κλίση επάνω από τον αποδέκτη, και σαρώσαμε τον στόχο για διάφορες ροές φωτεινής ακτινοβολίας σε διαφορετικές αποστάσεις μεταξύ τους. Ύστερα επιλέχθηκεαν οι ιδανικότερες συνθήκες (απόσταση δότη-αποδέκτη, ροή φωτεινής ακτινοβολίας) για την κατασκευή βέλτιστων pixel.

Σημαντικό πρόβλημα παραμένει η μορφολογία των pixel. Ύστερα από την βελτιστοποίηση η ύπαρξη ρωγμών και οπών στην επιφάνεια, μικροσωματιδίων περιφερειακά του pixel όπως και στρωματικών αναδιπλώσεων στις αιχμές τους καθιστά δύσκολη την παρασκευή μίας ολοκληρωμένης συσκευής. Τα πειράματα επαναλήφτηκαν σε διαφορετικής επιφάνειας αποδέκτες (ITO, quartz, κοινό γυαλί, γυαλί υψηλής καθαρότητας) και παρουσιάζουν παρόμοια αποτελέσματα. Ο χαρακτηρισμός των pixel έγινε με χρήση οπτικής συμβολομετρίας, μικροσκοπίας ατομικής δύναμης και οπτικής μικροσκοπίας.

Σημαντικό είναι πως οι ιδιότητες φωταύγειας του υλικού παραμένουν σχεδόν ανεπηρέαστες μετά την διαδικασία LIFT στην περίπτωση των Alq_3. Ακόμα και όταν η διαδικασία εκτύπωσης πραγματοποιείτε σε περιβαλλοντικές συνθήκες .

Βέλτιστη ελάχιστη απόσταση εναποτιθέμενων pixel

Ακόμα, το ωστικό κύμα μπορεί να επηρεάσει την εκτύπωση καταστρέφοντας ή επηρεάζοντας το ήδη εναποτιθέμενο pixel. Η μικρή δύναμη πρόσφυσης του Alq_3 με την επιφάνεια του αποδέκτη σε συνδυασμό με την μηχανική αστάθεια του υλικού, επιτρέπει την παραμόρφωση του, είτε την αποκόλληση του pixel λόγω του ωστικού κύματος. Για αυτό τον λόγο απαιτείται ιδιαίτερη προσοχή στην ελάχιστη απόσταση που μπορούμε να εναποθέσουμε pixel δίπλα το ένα στο άλλο. Το ελάχιστο αυτής της απόστασης εξαρτάται σημαντικά από το πάχος του στρώματος το οποίο μεταφέρουμε και το μέγεθος του pixel.

Ανόπτηση

Η παραμονή των μορφολογικών ανωμαλιών στην επιφάνεια των pixel μας οδήγησε στην ανάγκη για εύρεση επιπλέον τεχνικών για την εξομάλυνσης τους μετά την διαδικασία εκτύπωσης. Η ανόπτηση των pixel παρουσία ατμόσφαιρας πλούσιας σε ατμούς μεθανόλης έδειξε να είναι μία πολλά υποσχόμενη τεχνική. Μετά την παραμονή των δειγμάτων σε θάλαμο ελέγχου ατμοσφαιρικών συνθηκών παρουσία ατμών μεθανόλης σημειώθηκε διαστολή των pixel έως και 18% και μικρή επικάλυψη των οπών.

Τα πειράματα έγιναν παρουσία ατμών μεθανόλης και περιβαλλοντικής ατμόσφαιρας και παρουσία ατμών μεθανόλης και αζώτου. Και στις δύο περιπτώσεις σημειώθηκε σημαντική υποβάθμιση των ιδιοτήτων φωταύγειας του υλικού.

DRL-LIFT on IMEC's Sampes

Στη διάρκεια αυτής της διπλωματικής εργασίας, κάποια επιπλέον δείγματα τα οποία χορηγήθηκαν από την IMEC χρησιμοποιήθηκαν για την κατασκευή OLEDs. Τα αποτελέσματα ήταν παρόμοια με τα υπόλοιπα δείγματα τα οποία χρησιμοποιούσαμε έως τώρα, με την διαφορά ότι σημαντικό πρόβλημα παρέμενε η απώλεια ιδιοτήτων φωταύγειας μετά την εναπόθεση των pixel μέσω της τεχνικής LIFT.

Ένας θάλαμος κενού χρησιμοποιήθηκε ώστε να επαναληφτούν τα πειράματα σε ουδέτερες περιβαλλοντικές συνθήκες (συνθήκες χαμηλού κενού ή αδρανές περιβάλλον). Το ενεργό υλικό παρουσίασε ξανά απώλεια των ακτινοβολιτικών του

ιδιοτήτων, παρόλο που τα δείγματα διατηρόντουσαν σε αδρανές περιβάλλον, καθώς πριν και μετά την διαδικασία των πειραμάτων και δεν ήρθαν καθόλου σε επαφή με την ατμόσφαιρα πριν σταλούν για μετρήσεις φωταύγειας. Το τελικό συμπέρασμα από αυτά τα πειράματα είναι ότι κύριο αίτιο για την υποβάθμιση του υλικού ήταν προφανώς η επίδραση την φωτεινής ακτινοβολίας του laser στο υλικό μέσω θερμικών φαινομένων.

8.5 Παραλλαγές LIFT για την παρασκευή OLEDs

Μερικές ακόμα απόπειρες κατασκευής pixel με παραλλαγές της τεχνικής LIFT επιχειρήθηκαν. Οι τεχνικές που χρησιμοποιήθηκαν ήταν η τεχνική HA-LIFT, LITI, όπως και η εκτύπωση μέσω θερμο-αποδόμησης της τριαζήνης.

Οι τεχνικές HA-LIFT και LITI πραγματοποιήθηκαν χρησιμοποιώντας επίσης ένα excimer laser στα 198nm,50ns εκτός από το picosecond laser στα 355nm. Και στις δύο περιπτώσεις το υλικό εναποθετόταν κυρίως με την μορφή σκόνης και μικρο-σωματιδίων παρά σαν ένα συμπαγές στρώμα υλικού. Η απώλεια του DRL σε συνδυασμό με το πορώδες υλικό οδηγεί σε αυτό το αποτέλεσμα. Παρ όλα αυτά οι ακτινοβολιτικές ιδιότητες του υλικού φαίνονται να παραμένουν, με την χρήση μικροσκοπίας υπεριώδους ακτινοβολίας.

Η τριαζήνη παρουσιάζει επίσης υψηλή αποδόμηση παρουσία θερμοκρασιών μεγαλύτερες των 230^0C. Για αυτό το λόγω ένα διπλό στρώμα από χαλκό και τριαζήνη χρησιμοποιήθηκε ως DRL. Στόχος ήταν η θερμο-αποδόμηση της τριαζήνης από την τοπική θέρμανση του στρώματος χαλκού πριν αυτό αρχίσει να αποδομείτε.

Μετά από την βελτιστοποίηση του πάχους της τριαζήνης και του χαλκού, καλής μορφολογίας pixel κατασκευάστηκαν. Δεν υπήρχαν αναδιπλώσεις, οπές η ρωγμές στην επιφάνεια των pixel. Μετά των χαρακτηρισμό των pixel όμως αποδείχτηκε η ύπαρξη ενός επιπλέον στρώματος τριαζήνης από πάνω από το στρώμα του Alq_3.

Η παραπάνω τεχνικές επίσης εφαρμόστηκαν σε πολυμερές (Supper Yellow). Η DRL-LIFT τεχνική είναι αδύνατο να εφαρμοστεί σε αυτή την περίπτωση επειδή η

τριαζήνη διαλύεται κατά την εναπόθεση του Supper Yellow μέσω διαλύματος με βάση τολουήνη με την τεχνική spin coating.

Η τεχνική LITI και η τεχνική HA-LIFT που η επιφάνεια υποδοχής είναι χαλκός και SiN αντίστοιχα επιτρέπουν την συνέχεια της προετοιμασίας του δότη. Στην πρώτη περίπτωση η μεγάλες δυνάμεις συνάφειας μεταξύ του χαλκού και του Supper Yellow δεν επιτρέπουν την αποφύλλωση του ενεργού πολυμερούς. Στην δεύτερη περίπτωση η εκτύπωση του Supper Yellow επιτυγχάνεται αλλά με πολλές μορφολογικές ανωμαλίες. Και στις δύο περιπτώσεις δεν παρατηρείται κανέναν παράθυρο εργασίας προς βελτιστοποίηση.

8.6 Συμπεράσματα και Μελλοντικές προοπτικές

Για την ολοκλήρωση αυτής της διπλωματικής εργασίας απαραίτητη ήταν μία εκτενής ανασκόπηση της σχετικής βιβλιογραφίας, με την τεχνική LIFT όπως και ικανοποιητική αντίληψη της αρχής λειτουργίας της τεχνικής. Στις παρακάτω παραγράφους αναλύονται τα συμπεράσματα μετά το σύνολο των πειραμάτων που έγιναν. Επιπλέον προτείνονται κάποιες μελλοντικές προοπτικές όσον αφορά την συγκεκριμένη εργασία.

Συμπεράσματα

Η τεχνική LIFT είναι μία τεχνική για απ' ευθείας εκτύπωση υλικών, με την χρήση laser. Συνεπώς παράμετροι σχετικές με το laser επηρεάζουν σημαντικά τα αποτελέσματα. Η διάρκεια παλμού, το μήκος κύματος, η ένταση της δέσμης, η κατανομή της δέσμης όπως και η εστίαση είναι μερικές από αυτές. Ένας μικρότερης διάρκεια παλμός έχει ως αποτέλεσμα την στιγμιαία κατακόρυφη αύξηση της θερμοκρασίας στη διεπιφάνεια του προς μεταφορά στρώματος και του υποστρώματος, ενώ ένας μεγαλύτερης διάρκειας παλμός έχει μεγαλύτερο μήκος διάχυσης της θερμότητας στο προς μεταφορά υλικό με αποτέλεσμα να αποδομεί μεγαλύτερο πάχος υλικού επηρεάζοντας έτσι σημαντικά το προς μεταφορά υλικό, ή προκαλώντας την υποβαθμισή του μέσω θερμικών φαινομένων. Γενικώς συμπεραίνουμε πως για την εκτύπωση ευαίσθητων σε θερμικά φαινόμενα υλικών, προτιμότεροι είναι παλμοί της τάξης των picosecond από ότι nanosecond.

Το υλικό το οποίο παρεχόταν από την IMEC είναι πολύ ευαίσθητο στις ατμοσφαιρικές συνθήκες και σε συνδυασμό με την διαδικασία της τεχνικής LIFT, υποβαθμίζετε πλήρως μετά την εκτύπωση του. Αντιθέτως, το Alq_3 παρουσιάζει μεγαλύτερη σταθερότητα σχετικά με την ικανότητα του να εκπέμπει φώς μετά την διαδικασία εκτύπωσης. Επιπλέον το συγκεκριμένο υλικό διατηρεί της ιδιότητες του ακόμα και όταν η όλη διαδικασία διεξαχθει σε ατμοσφαιρικό περιβάλλον το οποίο είναι προαπαιτούμενο για την μείωση του κόστους παραγωγής.

Η τεχνική spin coating η οποία προτιμείτε για την μείωση του κόστους της όλης διαδικασίας έχει ένα μεγάλο μειονέκτημα. Ο διαλύτης ο οποίος χρησιμοποιείτε για το διάλυμα του προς εναπόθεση υλικού πρέπει να είναι συμβατός με το ήδη εναποτιθέμενο υμένιο. Σε αντίθετη περίπτωση το επόμενο διάλυμα προκαλεί μορφολογικές ανωμαλίες στην τελική δομή των στρωμάτων καθιστώντας αδύνατη την εφαρμογή τους στην τεχνική LIFT. Στη δική μας περίπτωση το χλωροφόρμιο και η τολουήνη που ήταν οι διαλύτες για το Alq3 και το Supper Yellow αντίστοιχα διαλύουν επίσης και την τριαζήνη. Αυτές οι αυξομειώσεις στο πάχος της τριαζήνης δεν μας επιτρέπουν τον έλεγχο των αποτελεσμάτων. Επιπλέον, όσον αφορά της εναπόθεση υμενίων με την μέθοδο spin coating μεγάλη προσοχή πρέπει να δοθεί στη ημερομηνία παραγωγής των διαλυμάτων. Γενικώς, μετά την παρασκευή ενός διαλύματος ή πριν την εναπόθεση κάποιου υμενίου απαιτείται η επανάληψη των μετρήσεων σχετικά με το πάχος του υμενίου.

Για την εφαρμογή οποιασδήποτε τεχνικής απαιτείται κάθε φορά βελτιστοποίηση σε παραμέτρους όπως την απόσταση του δότη με τον αποδέκτη, το πάχος των υμενίων στον δότη και τις παραμέτρους που είναι σχετικές με την δέσμη φωτός.

Στην τεχνική HA-LIFT δεν ανιχνεύεται κάποιο λειτουργικό παράθυρο και το υλικό εναποτίθεται κυρίως με την μορφή σκόνης και μικροσωματιδίων παρά σαν ένα συμπαγές στρώμα υλικού. Παρόμοια αποτελέσματα έχουν παλμοί τάξεως nanosecond και picosecond.

Η τεχνική DRL-LIFT όπου το στρώμα της τριαζήνης εκτίθεται άμεσα στη δέσμη laser, η εκτύπωση επιτυγχάνεται με χρήση μικρότερης έντασης δέσμης αλλά το προς μεταφορά υλικό παραμένει έντονα εκτεθειμένο στο φως επηρεάζοντας το

σημαντικά. Τα καλύτερης ποιότητας pixel τα οποία παρασκευάστηκαν, διατηρούν κάποιες μορφολογικές ανωμαλίες στην επιφάνεια τους όπως ρωγμές, οπές και αναδιπλώσεις στις αιχμές τους. Στην τεχνική όπου επιχειρήθηκε η θερμό-αποδόμηση της τριαζήνης τα αποτελέσματα είναι πολύ καλύτερα αλλά μέρος από το στρώμα της τριαζήνης εκτυπώνεται μαζί με το στρώμα του ενεργού πολυμερούς.

Το τελικό συμπέρασμα είναι ότι η πιο πολλά υποσχόμενη τεχνική για την παρασκευή OLEDs είναι η τεχνική DRL-LIFT, χωρίς να αποκλείουμε κάποιες άλλες προσεγγίσεις που με κάποιες βελτιστοποιήσεις θα μπορούσαμε να αποκλείσουμε τα ανεπιθύμητα αποτελέσματα. Όσον αφορά τις βελτιστοποιήσεις αυτές, τις προτείνω στο επόμενο κεφάλαιο. Στην περίπτωση της τεχνικής DRL-LIFT, το γεγονός ότι το ALq_3 διατηρεί τις ιδιότητες του ακόμα και μετά την εκτύπωση του σε ατμοσφαιρικό περιβάλλον είναι πολύ σημαντικό.

Επίσης, το μέγεθος των pixel είναι καίριας σημασίας. Παρατηρείται έντονα, πως όσο πιο μεγάλου μεγέθους pixel θέλουμε να εκτυπώσουμε, τόσο πιο πολλές μορφολογικές ανωμαλίες συναντάμε. Αυτό συμβαίνει προφανώς λόγω των μηχανικών δονήσεων του υλικού κατά την μεταφορά του, που σε συνδυασμό με το χαρακτήρα του υλικού οδηγεί σε ανεπιθύμητα αποτελέσματα.

Το πολυμερές Supper Yellow που έχει καλύτερες μηχανικές ιδιότητες από το ALq_3, είναι αδύνατο να εναποτεθεί με την τεχνική spin coating επάνω στο στρώμα της τριαζήνης. Για αυτό το λόγω η τεχνική LITI προτιμήθηκε. Παρόλα αυτά δεν παρατηρήθηκε κάποιο λειτουργικό παράθυρο λόγω των έντονων δυνάμεων συνάφειας μεταξύ του Supper Yellow και του χαλκού.

Μελλοντικές Προοπτικές

Στην περίπτωση της τεχνικής DRL-LIFT υπάρχουν ακόμα πολλοί παράμετροι που πρέπει να ελεγθουν και να βελτιστοποιηθούν για την εκτύπωση καλής μορφολογίας pixel χωρίς να επηρεάζονται οι ιδιότητες του Alq_3.

Μία από τις παραμέτρους που μπορούν να επηρεάσουν σημαντικά τα αποτελέσματα είναι το σχήμα του παλμού και η κατανομή ενέργειας. Στο επόμενο βήμα προτείνετε να χρησιμοποιηθεί δέσμη επίπεδου προφίλ. (Flat-top optics).

Επιπλέον στην περίπτωση της τριαζήνης είναι πιθανό, ακόμα μικρότερης διάρκειας παλμός να φέρει καλύτερα αποτελέσματα.

Το παραγόμενο ωστικό κύμα επηρεάζει έντονα τα αποτελέσματα της τεχνικής. Προτείνετε μία εκτενής μελέτη και μοντελοποίηση του φαινομένου σε συνδυασμό με τις παραμέτρους τις ατμοσφαιρικής πίεσης, του κενού μεταξύ δότη και αποδέκτη, του πάχους του προς μεταφορά υλικού, της μορφής και της διάρκειας του παλμού, όπως και του πάχους του DRL. Μία εκτενής μελέτη των παραπάνω μπορεί να βελτιώσει σημαντικά τα αποτελέσματα και να μας διαφωτίσει σχετικά με την διαδικασία.

Ένας ακόμα σημαντικός περιορισμός είναι το μέγεθος του pixel. Όπως έχει ήδη αναφερθεί , οι μηχανικές ταλαντώσεις κατά την εκτύπωση προκαλούν αυτές τις οπές και ρωγμές στα επιφάνεια των pixel. Για την αποφυγή αυτών των μηχανικών ταλαντώσεων, πρέπει να κατευθύνουμε προς τις μεθόδους όπου δεν απαιτείται η ύπαρξη απόστασης μεταξύ του δότη και του αποδέκτη. Επιπλέον μπορούμε να εναποθέσουμε διαφορετικά στρώματα καθ' επανάληψη ώστε να καλύψουμε αυτές τις ρωγμές.

Στην περίπτωση της τεχνικής με αρχιτεκτονική δομή στο δότη χαλκό/τριαζήνη/Alq_3 προτείνετε κάποιο άλλο μεταλλικό στρώμα να δοκιμαστεί. Στην διάρκεια αυτής της εργασίας μερικές απόπειρες έγιναν με στρώμα χρωμίου. Τα pixel που κατασκευάστηκαν είχαν καλή μορφολογία αλά στρώμα της τριαζήνης παρέμενε στην επιφάνεια μολύνοντας το Alq_3. Μερικές λύσεις για αυτό το πρόβλημα είναι οι εξής: να μειωθεί ακόμα περισσότερο το πάχος της τριαζήνης ώστε να αποδομείτε πλήρως κατά την εκτύπωση ή να αντικατασταθεί η τριαζήνη με ένα άλλο πολυμερές που θερμό-αποδομείτε εύκολα σε χαμηλές θερμοκρασίες. Επιπλέον, ένα επιπρόσθετο βήμα στην όλη διαδικασία όπου θα αφαιρείτε το ανεπιθύμητο στρώμα της τριαζήνης, μπορεί να είναι η λύση. Προτείνετε η φωτο-αποδόμηση της ύστερα από την εκτύπωση.

Στην περίπτωση του χαλκού/Alq3 δεν παρατηρήθηκε κανένα λειτουργικό παράθυρο. Το Alq3 φαίνεται να αναπτύσσει έντονες δυνάμεις με την επιφάνεια του χαλκού με αποτέλεσμα να εμποδίζεται η ομαλή αποφύλλωση του. Ίσως είναι πιθανό, απενεργοποιώντας την επιφάνεια του χαλκού να μπορέσουμε να επιτύχουμε καλύτερα αποτελέσματα. Προτείνετε να επαναληφτούν τα πειράματα και όλη η

διαδικασία να ολοκληρωθεί διατηρώντας τα δείγματα φύλλου χαλκού σε αδρανές περιβάλλον ώστε να αποφευχθεί η οξείδωση της επιφάνειας του.

Όσον αφορά τον χαρακτηρισμό των pixel, η τεχνική οπτικής συμβολομετρίας μπορεί να χρησιμοποιηθεί και να αποδώσει καλύτερα αποτελέσματα εάν στην επιφάνεια των δειγμάτων εναποτεθεί πριν της μετρήσεις ένα λεπτό στρώμα ασημιού ή χρυσού. Διότι, στην διάρκεια των μετρήσεων παρατηρήθηκε ότι η διαπερατότητα του Alq3 οδηγούσε σε λανθασμένα συμπεράσματα

9 Bibliography

[1] J. Bohandy, B. Kim and F. Adrian, “Metal deposition from a supported metal film using an excimer laser,” *Applied Physics,* vol. 60, no. 4, pp. 1538-1539, 1986.

[2] R. Osgood and H. Gilgen, “Laser Direct Writing of Materials,” *Ann. Rev. Mater. Sci.,* vol. 15, pp. 549-576, 1985.

[3] B. Thomas, A. P. Alloncle, P. Delaporte, M. Sentis, S. Sanaur, M. Barret and P. Collot, “Experimental investigations of laser-induced forward transfer process of organic films,” *Applied Surface Sience,* vol. 254, pp. 1206-1210, 2007.

[4] J. Wei, N. Hoogen, T. Lippert, O. Nuyken and A. Wokaun, “Novel Laser Ablation Resists for Excimer Laser Ablation Lithograpfy. Influence of Photochemical Properties on Ablation,” *J. Phys. Chem.,* vol. 105, no. 6, pp. 1267-1275, 2001.

[5] “A novel laser transfer process for direct writing of electronic and sensor materials,” *Applied Physics,* vol. A, no. 69, pp. S279-S284, 1999.

[6] N. Kattamis, N. McDaniel, S. Bernhard and C. Arnold, “Ambient laser direct-write printing of a patterned organo-metallic electroluminescent device,” *Organic Electronics,* no. 12, pp. 1152-1158, 2011.

[7] M. Brown, N. Kattamis and C. Arnold, “Time-resolved study of poluimide absorption layers for blister-actuated laser-induced forward transfer,” *Applied Physics,* vol. 107, no. 083103, pp. 1-8, 2010.

[8] M. Wolk, J. Baetzold, E. Bellmann, T. Hoffend, S. Lamansky, Y. Li, R. Roberts, V. Savvateev, J. Staral and W. Tolbert, “Laser Thermal Patterning of OLED Materials,” *SPIE,* vol. 5519, no. 13, pp. 12-23, 2004.

[9] D. Toet, M. Thompson, P. Smith and T. Sigmon, “Laser-assisted transfer of silicon by explosive hydrogen release,” *Apllied Physics Letters,* vol. 74, no. 15, pp. 2170-2172, 1999.

[10] D. Banks, C. Grivas, I. Zergioti and R. Eason, “Ballistic laser-assicted solid transfer (BLAST) from a thin film precursor,” *OPTICS EXPRESS,* vol. 16, no. 5, pp. 3249-3254, 2008.

[11] X. Yang, Y. Tang, M. Yu and Q. Qin, “Pulsed laser deposition of aluminum tris-8-hydroxyquinline thin films,” *Thin Solid Films,* vol. 358, pp. 187-190, 1999.

[12] L. Berthelot, J. Tardy, M. Garrigues, P. Cremillieu, J. Joseph and B. Masenelli, “ITO/PVK/ALq/matel LEDs: influence of PVK doping with DCM and of passivation with sputtered Si3N4,” *Optical Materials,* no. 12, pp. 261-266, 1999.

[13] J. R. H. Stewart Shaw, “Optimising the fabrication of organic light emitting

diodes by laser-induced forward transfer," University of Camprige, Camprige, 2012.

[14] P. T. Chou and Y. Chi, "Phosphorescent Dyes for Organic Light-Emitting Diodes," *Chemistry - Aeuropean Journal,* vol. 13, no. 2, pp. 380-395, 2007.

[15] J. Stewart, T. Lippert, M. Nageel, F. Nuesch and A. Wokaun, "Sequential Printing by Laser Induced Forward Transfer To Fabricate a Polymer Light-Emitting Diode Pixel," *ACS Applied Materials & interfaces,* vol. 4, pp. 3535-3541, 2012.

[16] C. Tang and S. VanSlyke, "organic electroluminescent diodes," *Applied Physics Letters,* vol. 51, no. 12, pp. 913-915, 1987.

[17] M. Boroson, L. Tutt, K. Nguyen, D. Preuss, M. Culver and G. Phelan, "Non-Contact OLED Color Patterning by Radiation-Induced Sublimation Transfer (RIST)," Eastman Kodak Company, NY.

[18] X. jiang, Z. Zhang, B. Zhang, W. Zhu and S. Xu, "Stable and current independent white-emitting organic diode," *Synthetic Metals,* vol. 129, pp. 9-13, 2002.

[19] A. Meyers and M. Weck, "Solution and Solid_state Characterization Of Alq3-finctionalized Polymers," *Chem. Mater.,* vol. 16, no. 7, pp. 1183-1188, 2004.

[20] M. Baldo, D. Brien, Y. You, A. Shoustikov, S. Sibley, M. Thompson and S. Forrest, "Highly efficient phosphorescent emission from organic electroluminescent devices," *NATURE,* vol. 395, pp. 153-154, 1998.

[21] Y. Seok Kim, S. Y. Jung, K. H. Koh and S. Lee, "Electroluminescence of Devices Fabricated using a Soluble Alq3 Pendent Polymer," *Korean Physical Society,* vol. 53, no. 6, pp. 3563-3567, 2008.

[22] P. Serra, M. Colina, J. Fernadez-Pradas, L. Sevilla and J. Morenza, "Preparation of Functional DNA microarrays through laser-induced forward transfer," *Applied Physics Letters,* vol. 85, no. 9, pp. 1639-1641, 2004.

[23] M. Joshi, S. Mohan, S. Tiwari, T. Dhami, T. Shripathi, U. Deshpande, M. Singh and H. Ghosh, "Broad-band visible emission from UV-exposed TPD solution," in *Proc. of ASID*, New Delhi, 2006.

[24] m. Mazzeo, f. Mariano, A. Genco, S. Carallo and G. Gigli, "High efficiency ITO-free flexible white organic light-emitting diodes based on multi-cavity technology," *Organic electronics,* vol. 14, pp. 2840-2846, 2013.

[25] G. Lei, L. Wang and Q. Yong, "Blue phosphorescent dye as sensitizer and emitter for organic light-emitting diodes," *Applied Physics Letters,* vol. 85, no. 22, 2004.

[26] B. D Andrade and S. Forrest, "White Organic light-Emitting Devices for Solid-Stete Lighting," *Advanced Materials,* vol. 16, no. 18, pp. 1585-1595, 2004.

[27] L. Hung and C. Chen, "Recent progress of molecular organic electroluminescent materials and devices," *Materials Science and Rngineering,* vol. 39, pp. 143-222,

2002.

[28] S. Taek Lee, J. Yeob Lee, M. Hyun Kim, M. Chul Suh, T. Min Kang, Y. Jin Choi, J. Young Park, J. Hyuk Kwon and H. Kyoon Chung, "A new Patterning Method For Full-Color Polymer Light-Emitting Devices: Laser Induced Thermal Imaging (LITI)," *S.T.Lee,* vol. 21, no. 3, pp. 784-787, 2002.

[29] Y. L. Jun and T. L. Seong, "Laser-Induced Thermal Imaging of Polymer Light-Emitting Materials on Poly(3,4-ethylenedioxythiophene): Silane Hole-Transport Layer," *Advanced Materials,* vol. 16, no. 1, pp. 51-54, 2004.

[30] R. Fardel, M. Nagel, F. Nuesch, T. Lippert and A. Wokaum, "Fabrication of organic light-emitting diode pixels by laser-assisted forward transfer," *Applied Physics letters,* vol. 91, 2007.

[31] J. Shaw-Stewart, T. Mattle, T. Lippert, M. Nagel, F. Nuesch and Wokaun, "The fabrication of small molecule organic light-emitting diode pixels by laser-induced forward transfer," *Applied Physics,* vol. 113, pp. 043104 1-7, 2013.

[32] N. Kattamis, M. Brown and C. Arnold, "Finite element analysis of blister formation in laser-induced forward transfer," *Materials Research Society,* pp. 1-12, 2011.

[33] K. Matsuo, K. hanawa, T. Hirano, T. Sasaoka and T. Urabe, "LIPS (Laser-Induced Patternwise Sublimation) Technology for Manufacturing Large-Sised OLED Displays," 2007.

[34] L. Urech, T. Lippert, C. Phipps and A. Wokaum, "Polymer ablation : From fundamentals of polymer design to laser plasma thruster," *Applied Surface Science,* vol. 253, pp. 6409-6415, 2007.

[35] J. Shaw Stewart, Fardel, Nagel, Delaporte, Rapp, Cibert, Alloncle, Nuesch, Lippert and Wokaun, "The effect of laser pulse length upon laser-induced forward transfer using a triazene polymer as a dynamic release layer," *Optoelectronics and Advanced Materials,* vol. 12, no. 3, pp. 605-609, 2010.

[36] J. Shaw-Stewart, T. Lippert, M. Nagel, F. Nuesch and A. Wokaun, "A simple model for flyer velocity from laser-induced forward transfer with a dynamic release layer," *Applied Surface Science,* vol. 258, pp. 9309-9313, 2011.

[37] t. Mattle, J. Shaw-Stewart, A. Hintennach, C. Schneider, T. Lippert and A. Wokaun, "Shadowgraphic investigations into the laser-induced forward transfer of different SnO2 precursor films," *Applied Surface Science,* pp. 24729/0-5, 2012.

[38] J. Stewart, b. Chu, T. Lippert, Y. Maniglio, M. Nagel, F. Nuesch and A. Wokaun, "Improved laser-induced forward transfer of organic semiconductor thin films by reducing the environmental pressure and controling the substrate-substrate gap width," *Applied Physics,* vol. 105, pp. 713-722, 2011.

[39] "Nanosecond time-resolved interferometric study on morphological dynamics of doped poly(mathyl methacrylate) film upon laser ablation," *Applied Physics Letter,* vol. 65, no. 26, pp. 3413-3415, 1994.

[40] O. Nuyken, J. Stebani, T. Lippert, A. Wokaun and A. Stasko, “Photolysis, thermolysis, and protolytic decomposition of a triazene polymer in solution,” *Macromol. Chem. Phys.*, vol. 196, pp. 751-761, 1995.

[41] S. Jingyao, Charge transport and excited states in organic semiconductors, University of London: Phd Thesis, 2010.

[42] B. Chichkov, C. Momma, S. Nolte, F. Alvensleben and A. Tunnerman, “Femtosecond, picosecond and nanosecond lase ablation of solids,” *Appl.Phys. A.*, vol. 63, no. 2, pp. 109-115, 1996.

[43] M. Sanz, M. Walczak, M. Oujjia, A. Domingo, A. Klini, E. Papadopoulou, C. Fotakis and Castillejo, “Femtosecond laser deposition of TiO2 by laser induced forward transfer,” *Elsevier*, pp. 5525-5529, 2010.

[44] X. Jiang, Y. Liu, X. Song and D. Zhu, “Organic light-emitting Diodes made with poly (N-vinylcarbazole) (PVK) and 8-hydroxyquinoline aluminium (Alq3),” *Synthetic Metals*, vol. 87, pp. 175-178, 1997.

[45] Gamaly, Madsen, Duering, Rode, Kolev and Luther-Davies, “Ablation of metals with picosecond laser pulses: Evidence of long-lived nonequilibrium conditions at the surface,” *Phusical review*, vol. B, no. 71, p. 174405, 2005.

[46] M. Kandyla, S. Chatzandroulis and I. Zergioti, “Laser induced forward transfer of contucting polymers,” *Optoelctron. Rev.*, no. 18, p. 345, 2010.

[47] T. Nguyen, J. Ip, P. Jolinat and P. Destruel, “XPS and sputtering study of the Alq3/electrode interfaces in organic light emitting diodes,” *Applied Suurface Science*, no. 172, pp. 75-83, 2001.

[48] T. Mattle, J. Shaw-Stewart, C. Schneider, T. Lippert and A. Wokaum, “Laser induced forward transfer aluminum layers: Process investigation by time resolved imaging,” *Applied Surface Ecience*, no. 258, pp. 9352-9354, 2012.

[49] D. Muller, A. Falcout, N. Reckefuss, M. Rojahn, V. Wiederhirn, P. Rudati, H. Frohne, O. Nuyken, H. Becker and K. Meerholz, “Multi-colour organic light-emitting displays by solution processing,” *NATURE*, vol. 421, pp. 829-833, 2003.

[50] T. Lippert, J. Dickinson, M. Hauer, G. Kopitkovas, S. Langford, H. Masuhara, M. Nuyken, J. Robert, H. Salmio, T. Tada, L. Tomita and A. Wokaun, “Polymers designed for laser ablation-influence of photochemical properties,” *Applied Surface science*, Vols. 197-198, pp. 746-756, 2002.

[51] J. Stewart, T. Lippert, M. Nagel, F. Nuesch and A. Wokaum, “Laser-Induced Forward Transfer Using Triazene Polymer Dynamic Releaser Layer,” *Amarican Institute of Physics*, 2010.

[52] J. Stewart, T. Lippert, M. Nagel, F. Nuesch and A. Wokaun, “Red-green-blue polymer light-emitting diode pixels printed by optimized laser-induced forward transfer,” *Applied Physics Letters*, vol. 100, pp. 203303 1-4, 2012.

[53] “White organic light-emitting diodes prepared by fused organic solid solution method,” *Applied Physics Letters*, no. 86, pp. 073510 1-3, 2005.

[54] D. Karnakis, A. Kearsley and M. Knowles, “Ultrafast Laser patterning of OLEDs on Flexible Substrate for Solid-state lighting,” *JLMN=-Journal of Laser Micro/Nanoengineering,* vol. 4, no. 3, pp. 218-223, 2009.

[55] J. R. H. S. Stewart, Optimizing the fabrication of organic light-emitting diodes by laser-induced forward transfer, Zurich: ETH Zurich, 2012.

[56] R. Menzel, Photonics:Linear and Nonlinear Interactions of Laser Light and Matter, Berlin: Springer, 2007.

[57] T. S. Yu, *Solidification in a thin liquid film: Croqing Alq3 needles via methanol-vapor annealing,* Massachusetts: Massachusetts Institute of Technology, 2011.

[58] J. Knox, M. Halls, h. Hratchian and B. Schlegel, “Chemical failure modes of Alq3-based OLEDs: Alq3 hydrolysis,” *physical Chemistry Chemical Physics,* vol. 8, pp. 1371-1377, 2006.

[59] K. Shepard, Y. Guo and C. Arnold, “Nanostructured morphology of polymer films prepared by matrix assisted pulsed laser evaporation,” *Applied physics A,* 2012.

[60] C. Arnold, R. Wartena, B. Pratap, K. Swider-Lyons and A. Pique, “Direct writing of planar ultracapacitors by laser forward transfer processing,” *SPIE LASE,* vol. 4637, pp. 353-360, 2002.

[61] L. Basirico, Ph.D. "inkjet Printing of Organic Transistor Devices", Cagliari: University of Cagliari, 2012.

[62] S. Hong, J. Lee, H. Kang and K. Lee, “Slot-die coating parameters of the low-viscosity bulk-heterojunction materials used for polymer solar cells,” *Solar Energy Materials & Solar Cells,* vol. 112, pp. 27-35, 2013.

[63] M. Singh, H. Haverinem, P. Dhagat and C. Jabbour, “Inkjet Printing- Process and its Applications,” *Advanced Materials,* vol. 22, pp. 673-685, 2010.

[64] M. Zenou, O. Ermak, A. Saar and Z. Kotler, “Laser sintering of copper nanoparticles,” *Physics D:Applied Physics,* vol. 47, pp. 025501-11, 2013.

[65] “The optimisation of the laser-induced forward transfer process for fabrication of polyfluorene-based organic light-emitting diode pixels,” *Applied Surface Science,* pp. 24659/0-6, 2012.

[66] N. Arnold, N. Bityurin and D. Bauerle, “Laser-induced thermal degradation and ablation of polymers: bulk model,” *Applied Surface Science,* Vols. 138-139, pp. 212-217, 1999.

[67] W. Chen, M. Tseng, C. Liao, P. Wu, S. Sun, Y. Huang, C. Chang, C. Lu, L. Zhou, D. Huang, A. Liu and D. Tsai, “Fabrication of Three-Dimensional plasmonic cavity by femtosecond laser-inducede froward transfer.,” *OPTICS EXPRESS,* vol. 21, no. 1, p. 618, 2013.

[68] N. Kattamis, N. McDaniel, S. Bernhard and C. Arnold, “laser direct write printing of sensitive and robust light emitting organic molecules,” *Applied Physics Letters,* vol. 94, no. 103306, pp. 1-3, 2009.

[69] C. Sones, M. Feinaeugke, A. Sposito, B. Gholipour and R. Eason, “Laser-Induced forward Transfer-printing of focused ion beam pre-machined crystalline magneto-optic yttrium iron garnet micro-discs,” *OPTICS EXPRESS*, vol. 20, no. 14, p. 15171, 2012.

A Appendix

A.1 Excited states in organic devices

Categories of excited states

Light emission from organic devices requires the formation of excited states. These are called excitons. Generally speaking, the exciton is an electron and hole pair. They attractively interact with each other via coulomb attraction. There are two different ways to classify the exciton.

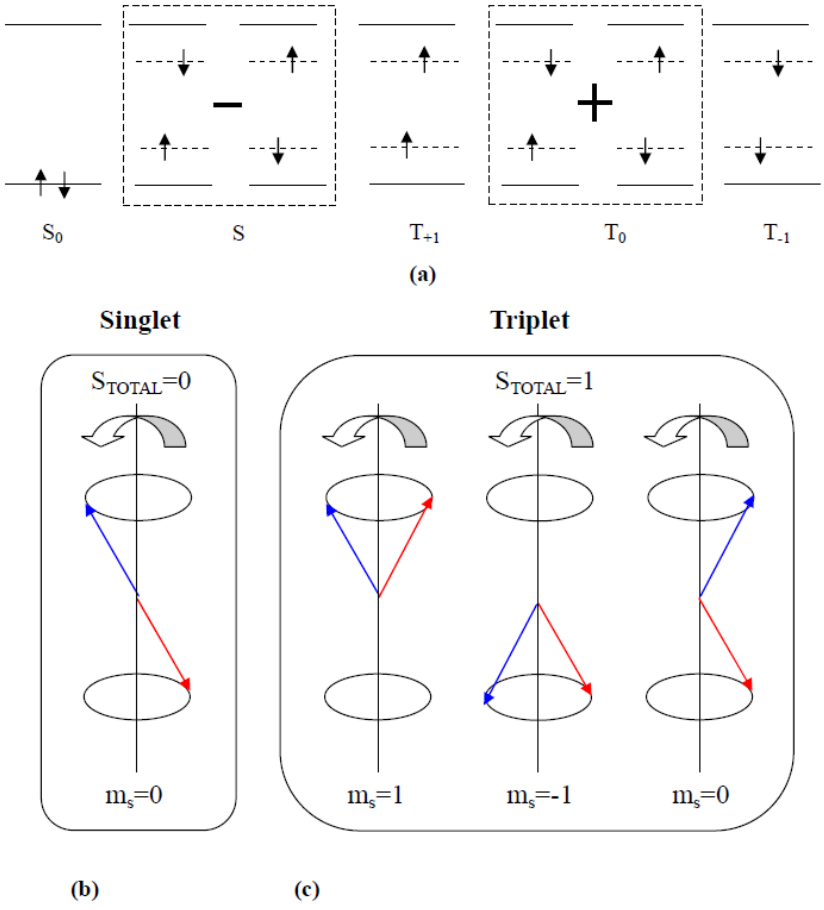

Figure 9-1: Exciton spin arrangements

An exciton can be categorized as Frenkel exciton if the electron-hole pair is located on the same molecular unit, or a Wannier-Mott exciton if the pair spans over a few adjacent molecular units, also known as transfer exciton. Unlike inorganic

semiconductors, the excitons in organic materials are mostly Frenkel excitons, which means that the exciton is localized on a single polymer unit or a small molecule.

The exciton can be classified by the different spin orientations of the electron-hole pair. The first group is called singlet states (Figure 9-1 (b)), whereby the electron and hole are orientated with spin anti-parallel and opposite (spin momentum m_s=0), and the total angular momentum equals to zero (S_{total}=0, with combination ($\frac{1}{\sqrt{2}}$(↑↓-↓↑)). The second group is call triplet states (Figure 9-1(c)), and contains three possible spin orientations. First, both electron and hole are spin up (with spin momentum m_s=1 and total angular momentum S_{total}=1). Secondly, both the electron and hole are spin down (m_s=-1, S_{total}=1). Thirdly, both of them are spin opposite but with a non-zero resultant spin component (m_s=0, S_{total}=1, with combination $\frac{1}{\sqrt{2}}$(↑↓+↓↑)).

Last but not least, because of the spin-allowed radiative decay, the singlet states have a much shorter lifetime, compared to the decay of triplet states, which is generally forbidden by the conservation of spin symmetry. Ordinarily, it is at least a factor of one thousand shorter than triplets, for example the radiative recombination time for singlets in Alq_3 is of the order of 10- 20 ns whilst that for triplets is of the order of 25 μ_s^{-1} ms.

Generation of excited states

Excitons can be generated in two different ways: photo excitation (or photoluminescence) and electrical excitation (or electroluminescence). Both ways can achieve light emission in an OLED device

Photo excitation is usually achieved using a laser. Light is incident on the diode and is absorbed by molecules in the organic semiconductor, the energy of the incident light lifts an electron into a higher energy state, leaving a hole behind it (Figure 9-2). However this excited state is very unstable, and it can easily lose energy. Both electron and hole recombine, emitting a photon. This is called photoluminescence. The exciton can also dissociate to a free electron and hole at the hetero-interface or at defects.

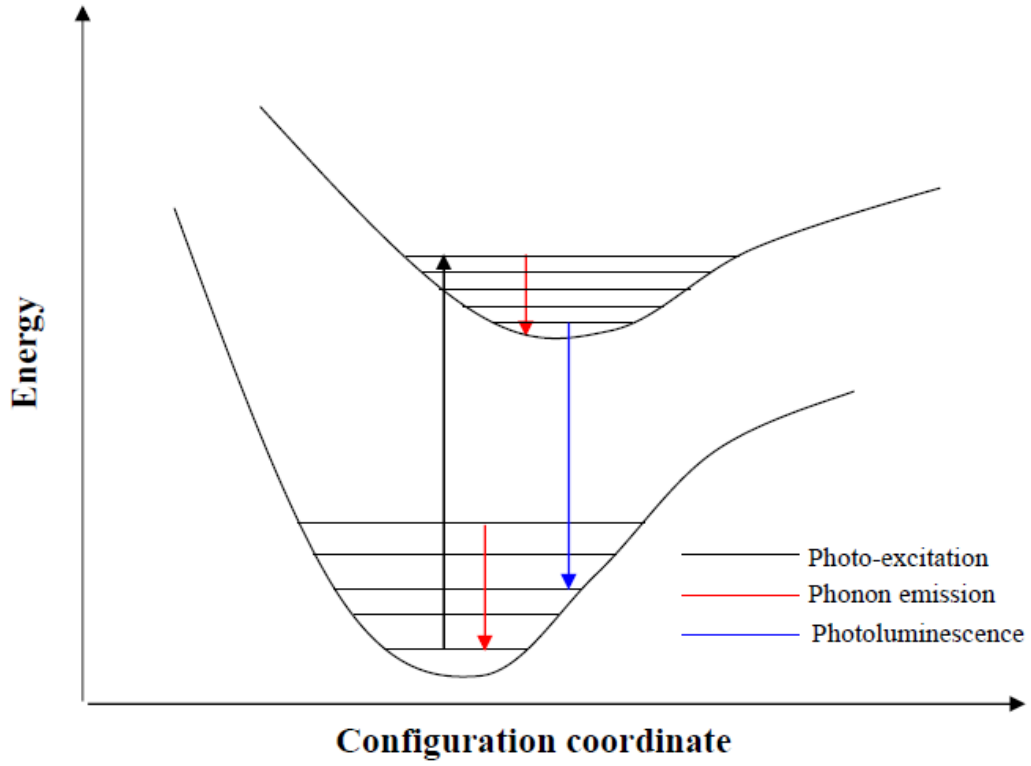

Figure 9-2:Schematic of photoluminescence process

Electrical excitation can be observed by applying a voltage to an OLED device. Holes are injected from the anode into the HOMO level of the hole transport layer and meet with the electrons that have been injected from the cathode into the LUMO of the electron transport/emission layer. Once both types of charge are present in the emission layer (or interface), excitons are generated by those electron hole pairs with required spin orientation. In this case, both singlets and triplets are formed. With singlet recombination, luminescence can be observed in the system, so it is called electroluminescence.

According to Figure 9-1, given the random spin of electron and hole, the triplet/singlet generation ratio is 3:1. The spins of injected charge carriers from anode and cathode are random, without any external influences exciton formation is solely governed by spin statistics, so the electrical excitation causes 25% of excitons to form singlets, and 75% of excitons to form triplets [41]

A.2 Influence of the pulse

The electron in a metallic material gets excited to a higher energy state upon laser irradiation, this leads to rapid thermalization of electrons and hence free hot electron gas is produced. The electron gas diffuses through the material and heats it up through electron-phonon collisions. The collision time is an important parameter that distinguishes between the physical processes of laser pulse interaction with a material and categorizes it as thermal and non-thermal processes respectively. Typically the electron-phonon (e-p) collision time is in sub-picosecond (10-14 s – 10-13 s) range at room temperature. Thermal processes are associated with laser pulses of pulse length longer than the e-p collision time such as a pulse length of typically below 10 ps, but, when the pulse length is comparable to the e-p collision time then it falls under non-thermal processes.

Below a discussion is presented respectively to understand the behavior while operating the laser energy in nanosecond, picosecond and femtosecond regimes. Let us assume that tp is the laser pulse length, electron cooling times, te and a lattice heating time, ti.

Nanosecond pulse

In case of a laser pulse length in nanoseconds(10-9 s) regime, the pulse duration is longer than the lattice electron-phonon thermal relaxation time i.e. tp > ti, the hot electrons gets enough time to establish thermal equilibrium with lattice and consequently both electrons and the lattice are at the same temperature [13]. It is assumed that the laser energy absorbed gets instantaneously converted into heat within the volume of absorption [14].

Picosecond pulse

In case of a laser pulse length in picosecond (10-12 s) regime, the pulse duration is between thermal electron cooling time and lattice heating time i.e. te << tp << ti. The lattice temperature can be neglected because at a time t >> te the electron temperature is said to be in quasistationary state and electron temperature is higher than lattice temperature [42].

Femtosecond pulse

In the case of a femtosecond (10-15 s) pulse length, the pulse duration is shorter than the electron phonon relaxation time i.e. tp << te. In this case the electron-phonon thermal relaxation time controls radiation energy transfer and hence it should be taken into consideration. Electrons and lattice are no longer in thermal equilibrium and therefore it should be treated as two separate subsystems. Heating of the material proceeds in two steps,

(i) Electrons absorb photon energy and

(ii) Lattice heating is done through electron phonon-coupling [13].